NTNU
Norwegian University of
Science and Technology

Iron Acquisition in *Cynobacteria Synechococcus* sp. PCC 7002 Culture

Ayten Pehlivan

Environmental Toxicology and Chemistry
Submission date: May 2018
Supervisor: Murat Van Ardelan, IKJ
Co-supervisor: Martin.F Hohmann-Marriott, IKJ

Norwegian University of Science and Technology
Department of Chemistry

Abstract

Iron is an essential micronutrient for the growth and health of phytoplankton and low overall iron concentrations in the High Nutrient Low Chlorophyll (HNLC) zones in the ocean have been reported. *Cyanobacteria* is one of the most important organism involved in primary productivity and iron-limitation could indirectly affect the global carbon cycle and CO_2 sequestration. This project aims to study the influence of the type of iron mineral and iron acquisition mechanism efficiency in *Cyanobacteria*. Two incubation experiments were carried out using a tropical strain of *Synechococcus* sp. PCC 7002 at room temperature (25 °C). Two different forms of Fe were used in cultures with different solubilities; one culture was added with 50 nM $FeCl_3$ (74.4 g/100 mL) and the other culture was added with 50 nM Goethite (FeO(OH)) (HCl soluble), respectively. Biological parameters such as growth and chlorophyll a concentration as well as particulate and intracellular Fe were analysed. Growth of *Synechococcus* sp. PCC 7002 was significantly slow in both cultures regardless of Fe concentrations which was predicted to be due to cells already being in stationary phase during the sampling period. High particulate and intracellular Fe were detected in $FeCl_3$ culture and no physiological stress response was observed. On the other hand, cells grown in FeO(OH), had less particulate and intracellular Fe however, the days where intracellular Fe was recorded, the Fe concentration was high. Overall, this study suggests that $FeCl_3$ is more available to cells than the less soluble goethite FeO(OH) and the cells grown in FeO(OH) culture are able to utilise the particulate Fe via PilA1 mechanism. However, future work must be carried out in order to conclude the experiment.

Acknowledgements

I would like to thank my supervisor, Professor Murat, for the opportunity to work on this project. I would also like to thank Annie Vera Hunnestad for being very helpful and supportive throughout this project, and for teaching me a lot of useful skills. This project would not be completed without the hard work of Maria Villegas, I would like to thank her for all the time and work she had put in this project with me. A big thank you to Cafe-Sito at Realfagbygget for providing delicious cinnamon buns on Wednesdays and fuelling us up on long lab days!

Table of Contents

Abstract iii
Acknowledgements v
List of Figures xi
List of Tables xiii
List of Equations xv
List of Appendix Tables xvii
Abbreviations xix

1 INTRODUCTION 1
2 HYPOTHESIS AND OBJECTIVES 3
3 BACKGROUND AND THEORY 5

3.1 Sources of iron 5
3.2 Iron in the oceans 7
3.2.1 Biogeochemistry and speciation of iron in the oceans 7
3.2.2 Oceanic iron cycling 9
3.3 Iron as a nutrient 11
3.3.1 Iron limitation and fertilization 14
3.4 Phytoplankton in the ocean 16
3.5 Iron uptake mechanisms in *Cyanobacteria* 18
3.5.1 Siderophores 18
3.5.2 Reductive iron uptake 19
3.5.3 Particulate bound iron via PilA1 21
3.6 Iron starvation in *Cyanobacteria* 22

4 MATERIALS AND METHODS 25

4.1 Clean work and acid washing 25
4.1.1 Acid cleaning procedure 25
4.2 Synthetic ocean water preparation 27
4.3 Cleaning of Aquil with Chelex-100 31
4.4 Microwave sterilisation 33
4.5 Experimental setup 34
4.6 Important biological indicators 35
4.6.1 Extracted chlorophyll a 35

4.6.2 Optical density (OD730nm) *36*
4.6.3 Particulate and intracellular iron *37*
4.6.4 Particulate Organic Carbon (POC)/ Particulate Organic Nitrogen (PON) *39*
4.6.5 Temperature and pH *39*

5 RESULTS **41**

5.1 Blanks and limit of detection 41
5.2 Growth 42
5.2.1 $FeCl_3$ *42*
5.2.2 FeO(OH) *44*
5.2.3 $FeCl_3$ vs FeO(OH) *46*
5.3 Temperature and pH 47
5.3.1 $FeCl_3$ *47*
5.3.2 FeO(OH) *49*
5.4 Chlorophyll a 52
5.4.1 $FeCl_3$ *53*
5.4.2 FeO(OH) *55*
5.5 Intracellular and particulate iron 57
5.5.1 $FeCl_3$ *59*
5.5.2 FeO(OH) *60*

6 DISCUSSION **63**

6.1 Growth 63
6.2 Temperature and pH 64
6.3 Chlorophyll a 65
6.4 Intracellular and particulate iron 67
6.4.1 $FeCl_3$ *67*
6.4.2 FeO(OH) *68*
6.4.3 $FeCl_3$ versus FeO(OH) *69*

7 CONCLUSION **71**
8 FUTURE WORK **73**
9 BIBLIOGRAPHY **75**

APPENDIX A: FE56 ICP-MS RESULTS I
APPENDIX B: CHLOROPHYLL A RESULTS VII
APPENDIX C: PH AND TEMPERATURE MEASUREMENTS XVI
APPENDIX D: CHLOROPHYLL A LINEAR REGRESSION XIX

List of Figures

Figure 1-1 Iron redox cycle and interactions with other elements. 1

Figure 3-1 Aeolian iron supply into the ocean. 6

Figure 3-2 Oceanic iron cycle in Atlantic Ocean. 11

Figure 3-3 Cyanobacteria. 17

Figure 3-4 Building blocks of iron binding molecules. 18

Figure 3-5 Siderophore structures. 19

Figure 3-6 Reductive iron uptake in *Synechocystis* PCC 6803 species. 21

Figure 3-7 PilA1 mechanism 22

Figure 4-1 Change in the structure of Chelex resin with increasing pH. 32

Figure 4-2 The experimental set up 35

Figure 4-3 Fluorometer - Turner Designs. 36

Figure 5-1 OD730nm vs Days for cells grown in culture $FeCl_3$ and FeO(OH). 46

Figure 5-2 Log(number of cells mL^{-1}) vs Days for $FeCl_3$ and FeO(OH) culture. 47

Figure 5-3 An ideal growth curve. 47

Figure 5-4 OD730nm and Temperature vs incubation days for $FeCl_3$. 49

Figure 5-5 OD730nm and pH vs incubation days for $FeCl_3$. 49

Figure 5-6 OD730nm and Temperature vs incubation days for FeO(OH). 51

Figure 5-7 OD730nm and Temperature vs incubation days for FeO(OH). 51

Figure 5-8 Extracted chlorophyll a versus in vivo fluorescence. 53

Figure 5-9 Chl a vs Days for $FeCl_3$ culture. 55

Figure 5-10 Chl a vs Days for FeO(OH) culture. 57

Figure 5-11 Fe concentrations for $FeCl_3$ culture. 60

Figure 5-12 Fe concentration for FeO(OH) culture. 61

List of Tables

Table 4-1 List of anhydrous salts. 28

Table 4-2 Hydrous salts..... 28

Table 4-3 Major Nutrients. 29

Table 4-4 Materials / Metalloids. 30

Table 4-5 Iron minerals. 30

Table 4-6 Vitamins. 31

Table 5-1 Limit of detection (LoD) calculated for Particulate and Intracellular Fe. 41

Table 5-2 Biological parameters showing growth in OD730 nm, number of cells mL^{-1}, Log (No of cells mL^{-1}) for $FeCl_3$ culture..... 43

Table 5-3 Biological parameters showing growth in OD730 nm, number of cells mL^{-1}, Log (No of cells mL^{-1}) for FeO(OH) culture. 45

Table 5-4 Temperature and pH for $FeCl_3$ culture. 48

Table 5-5 Temperature and pH for FeO(OH) culture. 50

Table 5-6 In vivo fluorescence and extracted chlorophyll a. 52

Table 5-7 Chlorophyll a concentrations for $FeCl_3$ culture. 54

Table 5-8 9 Chlorophyll a concentrations for FeO(OH) culture. 56

Table 5-10. Particulate and Intracellular Fe concentrations in control medium. 58

Table 5-11. Particulate, Intracellular and Extracellular Fe concentrations in $FeCl_3$ culture.... 58

Table 5-12. Particulate, Intracellular Fe concentrations in FeO(OH) culture. 59

List of Equations

Equation 1 Relationship between Number of cells mL^{-1} and OD730nm. 42

Equation 2 Chlorophyll a concentration calculation. 52

Equation 3 Linear relationship between in vivo FL and chl a/NA. 52

Equation 4 Carbonate equilibrium 65

List of Appendix Tables

Table A1 UltraCLAVE and filter blanks. I

Table A2 Particulate and Intracellular Fe ICP-MS results for $FeCl_3$ and FeO(OH) culture. II

Table B1 In vivo Chlorophyll a for $FeCl_3$ culture. VII

Table B2 Converted Chlorophyll a (extracted) for $FeCl_3$. VIII

Table B3 Calculated Chlorophyll a for $FeCl_3$ culture and control. X

Table B4 In vivo Chlorophyll a for FeO(OH) culture. XI

Table B5 Converted Chlorophyll a (extracted) for FeO(OH). XII

Table B6 Calculated Chlorophyll a for FeO(OH) culture and control. XIV

Table C1 Recorded pH and temperature values for $FeCl_3$ culture and control. XVI

Table C2 Recorded pH and temperature values for FeO(OH) culture and control. XVII

Table D1 Linear regression correlation results. XIX

Table D2 ANOVA results of regression analysis of chlorophyll a conversion. XIX

Table D3 Linear regression statistical results. XX

Abbreviations

Chemicals

Ammonia	NH_4^+
Ammonium hydroxide	NH_4OH
Bicarbonate	HCO_3
Boric acid: (hydrogen borate)	H_3BO_3
Calcium	Ca
Calcium Chloride Dihydrate	$CaCl_2 .2H_2O$
Carbon	C
Carbon dioxide	CO_2
Cobalt (II) Chloride Hexahydrate	$CoCl_2 .6H_2O$
Copper (II) Sulfate Pentahydrate	$CuSO_4 .5H_2O$
Disodium EDTA	$Na_2C_2O_4$
Disodium oxalate	$C_{10}H_{14}N_2Na_2O_8$
Fe(III) hydroxy species	$Fe\ (OH)_2^+$
	$Fe\ (OH)^{2+}$
	$Fe\ (OH)^-_4$
Ferric Iron	Fe(III)
Ferrous Iron	Fe(II)
Hydrochloric acid (Hydrogen Chloride)	HCl
Hydrogen peroxide	H_2O_2
Iron	Fe
Iron (III) chloride hexahydrate	$FeCl_3. 6H_2O$
Iron (III) oxide-hyrdroxide (Goethite)	FeO(OH)
Magnesium	Mg
Magnesium Chloride	$MgCl_2$
Magnesium Chloride Hexahydrate	$MgCl_2 .6H_2O$
Manganese (II) Chloride Tetrahydrate	$MnCl2. 4H_2O$
Nitrate	NO_3
Nitric acid	HNO_3
Nitrogen	N_2
Oxygen	O_2
Phosphorus	P

Potassium bromide	KBr
Potassium Chloride	KCl
Sodium bicarbonate	$NaHCO_3$
Sodium Chloride	NaCl
Sodium Dihydrogen Phosphate Monohydrate	$NaH_2PO_4.H_2O$
Sodium fluoride	NaF
Sodium hydroxide	NaOH
Sodium Metasilicate Nonahydrate	$Na_2SiO_3.9H_2O$
Sodium Molbdate Dihydrate	$Na_2MoO_4 .2H_2O$
Sodium nitrate	$NaNO_3$
Sodium selenite	Na_2SeO_3
Sodium sulfate	Na_2SO_4
Strontium Chloride Hexahydrate	$SrCl_2 .6H_2O$
Sulphate	SO_4
Zinc	Zn
Zinc Sulfate Heptadhyrate	$ZnSO_4 .7H_2O$

Prefixes

giga (10^9)	G
mega (10^6)	*M*
kilo (10^3)	k
mili (10^{-3})	m
micro (10^{-6})	µ
nano (10^{-9})	n
pico (10^{-12})	p

Units of Measure

Day	d
Degrees Celsius	°C
Gram	g
Hydrogen ion activity (negative log of)	pH
Litre	L
Meter	m
Molar	M
Mole	mol

Second	s
Ton	t
Water exchange rate	k_{ex}
Year	Yr

Acronyms

Acid phosphatases	APase
Adenosine triphosphate	ATP
Approximately (circa)	ca.
Capacity of seawater for soluble Fe	cFe
Chlorophyll a	chl a
Colloidal Iron	FeC
Concentration	Conc.
Cyanocobalamin	Vit. B12
Deionized water	DI water
Dissolved inorganic phosphorus	DIP
Dissolved Iron	DFe
Dissolved organic phosphorus	DOP
Ethylenediaminetetraacetic acid	EDTA
Fe(II) transporters	FeoB
Fe(III) trasnporters	FutABC
Flow injection analysis	FIA
glass microfiber filter	GF/F
Growth rate	μ
High efficiency particulate filter	HEPA filter
High Nutrient Low Chlorophyll	HNLC
High Resolution Inductively Couples Plasma Mass Spectrometry	HR-ICP-MS
Inorganic Fe3+ species	F'
Light-emitting diode	LED
Limit of detection	LoD
Logarithm base 10	log
Logarithm base *e*	ln
Low-density polyethylene	LDPE
Maximum fluorescence	Fv/F~

National Center for Marine Algae and Microbiota	NCMA
Optical density	OD
Particulate Iron	PFe
Particulate Organic Carbon	POC
Particulate Organic Nitrogen	PON
Parts per million	ppm
Phosphate Monoesterases	PhoA
	PhoX
	PhoD
Photosystem I	PSI
Photosystem II	PSII
Polyethylene	PE
Relative standard deviation	RSD
Soluble Iron	SFe
Standard deviation	SD
Strong Iron binding ligand	L1
Surface Microlayer	SML
Synthetic Ocean Water	SOW
Ultra-high purity	UHP
Ultra-pure	UP
Weak Iron binding ligand	L2

1 Introduction

Iron is the fourth most abundant element in Earth's crust after oxygen, silicon and aluminium. Today, iron forms 5% by mass of the crust and the rest is accumulated in the core over the history of evolution and differentiation. Iron plays a vital role in many biological and chemical processes both in eukaryotes and prokaryotes (Taylor and Konhauser, 2011). Despite the high concentrations of iron on the Earth's crust, there is an iron limitation in ocean waters. Before the oceans became oxygenic about 1 billion years ago, the anoxic oceans had a vast concentration of ferrous iron, Fe(II) which is known to be the most bioavailable form of Fe. *Cyanobacteria*, the oldest known photosynthetic organism, could easily acquire Fe(II) as a nutrient due to its high solubility in anoxic conditions. The largest biogeochemical change in the oceans occurred when *Cyanobacteria* grew rapidly, producing a gross amount of oxygen which had resulted in oxygenation of the oceans. In new oxic conditions, the Fe(II) is very unstable and on a time scale of few hours it is oxidised to its ferric Fe(III) form, which then precipitates as ferric hydroxides known as rust, a very important paleoceanographic mark. (Figure 1-1). Because Fe(III) has a significantly low solubility in water, today's ocean is poor in iron compared to the palaeo-ocean and phytoplankton growth is under stress due to iron limitation (Sakshaug et al., 2009).

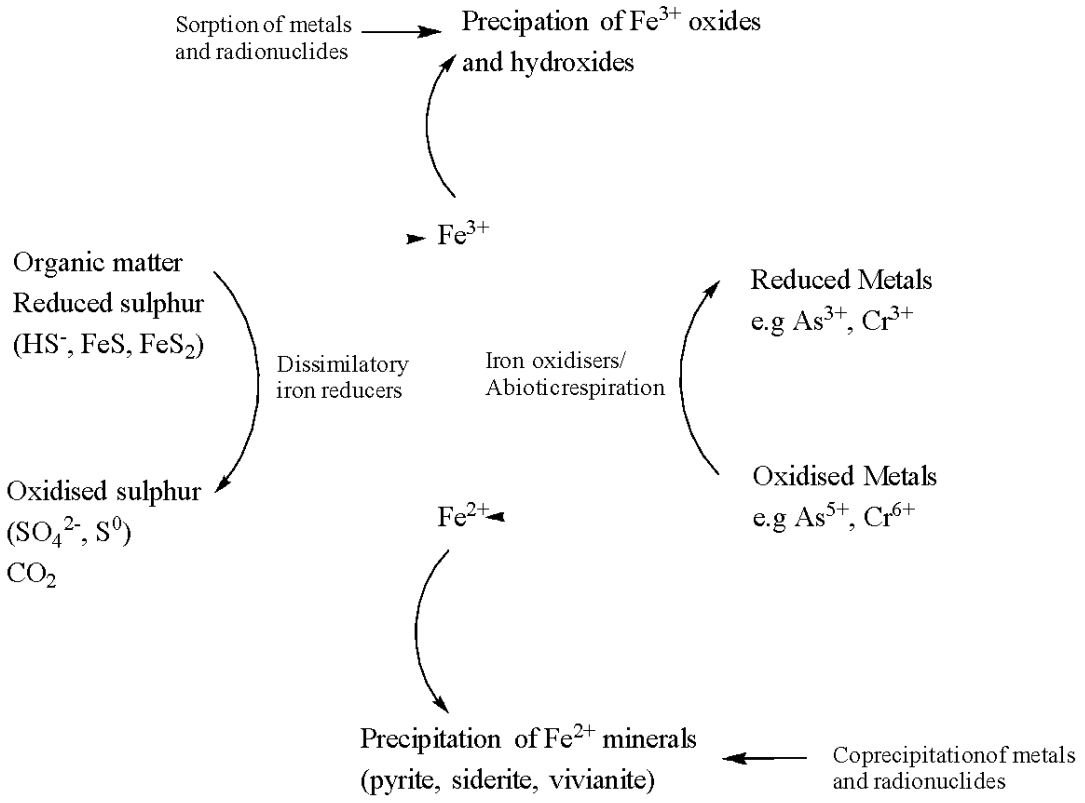

Figure 1-1 Iron redox cycle and interactions with other elements. (Taylor and Konhauser, 2011)

The importance of iron in the environment and biological systems was brought to the surface by John Martin and his work on phytoplankton's and their involvement in the carbon cycle which lead to the well-known "iron hypothesis" (Martin, 1990). His studies included High nutrient, low chlorophyll (HNLC) zones in the sub-arctic North Pacific, equatorial Pacific and the Antarctic Ocean. Despite the high levels of nutrients in those regions, phytoplankton population was significantly low. According to Martin, iron is an essential micronutrient for the reproduction of phytoplankton and his measurements indeed showed very low iron concentrations or no iron in those HNLC regions confirming his hypothesis (Weier, 2001). Therefore, it is very important to understand the iron acquisition mechanisms in order to come up with solutions for iron limitation in the world's oceans.

Iron acquisition in microorganisms such as *Cyanobacteria* can take place via several mechanisms, depending on the species (Rudolf et al., 2015). Iron uptake in *Synechococcus* sp. PCC 7002 is still being researched and a pili mediated reductive mechanism is suggested. Pili structures are hair-like appendages found on the surface of bacteria and they are associated with iron acquisition. The electrically conductive pili is able to reduce extracellular particulate bound Fe(III) into Fe(II) for cellular uptake (Årstøl, 2017).

Additionally, iron acquisition also depends on the mineral form of iron within the aquatic environment as well as other factors influencing the speciation such as redox processes, etc. (Rudolf et al., 2015). Hence, the aim of this project was to study the efficiency of the pili mediated iron reduction mechanism in a *Cyanobacteria* species of *Synechococcus* sp. PCC 7002, by manipulating the type of iron mineral and speciation under controlled conditions. The hypothesis and objectives of this project is mentioned in the following section.

2 Hypothesis and Objectives

Hypothesis

The efficiency of iron acquisition in *Synechococcus* sp. PCC 7002 via reduction of iron mineral using the electron flux in the pili structure may depend on mineral forms (speciation of particulate iron).

Objectives

- To determine the cellular iron quota/concentration of a *Cyanobacteria* species, *Synechococcus* sp. PCC 7002 in the culture medium and follow the concentrations of Fe(II) and Fe(III) which will be carried out by another MS student, using FIA-CL and HR-ICP-MS after pre-concentrating with SeaFAST, respectively.
- To estimate the iron acquisition efficiency by *Synechococcus* sp. PCC 7002 in the culture for different Fe mineral forms.

3 Background and Theory

3.1 Sources of iron

As briefly mentioned in the introduction, iron is an essential element for many natural processes and its availability is restricted in the oceans due to rapidly oxidised Fe(II) into the less soluble Fe(III) form. Dissolved Fe (DFe) is required for photosynthetic processes and growth of phytoplankton that will be explained in detail in the following chapters. The availability of DFe is controlled by several processes such as chelation with organic ligands which increases the solubility of Fe and it has been known that approximately all of the DFe in the oceans are bound to natural ligands (Benner, 2011). This chelation process is affected by the physical and chemical properties of the sea water including the pH, salinity and temperature. The DFe concentration also depends on the sources of Fe, mechanisms that keep Fe in the solution and processes which convert DFe into its particulate (PFe) form such as; scavenging, precipitation, and uptake by phytoplankton. (Gerringa et al., 2012)

Fe is transferred into the oceans via several modes of supply which determines the concentration of Fe entering to the seawater. Aeolian iron deposition has been recognised as the major iron supply to the world's oceans (Boyd et al., 2010). Aeolian iron is the iron that is deposited from atmospheric dust and is described as a three-phase system consisting of; air, sea and the interphase between them. Figure 3-1 summarises the entrance mechanism of aeolian iron which is shown by dry deposition of dissolved and wet deposition of soluble iron. On the surface of the Monolayer, organic compounds with hydrophilic and hydrophobic properties are found which provide coating for the entering wet and dry deposition. When reaching to the surface microlayer (SML) consisting of many organic compounds, competitive ligand exchange can take place. In this SML zone, ligand complexation controls iron solubility and bioavailability of dissolved and soluble iron due to the interactions between the wet and dry deposition with ligands. The iron then moves towards to the Euphotic zone in the form of dissolved, ligand bound iron and particulate, dust bound iron. The aerosol dissolution process of dissolved, ligand bound iron is short term which can take up to minutes to hours whereas the particulate, dust bound iron requires longer term dissolution consisting of days to weeks, which both take place in Euphotic zone. The Euphotic zone is dominated by microorganisms which carry out biological uptake and release of dissolved and aerosol iron such as; phytoplankton, bacteria and zooplankton. Dissolved form is taken up by phytoplankton whereas the aerosol iron is further accessed via mechanism such as; grazer/particle interactions or photoreduction in the presence of siderophores released by the microorganisms. After spending a residence time of days to

months in this layer, aerosol iron leaves the Euphotic zone in the form of lithogenic particulate (un-modified) or biogenic particulate (modified) and enters to the Apotic zone via gravitational settling. The aerosol iron then can be reintroduced back to Euphotic zone by water mass movements (Boyd et al., 2010).

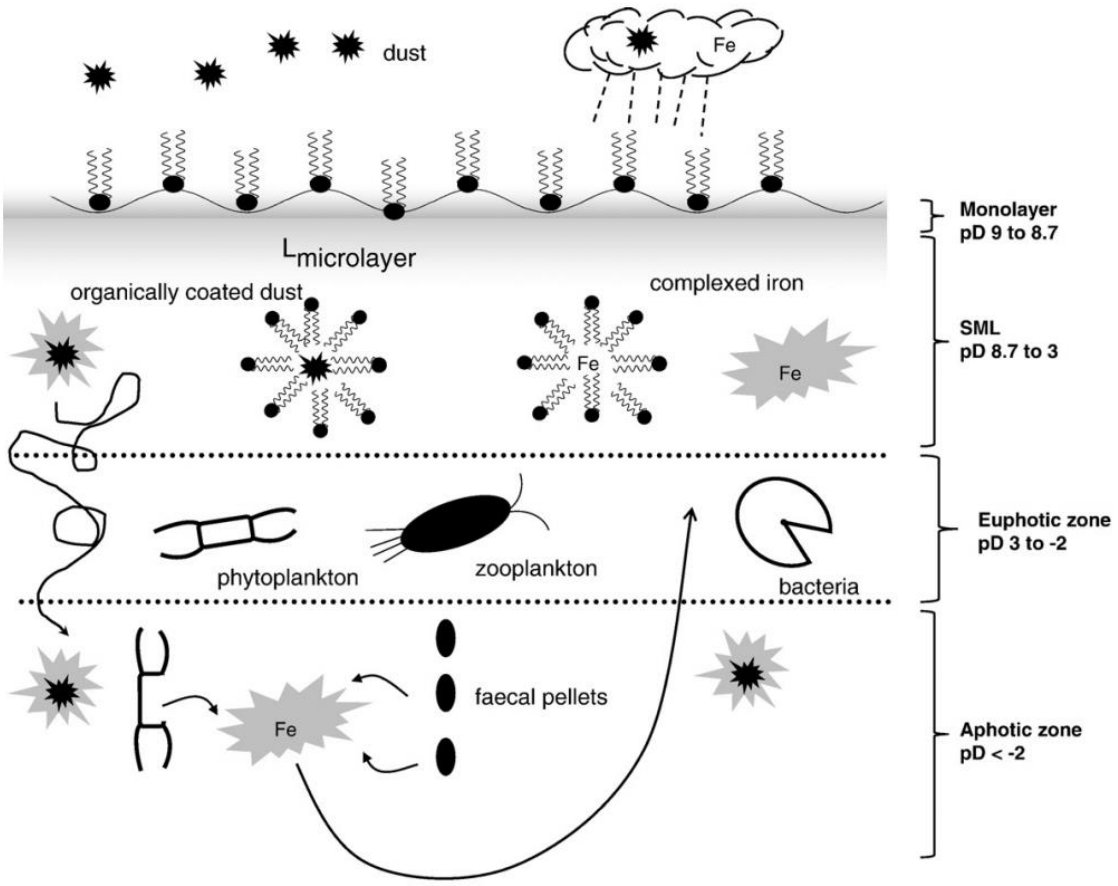

Figure 3-1 Aeolian iron supply into the ocean. Illustrates the supply of aeolian iron from its entrance to the ocean to its biological uptake by microorganisms. In this scheme, the upper ocean is divided into four sections; Monolayer, Surface microlayer (SML), Euphotic zone and Aphotic zone, corresponding to depth which is shown in pD (=negative log of depth in m) that is analogous to pH. (Boyd et al., 2010)

In addition to the aerosol iron, melting sea-ice has been identified as a Fe reservoir with several studies reporting Fe enrichment in oceans due to Fe being released from melting sea-ice during spring-time which brings light availability and surface-water stratification, resulting in phytoplankton blooms. Iron accumulates in sea-ice via external sources entering to the surface ocean such as; dust, rivers, glacial flow, hydrothermal vents, continental shelves, glaciers, icebergs and ice shelves. (Lannuzel et al., 2016)

Melting sea-ice results in rapid release of Fe and it is considered as a "pulsed source" where the supply of Fe to the surface water is sudden and occurs over a short period of time, i.e. spring

and summer. The sea-ice has shown to contain a significant amount of PFe (20.6 μmol m^{-2}) and when PFe enters the seawater, it can remain in suspension, be mineralised by microorganisms such as bacteria or zooplankton or can be transferred to the sea floor (Lannuzel et al., 2016). In addition to PFe, it has been found that Antarctic sea ice stores 4.7 μmol m^{-2} of DFe. When DFe enters the seawater, it can either be taken up by phytoplankton or scavenged into particles by other microorganisms.(Lannuzel et al., 2016).

Volcanoes which are rich in variety of minerals are also known sources of Fe. As a result of volcanic eruptions, the volcanic ash which can be transported up to several tens of kilometres high into the atmosphere, releases soluble and bioavailable iron in contact with water. The supply of iron is quick and the ash can reach even the remotest and most iron limited oceans (Breitbarth et al., 2010). Horizontal advection of water from South of the Plateau has also been described as a source of PFe and DFe. Where Fe is brought via horizontal advection from coastal interface to above the plateau. Additionally, the continental margins have been reported to play a key role as a Fe source (Breitbarth et al., 2010). As described by Lam and Bishop (2008), in HNLC North Pacific Ocean, the subsurface supply of Fe from continental margin is shallow enough that the phytoplankton is able to access Fe through winter upwelling and vertical mixing. This mechanism is thought to be a potential key source of bioavailable Fe to the HNLC North Pacific (Lamb et al., 2014). The following chapter will explain in detail how Fe behaves in the oceans after entering to the seawater via aforementioned modes of supply.

3.2 Iron in the oceans

3.2.1 Biogeochemistry and speciation of iron in the oceans

Chemical speciation including organic complexation and redox speciation is an important factor which determines the solubility and bioavailability of Fe. For example, as previously mentioned, the solubility of DFe is enhanced via strong organic ligand complexation. Ligand complexation can be explained by looking at two classes of iron-binding ligands which are differentiated with respect to their different binding affinities to iron. The strong iron binding ligands are known as L1 which are dominant on the upper ocean whereas, the weak binding ligands, L2 are observed throughout the water column (Boyd and Ellwood, 2010). The presence of these ligands in the ocean and their interactions affect the biogeochemistry of iron. As previously mentioned, biological activity is observed in the mixed layer of the ocean where uptake of bioavailable iron takes place via microorganisms such as *Cynaobacteria*. Since L1 class ligands are associated with siderophores, the highest concentration of L1 will be on this

layer accordingly. The movement of these ligands will be from the mixed layer towards deep ocean via vertical water exchange processes such as; advection, diffusion and down-welling which are dependent on the time of the year. The L2 ligand class on the other hand, is concentrated in the subsurface ocean where sinking particles decompose, and release chemicals associated with L2. The iron bound to L2 will be transported to the mixed layer in a similar fashion as L1 bound iron, instead via upwelling, vertical advection and diffusion. (Hunter and Boyd, 2007)

Iron exists in two oxidation states, reduced ferrous Fe(II) and oxidised ferric Fe(III), each having different chemical characteristics. When looking at kinetics of iron in seawater, it is known that Fe(III) is thermodynamically favorable redox form of Fe which has significantly low solubility as already established. The ferrous Fe(II) form is described as transient species existing in oxic waters that are mainly resulting from photochemical reactions which will be described later in the text. This soluble form of Fe is found in oceans in very low concentrations due to rapid oxidation by O_2 and H_2O_2 species in warm surface waters. When oxidised to Fe(III), colloidal oxyhydroxide species form which then coagulate resulting in the formation of particulate iron. DFe is strongly complexed with the aforementioned L1 class ligands and relevant colloidal material which makes it soluble. Iron solubility becomes significantly low (<80 pM) in the absence of these ligands. Dust deposition being one of the major supplies of iron, influences the thermodynamic equilibrium of iron species (soluble, particulate, colloidal) in the euphotic layer of the ocean. Another factor altering the speciation on the euphotic zone, is the sun which results in formation of transient Fe(II) species via photochemical processes. It has been established that the iron uptake by phytoplankton is controlled kinetically rather than thermodynamically and kinetics of exchange between the iron species is being used to study the biogeochemical iron cycle in the ocean. When studying kinetics of Fe in seawater, the rate of water exchange or loss for the inner coordination sphere of Fe is considered to be a key controlling factor represented as k_{ex}. In seawater, the inorganic speciation of Fe(III) is mainly consisting of hydroxide complexes and the rate of water exchange for the sum of inorganic Fe(III) species (F') was measured to be $k_{ex} = 8\times10^6\ M^{-1}s^{-1}$. The individual measurements of Fe(III) hydroxy species are as follows; Fe^{3+} $1.6\times10^2 M^{-1}s^{-1}$ and $Fe(OH)^{2+}$ $1.2\times10^5 M^{-1}s^{-1}$, $Fe(OH)^{+}_{2} > 10^7\ M^{-1}s^{-1}$ and $Fe(OH)^{-}_{4} > 10^9\ M^{-1}s^{-1}$. Whereas, the rate of water exchange for Fe(II) is found to be $k_{ex} \sim 1 \times 10^7\ M^{-1}s^{-1}$ which is much faster than the Fe(III) 's water exchange rate. (Croot and Heller, 2012)

Solubility of Fe is a major factor which controls the biological uptake of iron (bioavailability) by phytoplankton, the more soluble Fe is and the easier it would be taken up by phytoplankton.

The capacity of seawater for soluble Fe (cFe_s) and the stability of soluble Fe species in the ocean is highly affected by chemical and physical conditions such as; above mentioned organic ligand concentrations, temperature and pH. As mentioned in previous sections, in seawater, iron exists in different size fractions and chemical forms such as particulate (PFe; > 0.2 μm) and dissolved iron (DFe; < 0.2 μm). The DFe is further catagorised into soluble (FeS; < 0.02 μm) and colloidal (FeC; 0.02–0.2 μm) size fractions, existing in organic ligand bound or inorganic complexed species. It has been established that 99% of DFe found in the ocean is ligand bound as discussed above. The concentration of dissolved ligands in the oceans has found to be in excess (0.5–6 nmol L^{-1}) compared to the DFe concentrations (ca. 0.02–0.5 nmol L^{-1}) creating availability for incoming Fe flux. (Schlosser et al., 2012)

As emphasised previously, DFe or soluble iron is vital for phytoplankton health and growth however, due to low solubility of Fe in oxygenated waters, the majority of Fe exists in nanoparticle (< 0.2 mm), biogenic and lithogenic colloid (> 0.2 mm) forms. And this particulate-bound Fe forms 65-85 % of the total dissolvable Fe fraction in the mixed layer of the Southern Ocean, making PFe an important source of Fe for the photosynthetic organisms. Studies have found that, there is a strong link between biological availability of PFe and its solubility which is influenced by factors such as; differences in Fe oxidation state, mineralogy, crystallinity, structural impurities, structure and concentration of dissolved organic ligands. For example, as mentioned before, F(II) is more soluble than Fe(III) and it is also stated that amorphous (non-crystalline) phases of PFe are more soluble than morphous minerals. Structural impurities such as association of aluminium in Fe(III) oxides have been found to be less soluble. Alongside these factors, the heterogeneity in the surface chemistry of different Fe particles in water column would influence the availability of PFe to microorganisms via scavenging. Additionally, availability of other essential trace elements such as Cu and Zn that are strongly associated with Fe particle surfaces, would also be influenced in the same manner (von der Heyden et al., 2012).

However it is important to note that in addition to chemical and physical factors, phytoplankton physiology and their acquisition mechanisms influence the bioavailability of iron. Different pathways of iron uptake will be discussed in the latter part of this text. (Lis et al., 2014)

3.2.2 Oceanic iron cycling

Ocean primary production is tremendously important for sustaining a well-balanced and functioning Earth System. The biogeochemical processes such as the carbon cycle and air–sea CO_2 exchange, are some of the drivers of this system. It has been established that iron is a key

micronutrient influencing the dynamics and the magnitude of these processes in the global ocean. When looking at iron cycle in the ocean, it is important to consider the interaction of iron with the main processes involved in the ocean, such as the cycling of carbon, ocean circulation as well as its interactions with other nutrients, metals and organisms (Tagliabue et al., 2017). This section will go through the oceanic iron cycling looking at the big picture, considering the iron cycling as a wholistic mechanism, focusing on the Atlantic Ocean.

This paragraph will discuss the processes involving iron in the high latitude Southern Ocean and low latitude regimes. As previously mentioned dust is a major source of iron and in the following illustration (Figure 3-2) aeolian dust is shown to be the major source of iron supply to the low latitude ocean. However, in high latitude Southern Ocean which is described as iron-limited, melting of sea-ice glaciers is shown as a greater input of iron than aeolian dust input. It is also important to note that, in the Southern Ocean, continental margin and upwelled hydrothermal sources of iron are more significant compared to the low latitude ocean regions. In low latitude regimes where dust remains dominant, limitation of major nutrients such nitrogen and phosphorus is observed, interactions between iron and the major nutrients will be discussed in the following paragraph. In mixed layer of the Southern Ocean, flexible iron uptake and biological/chemical cycling are carried out by organisms such as phytoplankton, zooplankton and bacteria. Previously mentioned ligands that are produced by these organisms in the process of iron uptake are released in excess into the ocean where they form complexes with iron. Due to iron limitation in high latitude areas, the iron depleted organisms release these ligands in excess, as a stress mechanism with exhaustion of dissolved iron stocks. The excess iron binding ligands then can be subducted and transported following an equatorward flow. This biological activity is fueled by the iron supplied via upwelling and mixing into the surface water and is maintained by iron recycling processes carried out by zooplankton and bacteria. As previously mentioned, iron regenerated from sinking organic matter is decoupled to major nutrients (phosphorus in Figure 3-2), this is because of the longer effective remineralisation length scales which result in more efficient iron export to the ocean interior than for major nutrients.

In the areas with nutrient limitation, iron supplied from dust is released and scavenged to be used as a nutrient for organism that carry out nitrogen fixation in order to overcome nitrogen limitation. The importance of iron is observable in low latitude regimes where dust supply is low and upwelling is absent, the rate of nitrogen fixation slows down respectively due to stress caused by lack of available iron for nitrogen fixing organisms. In such cases where there is not enough iron, processes such as scavenging help to release iron from dust in the form of

lithogenic and organic particles to the seawater to be used by nitrogen fixers. The balance between local regeneration of iron from scavenging and sinking organic material influences the subsurface iron at low latitudes. As mentioned with high latitude areas, this subsurface iron can also be remotely controlled by subduction and equatorward transport of high-latitude waters carrying excess ligands since scavenging rates concern the concentration of iron that is not organically complexed. (Tagliabue et al., 2017)

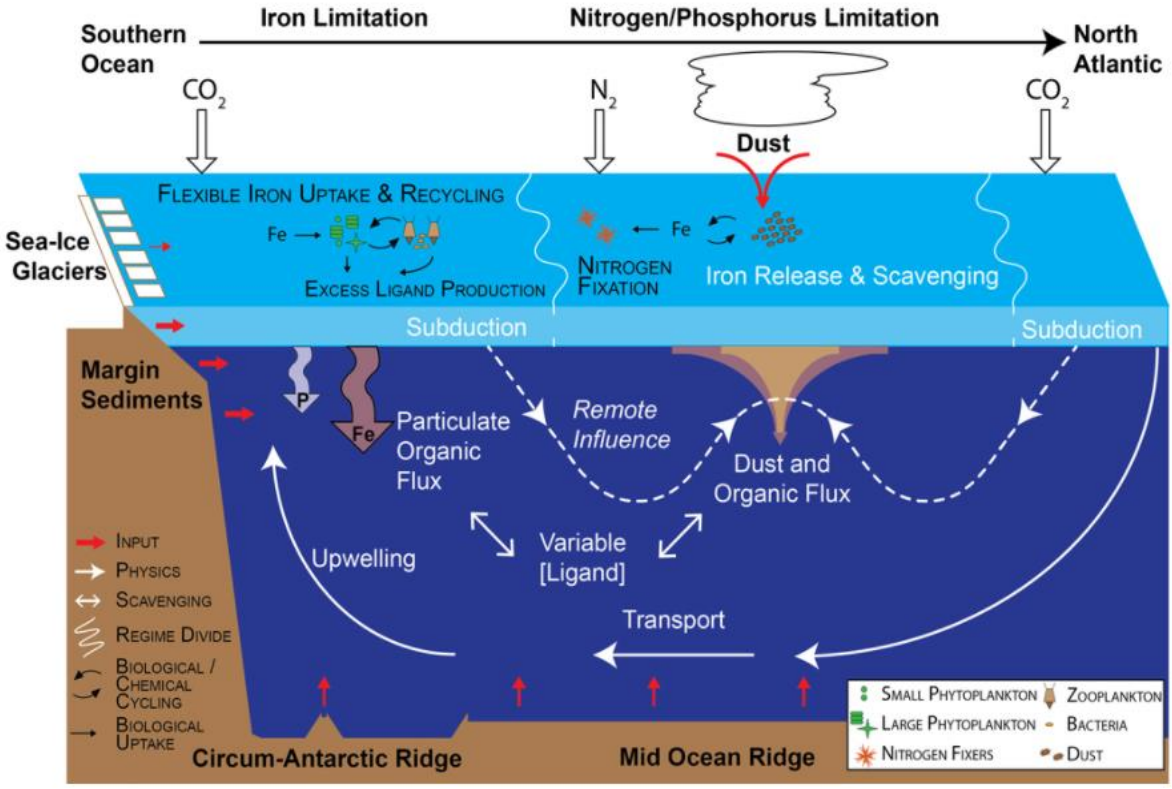

Figure 3-2 Oceanic iron cycle in Atlantic Ocean. This figure takes into consideration the major biogeochemical processes as well as release, transport and uptake mechanisms involved in the iron cycle. Processes such as flexible iron uptake, biological cycling and release of excess iron binding ligands are dominant in the iron-limited Southern Ocean to increase the availability of iron. In the low latitudes, where nitrogen fixation occurs, dust is the major source of iron, specifically, as the flux of lithogenic material. In higher latitudes, the particulate organic iron flux is decoupled from that of another important nutrient, phosphorus. Excess organic ligands are removed from the Southern Ocean which has an insignificant influence on the interior ocean at low latitudes. (Geotraces, 2010)

3.3 Iron as a nutrient

As aforementioned, interactions between iron and the major nutrients is observed in the oceanic iron cycle and iron metabolism in phytoplankton as well as diatoms has shown intersections with macronutrients. The studies done on the interactions with iron and nitrogen has shown that nitrogen source highly influences the iron requirements of phytoplankton as mentioned with the nitrogen fixing organisms. This is due to the phytoplankton's ability to incorporate nitrogen

species into amino acids. For instance, ammonia (NH^+_4) can be directly taken up whereas, nitrate (NO_3) and nitrogen (N_2) need to be reduced to ammonia before they can be processed by the organism. This process is known as nitrogen fixation where the nitrogen fixing organisms break the triple bonds holding N_2 very strongly, converting it to bioavailable NH^+_4. To carry out such energy consuming reaction, the organism requires a considerable amount of nutrients including iron. Hence, phytoplankton species that can process ammonia directly require less iron compared to others that grow on nitrate or those which carry out nitrogen fixation. (Schoffman et al., 2016)

Iron is an important nutrient which is required for biological and chemical processes in phytoplankton physiology, more specifically for nitrate assimilation. Nitrate assimilation involves the NO^-_3 reducing enzymes known as nitrate and nitrite reductase which have Fe cofactors that makes iron essential for guiding this chemical process. Additionally, the NO^-_3 reduction's reducing power is supplied by the photosynthetic electron transport chain. Studies done over the years have shown that iron addition to waters from the Equatorial Pacific and North Pacific Ocean results in increased NO^-_3 uptake rates by phytoplankton. Hence, it could be suggested that there is a correlation between limited iron availability and lowered nitrate uptake in natural waters. (Schoffman et al., 2016)

In the absence of iron, the nitrate and nitrite reductase enzyme activity decreases in eukaryotic phytoplankton due to the cells having limited availability to iron. Research done on *Phaeodactylum* diatoms had shown that under Fe-limited conditions there is a reduced nitrate uptake capacity due to down regulation of genes concerning nitrate assimilation as well as decreased functioning of the reductase enzymes. Interestingly, the outcome of this study suggested that the diatom had sufficient amounts cellular nitrogen despite the low enzyme activity and there was no increase in carbon to nitrogen ratios which is a sing of stress induced by nitrogen limitation. Hence, the role of iron in nitrate reducing enzymes seems insignificant. However, it has been found that iron limitation affects nitrate acquisition via photosynthetic electron transport. When the intracellular iron concentration is low, nitrate uptake by phytoplankton becomes less efficient under Fe-limited environments. The energy required for the reductive process of NO^-_3 assimilation is constrained by lack of iron which results from decrease in the photosynthetic activity. Additionally, the cultures grown on NO_3 show more light dependency than the ones grown on NH_4 in Fe-limited conditions. As with iron, light also plays an important role in photosynthetic processes and low levels of light also results in decreased nitrate assimilation rates in cells. Therefore, the influence of Fe-limitation on nitrate

acquisition is enhanced by the low light which is important to consider in low iron, high latitude natural waters. (Schoffman et al., 2016)

As previously mentioned, organisms carrying out nitrogen fixation require additional Fe for carrying out chemical processes involved in nitrogen fixation alongside their routine cellular uptake. The extra energy consumption is due to the N_2 fixing enzyme, nitrogenase which contains 38 Fe atom per holoenzyme. Nitrogenase has relatively slow reaction rates which means that the organism requires a large intracellular concentration of this enzyme. Nitrogenase is also irreversibly inhibited by molecular oxygen and nitrogen fixation requires a considerable amount of energy produced by photosynthetic reactions and reducing power. N_2 fixation is highly influenced by the size and surface area of an organism which determines how much iron is required for normal cellular functions as well as the concentration of iron that is available to the organism in its surroundings. For example, the heterocystous *Cyanobacteria Anabaena* are found in fresh, brackish and coastal waters where the iron concentration is high and are able to perform advanced iron acquisition due to their filamentous nature and large size. Filamentous *Cyanobacteria* such as *Anabaena* produce specialized heterocyst cells which can carry out nitrogen fixation in anaerobic conditions. Despite living in Fe rich environments, their large size hence additional iron requirements, make them prone to iron limitation in natural and laboratory conditions. In contrast, a smaller unicellular diazotroph, *Cyanothece* can survive in opens ocean waters where the Fe concentration is fairly low. This is due to their large surface area to volume ratio and ability to recycle Fe between photosynthetic apparatus during the day and nitrogen during the night which creates a cost-efficient diurnal separation of N_2 from photosynthesis. Another example is the non-heterocystous *Trichodesmium* living in iron limited open oceans despite its high cellular iron demand. This organism is capable of using Fe efficiently, so it can survive in low Fe concentrations by symbiotic association with bacteria, helping in iron acquisition and having the ability to access colloidal and particulate iron sources. (Schoffman et al., 2016)

It has been also suggested that iron together with phosphorus may limit nitrogen fixation. In regions with nitrogen limitation, co-limitation of phosphorus by microorganisms can also be observed where dissolved inorganic phosphorus (DIP) concentration declines due to diazotrophic N_2 fixation. In a situation as such, phosphate limited organisms access dissolved organic phosphorus (DOP) via enzymes known as alkaline phosphatase (APase) enzymes and supply additional DIP required for cell growth. In surface ocean waters, the DOP pool is larger than that of DIP and access to this pool is regulated by the phosphate monoesterases; PhoA, PhoX and PhoD families which are important contributors of phosphorus for primary

production. These phosphatases are activated by metal cofactors; two zinc (Zn) and one magnesium (Mg) ions for PhoA, three calcium (Ca) ions for PhoX and an unknown number of Ca ions for PhoD. Alongside the mentioned metal cofactors, it has been found that PhoX and PhoD phosphatases require additional Fe, two and one iron ions per enzyme, respectively. PhoX and PhoD are the dominating bacterial alkaline phosphatases hence, iron limitation in oceans could possibly influence microbial P acquisition by lowering the enzyme activity. (Browning et al., 2017)

The Fe dependence of PhoX and PhoD possibly comes from the APases which had evolved in Fe rich oceans that were also lacking Zn. It is also predicted that in the past, microbial communities had faced P stress due to elevated N_2 fixation which had resulted in depletion of excess DIP. As mentioned in above paragraph, in order to compensate for the depletion of DIP, microorganisms require additional Fe to access DOP. Followed by these assumptions, it can be hypothesised that, a strong dependence on APases would be present in iron rich waters which in turn would decrease the pressure on Fe- dependant PhoX and PhoD (Browning et al., 2017). The importance of Fe in nutrient cycles can be seen from the aforemnetioned examples of nitrogen and phosphorus however, interactions with Fe is a complex concept that requires more in-depth studies.

3.3.1 Iron limitation and fertilization

In this section, interaction of iron with the carbon cycle and CO_2 exchange will be discussed in the context of iron limitation and fertilization. According to John Martin's iron hypothesis, the geochemical cycle of iron in the oceans has an impact on primary productivity, hence, on atmospheric CO_2 concentrations (Martin, 1990). In his paper, glacial/interglacial CO_2 concentration change from 200 to 280ppm is hypothesized to be correlated to the variations in phytoplankton blooms in iron limited Southern Ocean. Iron deficient phytoplankton cannot consume the excess nutrients (nitrogen and phosphate), available on the surface ocean, decreasing primary productivity. This 80ppm change in the concentration of CO_2 brought about 170 Gt (gigatons) of C to the Earth's atmosphere causing a lot of changes in the global oceans. The ocean contains about 60 times more CO_2 than the atmosphere hence, oceanic processes have been thought to be the main reason behind these changes. As previously mentioned, in normal conditions, when the biological pump functions efficiently, CO_2 from atmosphere is removed by photosynthetic uptake via phytoplankton and transferred into deep ocean when the phytoplankton remains sink down from the surface ocean. This removal process results in lowered concentrations of CO_2 in the atmosphere and when the biological pump is not working

efficiently, CO_2 from the atmosphere cannot be removed resulting in increased CO_2 concentrations. The variation of CO_2 levels has also been explained by factors such as; phosphate extraction, denitrification, coral reef buildup, and/or changes in ratios of C:P and/or the organic/inorganic C ratio. Further models include assumptions that high-latitude circulation and/or productivity may be resulting in fluctuating CO_2 levels or even variations in polar surface water alkalinity may cause changes in CO_2 concentrations. (Martin, 1990)

However, according to Martin's iron hypothesis, if the excess nitrogen and phosphorus on surface ocean were able to be taken up by phytoplankton in iron limited Southern Ocean, a very large amount of C (2-3 Gt yr^{-1}) would be produced. Limited new productivity due to iron deficiency had resulted in high Holocene interglacial CO_2 levels (preindustrial) which is almost similar to the last interglacial CO_2 levels of 280ppm. Additionally, during the last glacial maximum, the aeolian Fe supply was 50 times higher resulting in iron enchainment of the oceans which in return might have led to increased primary productivity, enhanced phytoplankton growth, and increased withdrawal of atmospheric CO_2, respectively. Hence, the CO_2 concentrations were less than 200ppm during glacial period due to excess iron present in the waters. (Martin, 1990)

In case of iron limitation, various physiological responses of phytoplankton to adapt to this unfavorable condition is observed. Iron is an essential element for phytoplankton due to enzymes and proteins carrying out physiological processes involving iron either as a coenzyme as previously mentioned with N_2 fixation, or regulator for photosynthetic and respiratory election transport. Iron is also directly involved in reactions regarding chlorophyll synthesis and numerous biosynthetic or degradative reactions. Some of these reactions include oxygen cycling where iron functions as a component of the enzymes; catalase, peroxidase and some superoxide dismutases. The tricarboxylic cycle is also one of the processes that involves iron that is incorporated with the aconitase enzyme which carries out catalysis of the isomerisation of citrate to isocitrate. Another protein involving iron is ferrodoxin which is an iron-sulfur protein that acts as an electron donor for chemical reactions such as; SO_4 reduction, NO_3 reduction and N_2 fixation. Catalyst which regulate enzyme activity that contain iron also have important roles in cellular metabolism. As mentioned ferredoxin acting as an electron donor, donates electrons to thioredoxin, providing reductant to enzymes which in turn activate various chloroplast enzymes. It has been agreed by many scientists that decrease in chlorosis, the photosynthetic pigment is closely related with iron limitation. When there iron is not available for phytoplankton uptake, the above mentioned processes that are vital for survival are affected

adversely (Geider and La Roche, 1994). The physiological responses of *Cyanobacteria* to iron limitation will be discussed in detail in following sections.

Followed by John Martin's iron hypothesis, it is assumed that if iron deficiency is resulting in decreased phytoplankton bloom and primary productive, then adding iron into the ocean artificially would overcome this problem by enhancing phytoplankton growth which will in turn result in increased CO_2 sequestration. This artificial addition of iron into the oceans is called iron fertilisation which aims to increase primary production hence to increase CO_2 sequestration. This process alongside with phytoplankton bloom being grazed and excreted by microzooplankton as fecal pellets would facilitate CO_2 fixation (Singh et al., 2015). Many iron fertilization experiments are being done in the hope enhancing the removal of CO_2 from the atmosphere in today's increasing global CO_2 concentrations.

3.4 Phytoplankton in the ocean

Phytoplankton are microorganisms living in both salty and fresh waters. Phytoplankton can be species of bacteria, protists, and single-celled plants and some common types of these species include; *Cyanobacteria*, diatoms, dinoflagellates, green algae, and coccolithophores. These photosynthetic organisms contain chlorophyll pigments which capture sunlight to produce chemical energy, and as with other plants, phytoplankton consume CO_2 and release oxygen during this process. Some phytoplankton species that carry out photosynthesis also get additional energy from feeding on other organisms. (Lindsey and Scott, 2010)

Therefore, the growth of phytoplankton depends on CO_2, sunlight as well as nutrients that is available to the organism. Major nutrients required by phytoplankton are as mentioned in detail in previous chapters are; nitrate, phosphate, silicate and calcium depending on the species. The ability of some phytoplankton to fix nitrogen in low nitrate concentration is also discussed in previous chapters. Additional to abovementioned, phytoplankton requires iron as a macronutrient and low iron concentrations can limit phytoplankton growth. (Lindsey and Scott, 2010)

These organisms are important for the global ecosystem due to their role in climate and carbon cycle. Phytoplankton consume a very high amount of atmospheric CO_2 via photosynthesis, carrying some of the carbon to deep see when they die and some of the carbon is carried to different layers in the ocean when it is consumed by other organisms and these organisms complete the cycle by reproducing generating waste and eventually dying. As previously mentioned, via this biological carbon pump, atmospheric CO_2 concentrations are regulated in normal conditions. (Speer)

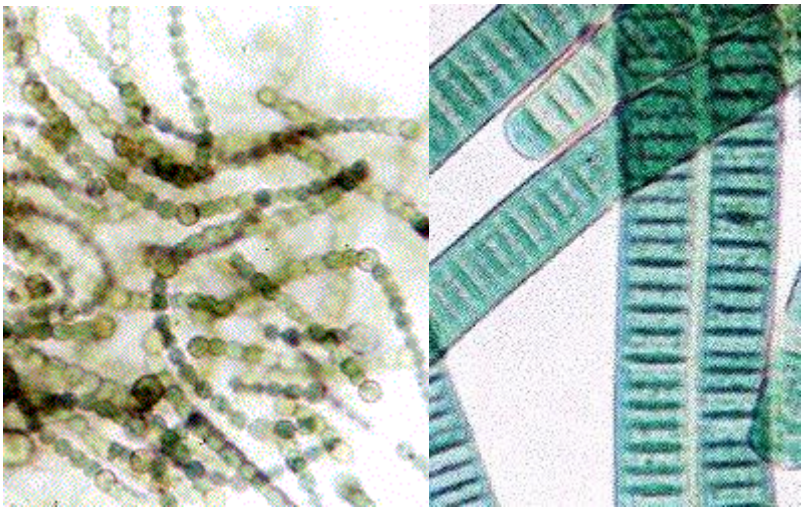

Figure 3-3 Cyanobacteria. Oldest photosynthetic organism which is a specie that is more than 3.5 billion years old. On the left is Nostoc and on the right is Oscillatoria. (Speer)

Cyanobacteria is known to be one of the most important phylum of bacteria involved in primary productivity on Earth. Their role in the supply of global oxygen, CO_2 sequestration and nitrogen fixation makes them an essential community of the ecosystem. These organism have various morphological forms and three of these forms are well known; unicellular, filamentous forms without heterocysts, and heterocystous filamentous forms with nitrogen fixing abilities in low nitrate conditions. As *Cyanobacteria* are also photoautotrophic, they use light as an energy source to generate their carbon cellular material and as a result of this process they produce oxygen. Some species of *Cyanobacteria* can also grow without carrying out photosynthesis heterotrophically where they use organic compounds as a source of carbon. In major nutrient (phosphorus and nitrogen) rich conditions, *Cyanobacteria* facilitate cellular uptake and store these essential nutrients which is an evolutionary response developed over billions of years ago due to extreme environmental conditions present in the past. (Percival and Williams, 2014)

Today, *Cyanobacteria* are the only known prokaryotes that carry out photosynthesis and generate oxygen while doing so. In this study a genus of *Cyanobacteria, Synechococcus* sp. strain PCC 7002 was used to study the iron acquisition mechanism in *Cyanobacteria*. This organism is considered to be the most commonly occurring photo-oxygenic microorganism on Earth. *Synechococcus is* an important component of primary productivity, accounting for 25% of net oceanic primary production together with *Prochlorococcus* (Dvořák et al., 2014). One of the reasons this organism was used in this study was because it lives in such diverse habitats from arctic to tropical waters to freshwater, terrestrial and subaerial environments, it would live in laboratory conditions with minimum stress and easily adjust (Dvořák et al., 2014). More

specifically, *Synechococcus* sp. strain PCC 7002 was chosen to be used for its high tolerance to high-light irradiation and rapid growth rates. (Ludwig and Bryant, 2012)

3.5 Iron uptake mechanisms in *Cyanobacteria*

There are several mechanisms that *Cyanobacteria* use for iron acquisition and the following chapters will discuss these mechanisms in detail.

3.5.1 Siderophores

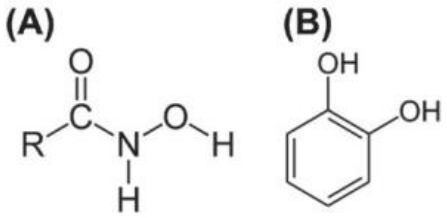

Figure 3-4 Building blocks of iron binding molecules. (Kranzler et al., 2013)

Siderophores are iron chelating compounds secreted by *Cyanobacteria* which have very strong binding affinities to Fe(III) and the building blocks of these molecules are shown in Figure 3-4. The production of siderophores are triggered under iron limiting conditions when the intracellular iron concentrations drops below the required threshold value for a functioning cell. Siderophores are divided into three main classes; the catecholates, the hydroxamates or mixed-types containing another iron complexing group such as α-hydroxy-carboxylate next to the hydroxamate or catecholate group. A specific siderophore is released depending on the chemical nature of organic ligand that is complexed to iron. When siderophore binds to Fe(III) the formed siderophore-iron complex called ferrisiderophore is transferred back into the host cell via specific acceptors found on the cell surface. (Kranzler et al., 2013)

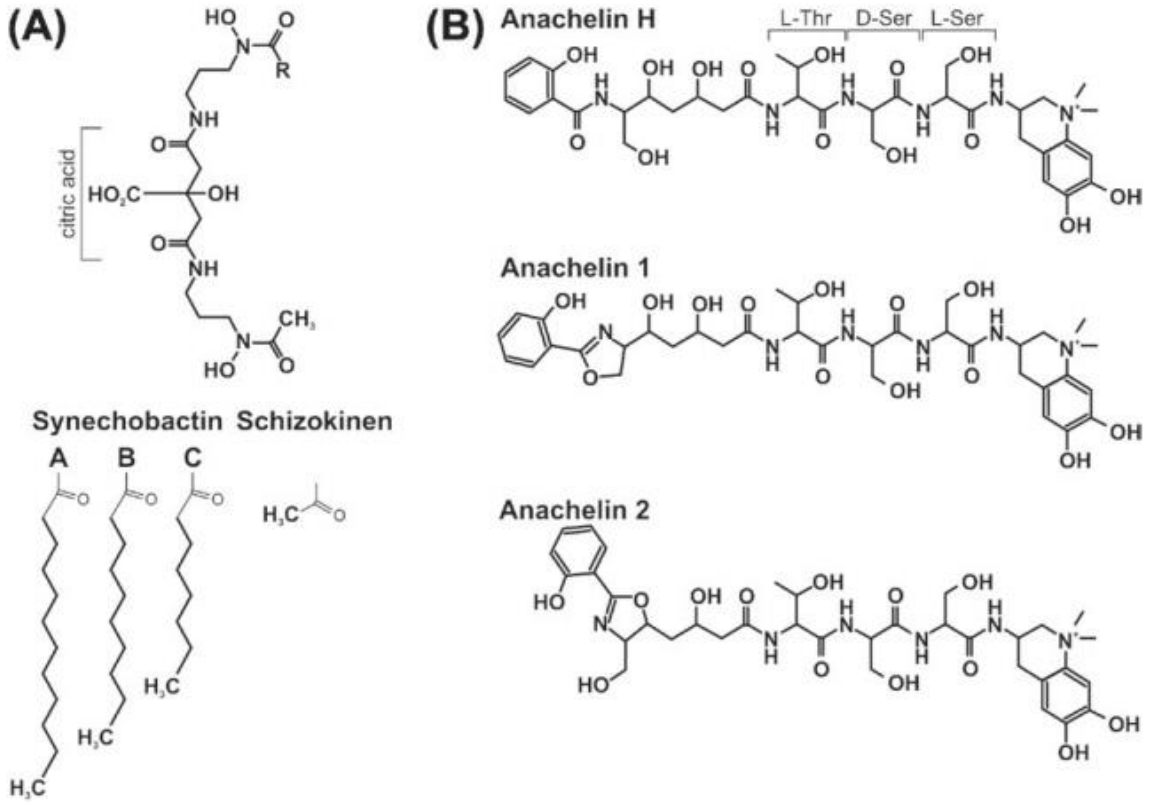

Figure 3-5 Siderophore structures. Figure showing hydroxamate-type siderophore schizokinen (A) and amphiphilic hydroxamate-type siderophores synechobactin (B). (Kranzler et al., 2013)

It has been also found that different *Cyanobacteria* species produce different siderophores. For example, the *Synechococcus* sp. strain PCC 7002 were found to be secreting hydroxamate-type siderophores which was then characterised as the amphiphilic hydroxamate-type siderophores synechobactin A–C. This compound is composed of a citric acid backbone and a fatty acid tail attached to the second α-hydroxamate group which may increase the binding affinity of the siderophore to the cell surface membrane Figure 3-5. Synechobactin on the other hand, is a photoreactive chelator that undergoes light-induced charge transfer reaction which in turn results in oxidative cleavage and two fragments; a hydrophilic peptide fragment and a fatty acid tail fragment. During this photochemical process, Fe(III) that is bound to the synechobactin ligand is reduced to Fe(II) for cellular uptake. (Kranzler et al., 2013)

3.5.2 Reductive iron uptake

Another Fe uptake mechanism suggested for many plants, yeast and eukaryotic algae is the reductive Fe uptake which involves the reduction of extracellular Fe(III) or Fe(III) chelates in the presence of a reductase enzyme on the plasma membrane. This way, the extracellular Fe(III) is reduced to Fe(II) before it is transported into the cell for an easier biological uptake (Kranzler

et al., 2013). A study done on reductive uptake mechanism of the marine cyanobacterium *Lyngbya majuscula* using a chemiluminescence system shows reduction of iron by superoxide. The reductive power of superoxide results in increased availability of Fe(II) and the production of this compound by *Lyngbya majuscula* is thought to be metabolically related and intentional. The role of superoxide in iron uptake is supported by the experiment where iron complexed with Ethylenediaminetetraacetic acid (EDTA) was introduced to the extracellular solution and with the addition of superoxide dismutase, Fe uptake by the organism was inhibited by 94%. This could suggest that superoxide does indeed play a role in iron acquisition in *Lyngbya majuscula.* Additionally, ferrozine, a ligand that forms a strong complex with Fe(II) was added to capture the Fe(II) produced as a result of the reduction process thus prevent its uptake. However, the iron uptake was not affected with the addition of 1 mM ferrozine which suggested that organically complexed Fe(II) may be directly transported into the cell. (Rose et al., 2005)
Figure 3-6 shows another example of reductive iron acquisition mechanism in Synechocystis PCC 6803. This organism is described as having no siderophore producing genes but has specific Fe transporters in its inner membrane which are identified as Fe(III) and Fe(II) transporters; FutABC and FeoB respectively. Fe is transported from the extracellular medium through the outer membrane in the form of organic/inorganic complexed and Fe(III) via TonB transport system which has specific substrate binding sites. Due to the short residence time of Fe(II) in oxic environments, iron reduction is carried out in the periplasmic space just before it is transported through plasma membrane. Some of the reduced Fe(II) is transported through plasma membrane via FeoB and some is oxidised back to Fe(III) which is then transported through plasma membrane via FutA2, FutB and FutC respectively. (Kranzler et al., 2013)

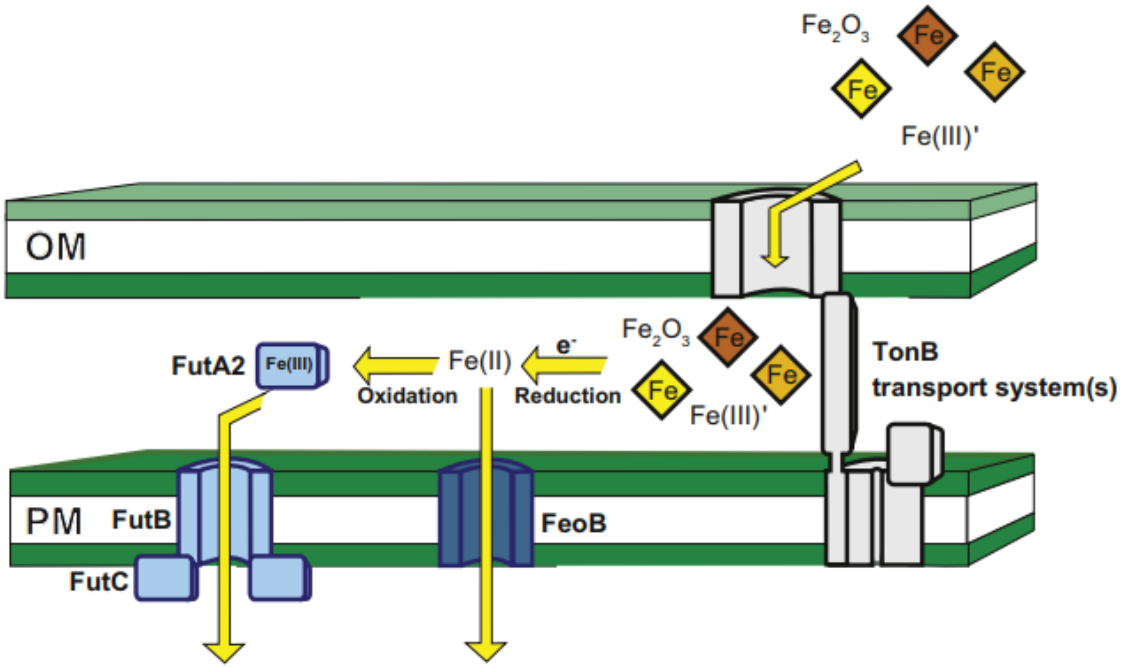

Figure 3-6 Reductive iron uptake in *Synechocystis* PCC 6803 species. (Kranzler et al., 2013)

Additionally, reductive siderophore uptake has also been observed in a nonphotosynthetic bacterium, *P. Aeruginosa*. The iron uptake mechanism in this organism includes ferrisiderophores which follow the same pathway as Fe(III) species, entering the outer membrane where they get reduced in the periplasm upon transportation through the plasma membrane. The siderophores are then recycled in the periplasm and sent back into the extracellular environment. (Kranzler et al., 2013)

3.5.3 Particulate bound iron via PilA1

The major pilin protein, PilA1 in has been found to have an important role in iron acquisition in *Cyanobacteria* due to their abilities in reducing metal oxides. A *Synechocystis* strain (PCC 6803) are able to utilise form of Fe that have very low solubilities such as; iron oxide and goethite FeO(OH). The organism uses pili to access this iron and the mechanism can be seen on Figure 3-7 where extracellular particulate Fe(III) is reduced into the more soluble and bioavailable Fe(II) by the electrons transported from the photosynthetic electron transport chain. The Fe(II) then can be taken up directly by the cells. However, transporters of these electrons that mediate the reduction of extracellular particles containing Fe(III) are yet to be defined. (Lamb et al., 2014)

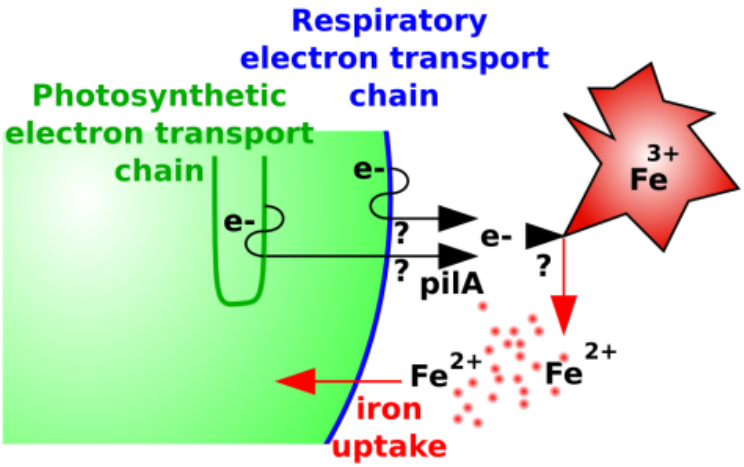

Figure 3-7 PilA1 mechanism. Electrons are transported to extracellular particles containing Fe(III) from the photosynthetic electron transport chain and insoluble Fe(III) is converted into soluble Fe(II) for cellular uptake (Lamb et al., 2014).

3.6 Iron starvation in *Cyanobacteria*

Physiological responses to iron limitation

As extensively discussed in the previous sections, iron is an essential macronutrient for *Cyanobacteria* species and when there is iron starvation, several physiological responses are observed which will be discussed in this section.

Chlorosis

Chlorosis is a condition where the chlorophyll content decreases significantly in a photosynthetic organism. This condition is known to be the most noticeable symptom of iron deficiency in *Cyanobacteria*. The reason behind this is that the enzyme coproporphyrinogen oxidase catalysing protochlorophyllide from Mg-protoporphyrin in chlorophyll synthesis, requires iron for functioning. However, iron limitation may not directly cause chlorosis, but the effects are visible when iron deficiency induced chlorosis is coupled with the decrease in the number of chloroplast per unit cross-sectional area. (Geider and La Roche, 1994)

Accessory pigments and light harvesting

Light absorbing pigments in *Cyanobacteria* such as chlorophylls and carotenoids are quite independent of iron status. For example, in iron limited conditions, it has been observed that the ratio of pigments; chlorophyll b, β-carotene, neoxanthin and lutein to chlorophyll a were not affected by chlorosis in Fe-starved sugar beet. In apricot and pear leaves, the β-carotene:chlorophyll a and neoxanthin:chlorophyll a ratios were independent of iron starvation.

However, a decrease in the ratios of chlorophyll b/a and an increase in the lutein:chlorophyll ratio were described. During iron starvation, light harvesting pigments of the diatom *Phaeodactylum tricornutum* behaved similar to the vascular plants where the ratio of chlorophyll c, fucoxanthin and β-carotene to chlorophyll a were independent of the degree of Fe-starvation. In *Cyanobacteria*, Fe limitation seem to affect the pigments where a greater loss of phycocyanin relative to chlorophyll a is observed. (Geider and La Roche, 1994) However, on recently done studies it has been reported that in iron limited conditions a decrease in intracellular photosynthetic pigments such as chlorophyll a is observed (Lis et al., 2015).

Photosynthetic electron transfer

Chloroplasts found in *Cyanobacteria* as with other green algae and vascular plants contain membranes that are involved in photosynthesis called thylakoid membranes. Thylakoid membranes have four multi-subunit protein complexes that are composed of at least 70 different proteins known as; photosystem I [PSI], photosystem II [PSII], ATP synthase, and cytochrome *b6f* complexes, each having multiple cofactors. The proteins forming these complexes are vital for a photosynthetic organism since they are responsible for carrying out the photosynthetic reactions in the cells. (Friso et al., 2004)

In iron limited cells and leaves it has been found that thylakoid proteins are affected the most compared to the stromal proteins and total cell proteins by significantly decreasing in number. As a result of chlorosis, alongside the reduction of pigment binding proteins and photosynthetic pigments, a reduction in the ratio of reaction center and electron transport chain proteins to chlorophyll is observed. The protein composition of the thylakoid membranes is altered in the presence of other factors such as; changes in the light absorption, fluorescence excitation and emission spectra. Also, in iron limited conditions, the photochemistry in Photosystem II functions less efficiently as could be seen from the decline in the ratio of variable to maximum fluorescence (Fv/F~) in *Cyanobacteria* as well as other diatom and vascular plant species. However, the reduction in the organism's photosynthetic ability does not solely result from iron limitation. The additional factor, chlorosis enhances the symptoms that is observable such as; decline in the cell specific and biomass specific rates of photosynthesis. Since aspecific chlorophyll rates of light-saturated photosynhtesis are not affected by iron limitaion, the photosynthetic apparatus is thought not to be affected by iron limitation alone. (Geider and La Roche, 1994)

Siderophore production

According to a study done in six *Bradyrhizobium* (lupin) strains, the biosynthesis of siderophores are found not to be solely regulated by the external iron concentrations in the specific WPBS 3201 D strain of this organism. The hydroxamate production in cells that were grown in iron limited conditions is less sensitive to iron suppression than the cells pre-grown in excess iron which show more sensitivity to iron deficiency. The reason behind this is thought to be due to cells having a mechanism that maintains minimum intracellular pools of iron. This mechanism may regulate siderophore production according to the availability of iron which is described as components of; "immediately available iron" and "storage iron". When both of these components are present in the cells, the siderophore production is expected to be suppressed due to having enough intracellular iron. Hence, when the cells which have high intracellular iron concentrations are transferred to zero iron concentration, siderophore production is regenerated due to depleted "immediately available iron". And when 10 μM/L Fe is added to the same cells, the siderophore biosynthesis is suppressed about after 2 hours due to the increase in the "immediately available iron" as well as the existing "storage iron". However, when cells are already grown in low iron concentrations such as 0.5 μM/L and reintroducing them to zero iron result in cells having low levels of both mentioned components. The siderophore production in these cells would not be suppressed with the addition of 10 μM/L Fe, since the cells already have a low iron concentration. (Abd-Alla, 1998)

4 Materials and Methods

4.1 Clean work and acid washing

Prior to the experiment, all the equipment was acid washed and the experiment was carried out in a trace metal clean room, due to samples being easily contaminated by extremely low concentrations of iron. Since this experiment was studying iron and its species at very low concentrations, it was important to keep the laboratory environment as clean as possible because as discussed in the introduction, dust and rust being two of the major sources of iron would result in contamination and the sensitive instruments used in detecting iron such as ICP-MS and FIA would have unwanted interferences.

Alongside this precaution, the labware, ultrapure water and reagents were chosen carefully. Low-density polyethylene (LDPE) and polyethylene (PE) containers (bottles, wash bottles, acid cleaning bath tanks and other containers) were used to prevent contaminant from dissolving out from the walls of the containers. Ultrapure water; Milli-Q and "TraceMetal" grade HNO_3 was used for the sample treatment as well as acid washing the equipment. (Liu et al., 2009)

The laboratory working space was covered with LDPE plastic film from the ceiling to the walls to the benches to prevent any contaminants coming in. Every once a week, the floors were cleaned with Milli-Q water. Cleanroom lab coats, disposable shoe covers, disposable vinyl gloves, surgical masks and disposable hair caps were worn at all times. After every workday, the rubbish that was stored in a zip lock bag was taken out and the benches were wiped with acid and Milli-Q water.

All the filtration and sample treatments were carried out in a vertical laminar flow workstation, AirClean® Systems AC600 Series. This flow hood provides clean, Class 100 laminar flow air by using two-stage filtration. First, the air in the room is passed through an electrostatically charged pre-filter then it is transported through a high efficiency particulate (HEPA) filter which promises to give ISO 5 clean air (Systems, 2018). This way, contamination was avoided from the point of sample collection, transport, processing and analysis.

The set up for the acid cleaning was as follows;

4.1.1 Acid cleaning procedure

All the cleaning was carried out in the Cleanlab. Before the process, powder free gloves were rinsed with Milli-Q water.

Cleaning of plastic for trace metal work

If necessary, the plastic bottles were rinsed with methanol or acetone to release oils from manufacturing. (Geotraces, 2014)

The bottles were immersed in 5% detergent bath that was prepared in a 10 L plastic box container due the large size of bottles being used and left for 1 week. Then the bottles were rinsed 3 times with deionized (DI) water followed by another 3 times rinse with UHP, Milli-Q water. Afterwards, a 10L plastic box containing 6M analytical grade HCl was prepared and the bottles were placed in for 2 weeks. After 2 weeks, the bottles were rinsed 3 times with Milli-Q water and this time immersed in 3M analytical grade HNO_3 bath for 2 weeks followed by a 3 times rinse with Milli-Q water. After this process, the bottles were filled up with Milli-Q water and the pH was adjusted to around 2 by the addition of 12M ultrapure (UP) HNO_3, which was equal to adding 1 mL 12M UP HNO_3 to 1 L Milli-Q water. The bottles were then placed in a double plastic bag, sealed and stored in a large plastic bag within the plastic box until use. Prior to use, the acidified Milli-Q water was emptied, and the bottles were rinsed 3 times with Milli-Q water. If the bottles were to use for sampling, then they were rinsed 3 times with Milli-Q water and rinsed 3 times with the sample additionally. (Achterberg)

*All the vials (15mL, 45mL), filter holders and petri dishes that were used for sampling were acid washed followed by the above procedure.

Washing tubes

The tubes used in the experiment were placed in a 10 L plastic box containing 2-3M HNO_3 for 1 week. After 1 week, the tubes were rinsed 4 times with Milli-Q water and placed in 0.5M UP HNO_3 for further 1 week. They were then rinsed 3 times with Milli-Q water and placed in another bath containing 0.1M UP HNO_3 for 3 days. Prior to use, they were rinsed with Milli-Q water 5 times starting from small amounts of Milli-Q and increasing. In case of time constraints, the time the tubes were kept in acid was reduced by 1/3.

Washing Chelex columns

The columns were rinsed by turning upside down and placing the tip on the Milli-Q water tap. If the columns were new they were left in 1M UP HNO_3 bath for 1-2 days followed by a 3 times rinse. They were filled up with 0.5M UP HNO_3 for 1 week then filled up with 0.1M UP HNO_3 and left for 5 days. Prior to use, the columns were rinsed 5 times as described above in small additions of Milli-Q water.

Washing large 20 L Aquil PE bottles

The PE bottles were filled up with super detergent (ca. 2-3 g/L) and left for 4 days (2+2 rinse in between) followed by a 4 times rinse with Milli-Q water. They were then filled with analytical grade methanol, left overnight and rinsed 4 times with Milli-Q water. Afterwards, the bottles were filled up with ca. 3.5M HNO_3 25 % v:v, reagent grade, ca. 250 mL HNO3 to 750 mL Water) and left for 4 additional days (2+2 rinse in between). Then they were rinsed 5 times with Milli-Q water, filled up with a 0.5 M HNO3 (ca. 3.5 % v:v that is ca. 1 liter water + 40 mL UP HNO3) and left for as long as possible (minimum 4 days). Finally, the bottles were rinsed 7 times with Milli-Q water and stored in Cleanlab, in a large double or triple PE bag. (NTNU, 2018)

4.2 Synthetic ocean water preparation

Types of iron used in the experiment

In this project two types of iron were studied: iron (III) chloride hexahydrate ($FeCl_3.6H_2O$) and goethite: FeO(OH) due to their differences in solubility hence, the different influence they would have on the growth of *Synechococcus*. $FeCl_3$ is known to be very soluble in water (cold water: 74.4 g/100 mL at 0 °C; in hot water: 535.7 g/100 mL at 100 °C) and solvents such as acetone and methanol (acetone: 63 g/100 mL at 18 °C; very sol in alc, ether, methanol). (PubChem, 2004) In contrast, goethite FeO(OH) is described as being very insoluble as with other Fe(lII) oxides with very low K_{sp} values. (Schwertmann, 1991)

Aquil medium in other words (SOW) enriched with macro- and micronutrients was prepared in 4x 20 L acid washed PE bottles; one for Abiotic control for $FeCl_3$, one for Culture for $FeCl_3$ and a batch of Abiotic and Culture for FeO(OH) experiment. The method of preparation was adapted from the National Center for Marine Algae and Microbiota (NCMA) at Bigelow Laboratories with several adjustments (Bigelow).

*Preparation of the Aquil medium was done in the environmental lab and the cleaning of Aquil by chelex was carried out in the Cleanlab.

Anhydrous and hydrous salts

The recipe given on NCMA was for a 1 L medium hence, calculations were made to have the correct amounts and concentration of chemicals for a 20 L medium (Table 4-1). The anhydrous salts were each placed on a weighing boat by using a plastic spoon, weighed correctly, transferred into a 20 L acid washed PE bottle by rinsing the leftover salts on the weighing boat with droplets of Milli-Q water. The anhydrous salts were then dissolved in 12 L of Milli-Q

water that was added to the 20 L PE bottle by using a 2 L plastic graduated cylinder (in 6 instalments) and a plastic funnel (Bigelow).

*Anhydrous and hydrous salts were dissolved in separate PE bottles and then combined to prevent any vigorous exothermic reactions from occurring.

Table 4-1 List of anhydrous salts.

Anhydrous salts	Quantity per 1L [g]	Final conc. [M]	Quantity per 20L [g]
NaCl	24.5400	4.20E-01	490.800
Na_2SO_4	4.0900	2.88E-02	81.800
KCl	0.7000	9.39E-03	14.000
$NaHCO_3$	0.2000	2.38E-03	4.000
KBr	0.1000	8.40E-04	2.000
H_3BO_3	0.0030	4.85E-05	0.060
NaF	0.0030	7.15E-05	0.060

The hydrous salts were each placed on a weighing boat by using a plastic spoon, weighed to the correct amount, transferred into a 4 L PE bottle by rinsing the leftover salts each time with droplets of Milli-Q water. The 4 L PE bottle was then filled up with 4 L of Milli-Q water to dissolve the salts using a 2 L plastic graduated cylinder and a plastic funnel. The 4 L dissolved hydrous salts were then added to the 20 L PE bottle containing 12 L dissolved anhydrous salts. Finally, 2 L of Milli-Q water was added into the final salt medium to make it up to 18 L in total.

Table 4-2 Hydrous salts. *$MgCl_2$ was used if $MgCl_2.6H_2O$ was not available.

Hydrous salts	Quantity per 1L [g]	Final conc. [M]	Quantity per 20L [g]
$MgCl_2.6H_2O$	11.1000	5.45E-02	222.000
$MgCl_2$	5.1900	5.45E-02	103.800
$CaCl_2.2H_2O$	1.5400	1.05E-02	30.8
$SrCl_2.6H_2O$	0.0170	6.38E-05	0.3

Nutrients

The nutrient concentrations were adjusted to higher concentrations to prevent stress that could be caused from nutrient limitation. The concentration of $NaH_2PO_4.H_2O$ used was 100 times more than the original stated concentration of 1.00E-05 M and $NaNO_3$ concentration used was

200 times more than the original described concentration of 1.00E-04 M. $Na_2SiO_3.9H_2O$ concentration was kept the same as the original concentration of 1.00E-04.

Table 4-3 Major Nutrients.

Major Nutrients	Stock [g L^{-1} dH_2O]	Stock conc. [M]	Quantity per 20 L [mL]	Final conc. [M]
$NaH_2PO_4.H_2O$	13.80	0.1	200	1.00E-03
$NaNO_3$	85.00	1	400	2.00E-02
$Na_2SiO_3.9H_2O$	28.40	0.1	20	1.00E-04

Three individual nutrient stock solutions of phosphate, nitrate and silicate were prepared as follows. 13.80 g of $NaH_2PO_4.H_2O$ was weighed in a weighing boat and transferred into a 1 L volumetric flask and the leftover powder was rinsed with droplets of Milli-Q water. The volumetric flask was then filled up to the mark and shaken to dissolve the powder. 200 mL of this solution was added into the 20 L PE bottle containing the salts. The rest of the solution was transferred into a 1 L PE bottle to be stored in the fridge until use.

The nitrate stock was prepared by weighing out 85.00 g of $NaNO_3$ in a plastic weighing boat and transferring into a 1 L volumetric flask. The leftover powder was rinsed with droplets of Milli-Q water and the volumetric flask was filled up to the mark. The solution was shaken until there were no precipitates and 400 mL of this stock was transferred into the 20 L PE Aquil bottle. The rest of the stock was placed in a 1 L PE bottle and stored in the fridge for later use.

The silicate stock was prepared by weighing 28.40 g $Na_2SiO_3.9H_2O$ in a weighing boat and transferring into a 1 L volumetric flask. The residues were rinsed with droplets of Milli-Q bottle and the volumetric flask was filled up to the mark and shaken. 20 mL of this stock solution was transferred into the 20 L Aquil bottle containing the salts and the abovementioned nutrients. The rest of the stock was placed in a 1 L PE bottle and kept in the fridge until further use.

Metals / Metalloids

Individual stock solutions were prepared by weighing out 4.9 g $CuSO_4.5H_2O$ and 1.9 g of Na_2SeO_3, respectively. The metals were each transferred in 1 L volumetric flasks and the residues were rinsed with droplets of Milli-Q water. The volumetric flasks were then filled up to the mark, shaken and transferred into 1 L PE bottles for storing.

The concentration of EDTA used in this experiment was 10 times lower than the suggested amount. This is because ferric EDTA has high binding affinity to iron and if there is too much

of it in the medium, the cells may not be able to acquire Fe as easily and unwanted stress on the organism might occur (Xue et al., 1995). 2.92 g of EDTA was dissolved in 950 mL Milli-Q water in a 1 L volumetric flask and 1 mL of each stock solution ($CuSO_4.5H_2O$ and Na_2SeO_3) was added to this flask. The other metals were weighed and also added to the solution containing EDTA. The resulting metal solution was brought up to 1 L and transferred into a 1 L PE bottle.

Table 4-4 Materials / Metalloids.

Metals/Metalloids	**Stock [gL^{-1} dH2O]**	**Quantity per 1 L [g]**	**Final concentration [M]**
EDTA		2.920	1.00E-05
$ZnSO_4.7H_2O$		0.0230	7.97E-08
$MnCl_2.4H_2O$		0.0240	1.21E-07
$CoCl_2.6H_2O$		0.0120	5.03E-08
$Na_2MoO_4.2H_2O$		0.0242	1.00E-07
		Quantity per 1 L [mL]	
$CuSO_4.5H_2O$	4.9	1	1.96E-08
Na_2SeO_3	1.9	1	1.00E-08

Iron

Iron concentrations used in this experiment were higher than the original concentrations suggested on NCMA to enhance phytoplankton growth. Iron stock solutions were prepared by weighing out 2.70 g of $FeCl_3.6H_2O$ and 0.44 g of FeO(OH) separately and dissolving in 1 L volumetric flasks. The obtained stock solutions were then transferred into 1 L PE bottles, wrapped in aluminum foil and kept in the fridge to prevent any changes in the chemistry of iron species.

Table 4-5 Iron minerals.

Iron type	**Stock [gL^{-1} dH2O]**	**Stock concentration [M]**	**Quantity per 20 L [mL**	**Final concentration [M]**
$FeCl_3.6H_2O$	2.70285	1.00E-03	1	5.00E-08
FeO(OH)	0.44425	1.00E-03	1	5.00E-08

Vitamins

Thiamine and biotin were found not to be essential for growth of *Synechococcus* hence in this experiment, the essential vitamin B12 was used. The vitamin stock solution was prepared by

weighing out 0.005 g of Cyanocobalamin in a weighing boat and transferring into a 1 L volumetric flask where it was shaken until it was dissolved. The volumetric flask was then filled up to the mark and the resulting stock solution was transferred into a 1 L PE bottle, wrapped in aluminum foil and kept in the fridge until it needed to be used. This was done due to the light and temperature sensitivity of vitamin B12.

Table 4-6 Vitamins.

Vitamin	Stock [gL^{-1} dH2O]	Quantity per 20 L [mL]	Final concentration [M]
Cyanocobalamin (Vit. B12)	0.0050	2	3.7E-06

4.3 Cleaning of Aquil with Chelex-100

Aquil containing the major nutrients was cleaned with Chelex® 100 resin, in order to remove all the possible contaminants. Chelex chelating ion exchange resin is used due to its high-performance ability to eliminate heavy metals such as copper and iron. Additionally, it has a strong attraction to transition metals even in high concentrated salt solutions which makes it suitable to use in SOW (Rad, 2000). This way the Aquil would be free of any trace metal metal contaminants especially iron, having solely the experimentally added known metal concentrations.

The chemical composition of Chelex-100 resin consists of styrene divinylbenzene copolymers containing paired iminodiacetate ions which act as chelating groups and bind to polyvalent metal ions. The chelating resin contains carboxylic acid groups on which could be considered as a weakly acidic cation exchange resin. However, its high selectivity for metal ions and its higher bond strength separates it from the ordinary exchangers. (Rad, 2000)

The structure of the Chelex chelating resin changes with the increasing pH; it is regenerated in dilute acid and functions at basic, neutral and weakly acidic conditions (pH 4 or higher) (Figure 4-1).

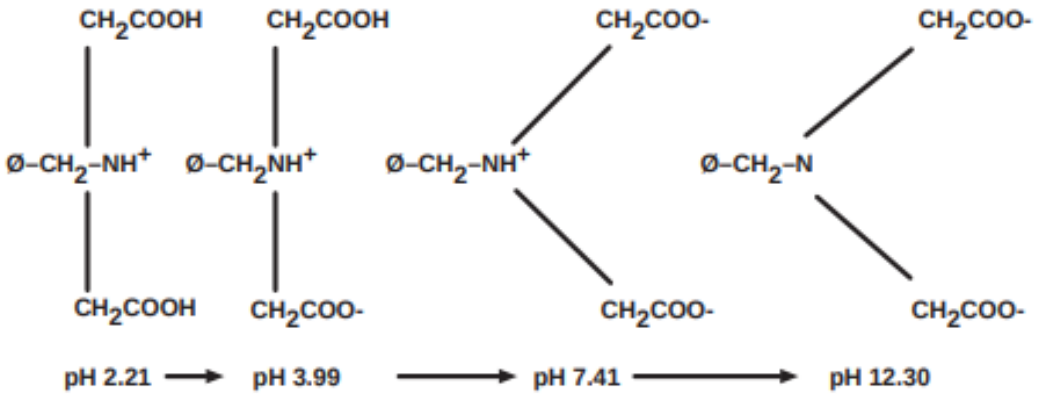

Figure 4-1 Change in the structure of Chelex resin with increasing pH. (Rad, 2000)

Making the chelex slurry

The method was adapted from Bio-Rad Laboratories, Chelex® 100 and Chelex 20 Chelating Ion Exchange Resin Instruction Manual (2000). (Rad, 2000)

Enough amount of Chelex resin was taken out from its container and placed in an acid washed 250 mL Nalgene bottle. To this bottle, 2-3 M UP HNO_3 was added up to the top, placed in a shaker horizontally and left for 2 hours. All the supernatant acid was emptied in one go and the leftover was rinsed 2 times with Milli-Q water each time shaking vigorously by hand, waiting for it to settle down and removing the supernatant. This process of acid washing was repeated 2 times more and, in the end, 2-3 mL of 13.4 SP NH_4OH was added followed by the addition of Milli-Q water until the slurry consistency was reached. (Rad, 2000)

Chelexing the Aquil

Four 20 L Aquil mediums containing the nutrients were pH adjusted to have the maximum removal efficiency. In the environmental lab, under fume hood, the pH was adjusted to 5.34-6.40 by adding 1.5-2 mL 12M UP HNO_3 to each Aquil bottle. To the each Aquil medium, 5 mL of the Chelex slurry was added and the bottles were placed on a shaker making the necessary adjustments so that the bottles would not trip over or get damaged throughout the shaking process. The Chelex was left in the Aqiul over the weekend. The shaker was then turned off and the Chelex was left to settle. The 20 L Aquil containers were moved to the Cleanlab and placed under the fume hood. Four new acid washed 20 L PE bottles were labelled, each placed in clean large PE bags and placed on the floor. The acid washed and cleaned Chelex columns were fitted on the wall of fume hood, attached to suitable sized acid washed and cleaned tubings and inserted into the full Aquil containers. The mouth of the containers was closed with parafilm to prevent any contamination. An acid washed and cleaned syringe was used to draw out Aquil

through tubing, the first flow was discarded, and the end of the tubing was rinsed again before it was inserted into the empty Aquil bottle. The flow was let to run with its own pace until it stopped, and it was made sure that the filter part of the column was not dislodged inside, and the containers were carefully protected by parafilm the whole time. When the process was done, the tubing from the bottom container was removed and the cap that has been rinsed before was placed on the container quickly. The containers now having clean Aquil were sealed in their large PE bags and moved to the laboratory where the experiment was conducted. The used columns were rinsed with Milli-Q water into acid washed and cleaned small 125 mL PE bottles, labelled, sealed in a plastic bag and placed in the fridge for recovery. (Rad, 2000)

4.4 Microwave sterilisation

The Chelexed Aquil containing the nutrients was divided into acid washed and cleaned 4 L PE bottles by using a plastic graduated cylinder and a plastic funnel that has been acid washed. Using a 700-W microwave oven, 4 L Aquil was microwaved for 20 mins, stopping in 10-minute intervals and placing the bottle horizontally each time. After the microwaving was done, the Aquil in 4 L PE bottles were let to cool down and placed into new acid cleaned, labelled 20 L PE bottles.

Microwave sterilisation was used for sterilising the Aquil as adapted from Price et al. (1989), because as stated it is one of the better options than Autoclaving, filter sterilisation etc. According to Price et al. (1989), Autoclaving may contaminate the medium by introducing some trace metals via the steam and additionally result in formation of carbonate species via precipitation, so this method was not considered. Another suggested method was using 0.25 or 0.45 μm acid washed Nuclepore filters and filter sterelising the medium through using a suitable metal clean filtering apparatus. However, due to the large quantity of the Aquil (20 L), this would be highly time consuming and not efficient. The same problem applies to using 2 L Teflon bottles which involves heating to 95 °C for 2 hours and freezing overnight and reheating again to 95 °C for 2 hours. Again, this would be very time consuming hence, microwave strelisation was the most efficient and possibly clean alternative. It was highly recommended that the metals and vitamin stock solutions should be filter sterilised and added after microwaving due to the harmful chemicals being released from heat for human health as well as changing the speciation of the metals in the medium. Also, according to Price et al. (1989) the addition of trace metals to the medium before microwaving had resulted in lower than maximum growth rates in a nutrient sufficient medium. (Price et al., 1989)

To the cooled Aquil, 20 mL, 1 mL and 2 mL of the EDTA+metal stock, iron and vitamin B12 were filter sterilised using an acid washed plastic syringe, plastic filter holder and a 0.25 µm acid washed Nuclepore filter, respectively. The pH of the medium was adjusted to 8.0-8.2 for optimum growth before adding the *Synechococcus* sp. PCC 7002 cells by adding approximately 1 mL UP 25% Ammonia solution. 1 mL of *Synechococcus* sp. PCC 7002 cells were then added to the final Aquil and the medium was made up to 20 L with Chelexed and microwave streilised water (De Farias Silva et al., 2016).

* *Synechococcus* sp. strain PCC 7002 were obtained from the Biotechnology faculty of NTNU.

4.5 Experimental setup

The experimental set up is shown in Figure 4-2 where a Plexiglas stand is supported by two 10 L PE boxes that inside, hold three round LED lights each. According to Thomas et al., (2005), *Synechococcus* sp. PCC 7002 is adapted to higher CO_2 concentrations, and few common freshwater strains were found to survive in conditions greater than 40% CO_2, so it was important to provide enough CO_2 by connecting two CO_2 pumps for each 20 L Aquil. (Thomas et al., 2005)

The acid washed and cleaned tubing was connected to an aquarium air pump and the other end of the tubing was inserted into an acid washed PE bottle containing Milli-Q water. The cap of this PE bottle had another entrance which was used to connect to the Aquil with another tubing. A 50 mm CA syringe filter, 0.45 µm was attached to the tubing connecting the Aquil to the bubbling bottle to prevent any contamination. The Aquil caps had two entrances; one for CO_2 and one for sample outtake. The tubing used for sample outtake was acid washed and cleaned and when in not use the tip of the tubing was kept sealed in a clean plastic bag which was kept in a larger double sealed plastic bag.

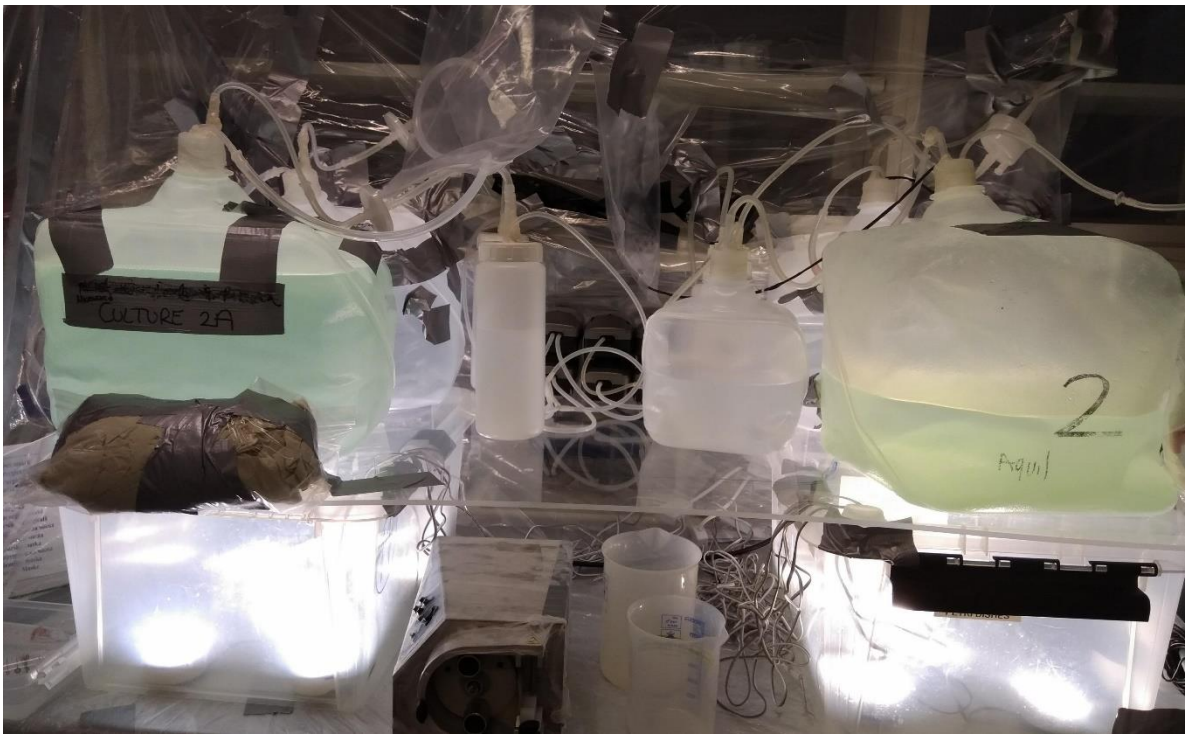

Figure 4-2 The experimental set up. On the left is the Culture Goethite FeO(OH), behind the culture is Abiotic control FeO(OH), on the right is the Culture $FeCl_3$ and behind that is the Abiotic control for $FeCl_3$. In the middle is the CO_2 bubbling set up. The lights were adjusted that they are directly below each Aquil.

The light intensity was measured as photosynthetically active radiation and was set to be 195 $\mu E\ m^{-2}\ s^{-1}$. The temperature was around room temperature, which was measured daily.

4.6 Important biological indicators

All the analysis was done in 3 replicates for reproducibility and repeatability.

4.6.1 Extracted chlorophyll a

Phytoplankton contain chl a, the primary photosynthetic pigment like all the other organisms that carry out photosynhtesis. Chl a fluorescence is known to be most versatile and sensitive way to measure the concentrations of phytoplankton in water (Turner Designs). In this experiment, alongside phytoplankton growth, chl a analysis was done in order to observe the physiological responses of phytoplankton in experimental conditions and examine the stress related variations in chl a concentrations if there was any.

The theory of chl a measurement comes from the phenomena called fluorescence where some compounds absorb specific wavelength of light and emit longer wavelengths of light almost instantaneously. In this case, chl a naturally absorbs blue light and emits red light. This fluorescence of chl a can be detected by transmitting an excitation beam of light in the blue range (440 nm for extracted analysis and 460 nm for in vivo analysis) and detecting the light

emitted by the chlorophyll in a sample in the red range (685 nm). It is assumed that the fluorescence emitted by the chl a is directly proportional to the concentration of the material (cells) in the sample. (Turner Designs)

Figure 4-3 Fluorometer - Turner Designs. Chlorophyll a content of the cells was measured by Trilogy® Laboratory. (Designs, 2017)

The sample preparation was as follows;

*The sample outtake and the filtration process were done in a dark room to prevent chl a from reacting to any incoming light.

The method was adapted from Sakshaug et al. (2009)

The Aquil was shaken well until it was homogonised before sampling. 1 mL of sample was taken from the culture and filtered using a 25 mm Whatman® glass microfiber filters, Grade GF/F, 10 mL syringe and a 25 mm Whatman® plastic filter holder with the help of a plastic tweezer. The filter was then placed in a glass bottle (wrapped with black tape) containing 10 mL cold 100% methanol and shaken. The tube was placed in a plastic bag and placed in the freezer for 1 hour. After 1 hour the tube was shaken again and left in the freezer overnight (not longer than 24 hours). Before analysis the fluorometer was turned on, the appropriate chl a/na module was chosen and the instrument was let to warm up for 10 minutes. The sample was then filtered using 0.2 μm syringe filter and syringe and transferred to a new tube. First, blank (2 mL 100% Methanol) was measured then the measurement of the sample was recorded) (Egil Sakshaug, 2009).

4.6.2 Optical density (OD730nm)

UV–vis spectrophotometric optical density (OD) is technique used for estimating chromophore formation and cell concentration in liquid culture. It could be used as a proxy measurement for biomass concentration including direct dry weight (DW), cell count as well as pigment levels. The theory behind OD is associates with the Beer-Lambert law where the concentration of a

sample is related to the attenuation of light passing through the sample medium. Scattering and adsorption of light enables measuring biomass and pigment concentrations (Myers et al., 2013). The choice of wavelength used was 730 nm as reported with several studies on monitoring growth of *Synechococcus* sp. strain PCC 7002 (Balasubramanian et al., 2006) (Vogel et al., 2017). This wavelength was used to prevent interferences by photosynthetic pigments such as chlorophyll a/b and carotenoids which have absorption maxima below 730 nm (Lichtenthaler and Buschmann, 2005).

The Aquil was shaken well until it was homogonised before sampling. 1 mL of the sample was taken out at the same time every day and if the samples were not measured immediately or within an hour, they were kept in a dark and cold environment until time of the measurement. OD730 was measured in the Biotechnology Department by a PhD student using a SPECTRONIC 200 E spectrophotometer (Thermo Scientific).

*Sample outtake for OD, chl a and pH were done daily at 11:30 am.

4.6.3 Particulate and intracellular iron

Particulate Fe for ICP-MS

The Aquil was shaken well until it was homogonised before sampling. 25 mL (enough to make the filter green) of the culture sample was taken out and ran through 47 mm 0.2 µ Whatman® Nuclepore Track-Etched Membrane that was placed inside Hellman filter system. The filter was then folded into a small compact form using a plastic tweezer and placed in a previously acid washed, clean petri dish, labelled and sealed with tape. The filters were stored in the freezer until ready for digestion. The blank filters (3x) were treated the same way expect instead of the sample solution, the filter was ran with 25 mL Milli-Q water.

Oxalate cell wash process

The cells were washed with an oxalate cell washed that was prepared to remove iron adsorbed to the surface of microorganisms and ideally measure solely the intracellular iron. (Hassler and Schoemann, 2009)

The oxalate was prepared according to Hassler and Schoemann (2009) in a 1 L acid washed and rinsed PE bottle, with NaCl (100 mM, 5.884 g/L), KCl (10 mM, 0.7454g/L), disodium oxalate (100 mM, 13.4g/L) and disodium EDTA (50 mM, 18.612g/L) at pH 7.0 (Hassler and Schoemann, 2009).

NaCl rinse

NaCl solution was prepared by mixing 0.6 M NaCl with 2.38 mM of HCO3 at pH 8 in a 1 L acid washed and rinsed PE bottle and this solution was then chelexed.

The Aquil was shaken well until it was homogonised before sampling. 25 mL(enough to make the filter green) of the culture sample was taken out and ran through 47 mm 0.2 μ Whatman® Nuclepore Track-Etched Membrane that was placed inside Hellman filter system. When there was approximately 5 mL of sample was left on the filter, the vacuum was stopped, and 10 mL of oxalate was added onto the filter to run through the filter (no vacuum). About 5 minutes later, the filter was then rinsed with ten 1.5 mL aliquots (15 mL in total) of prepared NaCl solution under vacuum. The filter was then folded into a small compact form using a plastic tweezer and placed in a previously acid washed, clean petri dish, labelled and sealed with tape. The filters were stored in the freezer until ready for digestion. The blank filters (3x) were treated the same way expect instead of the sample solution, the filter was ran with 25 mL Milli-Q water.

Sample preparation for HR-ICP-MS

Microwave Closed Vessel Digestion System, UltraCLAVE (MLS/Milestone) was used to digest filter samples prior to HR-ICP-MS analysis. UltraCLAVE digestion is used due to its efficient sample preparation for ICP-MS. The instrumentation is based on high pressure autoclave design with a single large reaction chamber at its centre where the samples are placed and are pre-pressurised with inert gas followed by heating via microwaves. The samples are digested at pressures and temperatures up to 200 bar and 260°C (MILESTONE, 2018).

The procedure is as follows. The filters containing the samples were transferred into Teflon tubes and 5 mL of 50% HNO_3 was added. The tubes with the samples and blanks were placed in the sample rack and transferred into the reaction chamber. The samples were left until the digestion process was completed, ca. two hours. After digestion, when the samples were cooled down, they were diluted to between 48-52 g with Milli-Q water and the exact weight was recorded. The solution was then transferred to 15 mL acid washed PE vials to be analysed by HR-ICP-MS.

4.6.4 Particulate Organic Carbon (POC)/ Particulate Organic Nitrogen (PON)

During the entire procedure of sampling, filtration, storage, fuming and analysis, care was taken to avoid contamination by both organic and inorganic forms of carbon and nitrogen. During storage, samples were placed in plastic box in a freezer room where they would not be exposed to other sources of volatile carbon and nitrogen. (Martin)

*All equipment that came in contact with sample filters were only metal, and always cleaned with methanol before use.

The Aquil was shaken well until it was homogonised before sampling and 25 mL (enough to give colour on the filter) of the culture sample was taken out. The sample was ran through a precombusted 25 mm Whatman® glass microfiber filter, Grade GF/F that was placed inside Hellman filter system using methanol washed metal tweezers. The filters were precombusted by wrapping in aluminum foil and placing in a muffle furnace for 4 hours at 450 °C to get rid of any contaminants. The vacuum was turned off and the filter containing the sample was folded into a small, compact form by using methanol washed metal tweezers. The folded filter was placed on an aluminum foil and the sides were closed carefully without touching the filter. The samples were then placed in a plastic box, closed securely and placed in a freezer room at –20 °C until further treatment.

*The samples were collected with the abovementioned method however, they have yet to be analysed hence, no POC/PON results are available to discuss.

4.6.5 Temperature and pH

Temperature and pH were recorded daily. The temperature was recorded using a digital thermometer with ±0.01 accuracy. For pH measurement WTW pH/ION 340i pH meter was used.

5 Results

The measurements of pH, chlorophyll a concentration, intracellular and particulate Fe were all done in three replicates and the mean values were used in data representation. The tables including the replicate values can be found in appendix. The highlighted values in red are considered to be anomalies and thus, they were not included for a better demonstration of results Regression analysis was used to observe if changes in one variable affects the other variable by using dependent and independent variables. Regression analysis was performed using Microsoft Excel using built in Analysis Toolpak. The p-value in the regression equation depends on the assumption that the rest of the model is correct, so the same results would be obtained if the experiment was carried out in the exact same conditions as previous.

5.1 Blanks and limit of detection

The term Limit of Detection (LoD) used in analytical chemistry, describes the smallest concentration of a substance that can be reliably measured by an analytical procedure (Armbruster and Pry, 2008). LoD is calculated by taking the mean value of three blank measurements, calculating the standard deviation and multiplying that value by three, respectively. The Table 5-1 shows calculated LoD where the RSD value for particulate Fe is 17.60% and for intracellular Fe is 29.44%. The values obtained below limit of detection were presented in tables as LoD and not shown in the graphs.

Table 5-1 Limit of detection (LoD) calculated for Particulate and Intracellular Fe.

Sample Number	Particulate nM	Intracellular nM
1	13.90	30.78
2	12.89	41.31
3	9.78	22.75
Mean	12.19	31.61
Std	2.15	9.31
Blank detection limit	6.44	27.92
RSD % <5, 5-10, >10	17.60	29.44

5.2 Growth

5.2.1 $FeCl_3$

Overall, from day 1, there is a steady increase in the optical cell density measured at 730nm. However, a decrease in cell density is observed on days 6, 9, 11, 14 20, 21 and on day 28 the cell density drops down nearly by a half (Table 5-2). The number of cells mL^{-1} was calculated for a better representation of cell growth. The calculation was done assuming that there is a direct correlation between the OD730nm and number of cell mL^{-1} using Equation 1.

$$y = 5 \times 10^8 \times x + 1 \times 10^8$$

Equation 1 Relationship between Number of cells mL^{-1} and OD730nm. Where y is the number of cells mL^{-1} and x is the OD730 (Biotechnology Department, 2018). Hence, number of cells mL^{-1} also shows the same trend as the OD730nm.

The Log no of cell mL^{-1} was calculated to demonstrate the logarithmic/exponential phase of cell population growth in the following section Figure 5-2.

Abiotic control medium was also measured for OD730 nm to check if there is any contamination that would result in cell population growth. The detected values range from 0.001-0.003 which is insignificant, however on day 13 and 24 the OD730 is 0.015 and 0.006, respectively.

Table 5-2 Biological parameters showing growth in OD730 nm, number of cells mL^{-1}, Log (No of cells mL^{-1}) for $FeCl_3$ culture. Additionally, the OD730 nm measurement for the Abiotic control is shown.

Day	Culture OD730nm	Abiotic OD730nm	*M*No of cells mL^{-1} (Culture)	*M*No of cells mL^{-1} (Log)
1	0.008	0.002	104	8.02
2	0.010	0.001	105	8.02
3	0.010	0.000	105	8.02
4	0.020	0.000	110	8.04
5	0.022	0.000	111	8.05
6	0.020	0.001	110	8.04
7	0.024	0.002	112	8.05
8	0.034	0.003	117	8.07
9	0.026	0.000	113	8.05
10	0.035	0.002	118	8.07
11	0.030	0.002	115	8.06
12	0.037	0.001	119	8.07
13	0.042	0.015	121	8.08
14	0.034	0.000	117	8.07
15	0.046	0.001	123	8.09
16	0.056	0.003	128	8.11
17	0.058	0.000	129	8.11
18	0.061	0.000	131	8.12
19	0.070	0.000	135	8.13
20	0.060	0.001	130	8.11
21	0.056	0.000	128	8.11
22	0.059	0.000	130	8.11
23	0.075	0.000	138	8.14
24	0.076	0.006	138	8.14
25	0.084	0.001	142	8.15
26	0.089	0.001	145	8.16
27	0.091	0.001	146	8.16
28	0.052	0.000	126	8.10

5.2.2 FeO(OH)

On day 22 and 24 there were no results recorded due to human error. A fluctuation in OD730 nm and number of cells mL^{-1} is observed for the cells grown in the FeO(OH) culture. There is a steady increase from day 1 until day 4 and thereafter the OD730 nm drops down to 0.012-0.011 until day 9. This trend continues where from day 9 the cells continue growing again followed by random decreases, reaching up to 0.036 (Table 5-3).

Growth detected in Abiotic control medium starts from the acceptable range 0.001-0.003 and goes up to higher values that were detected on day 4 and stays on the higher range from day 8 and thereafter until the end of the experiment.

Table 5-3 Biological parameters showing growth in OD730 nm, number of cells mL^{-1}, Log (No of cells mL^{-1}) for FeO(OH) culture. Additionally, the OD730 nm measurement for the Abiotic control is shown.

Day	Culture OD730nm	Abiotic OD730nm	*M*No of cells mL^{-1} (Culture)	*M*No of cells mL^{-1} (Log)
1	0.000	0.003	100	8.000
2	0.010	0.000	105	8.021
3	0.012	0.000	106	8.025
4	0.019	0.005	110	8.039
5	0.012	0.001	106	8.025
6	0.011	0.003	106	8.023
7	0.012	0.003	106	8.025
8	0.059	0.006	130	8.112
9	0.011	0.014	106	8.023
10	0.062	0.006	131	8.117
11	0.066	0.015	133	8.124
12	0.022	0.005	111	8.045
13	0.015	0.002	108	8.031
14	0.031	0.006	116	8.063
15	0.004	0.005	102	8.009
16	0.015	0.012	108	8.031
17	0.029	0.008	115	8.059
18	0.037	0.011	119	8.074
19	0.030	0.011	115	8.061
20	0.037	0.012	119	8.074
21	0.044	0.010	122	8.086
22	-	-	-	-
23	0.030	0.012	115	8.061
24	-	-	-	-
25	0.036	0.013	118	8.072

5.2.3 $FeCl_3$ vs FeO(OH)

The growth curves plotted on Figure 5-1 and Figure 5-2, compares the increase in OD730 nm value and Log number of cells mL^{-1} in cells grown in $FeCl_3$ and FeO(OH) mediums, respectively. There is a steady increase in both of the cultures from day 1 until day 4. Thereafter, the OD730 value for the cells grown in FeO(OH) declines drastically and continues to increase in a rather slow rate. The cells of $FeCl_3$ culture increases in density in a higher rate compared to the cells grown in FeO(OH) and reaches up to its optimum 0.091. FeO(OH) culture reaches its optimum density of 0.044 which is less than half of $FeCl_3$ culture density.

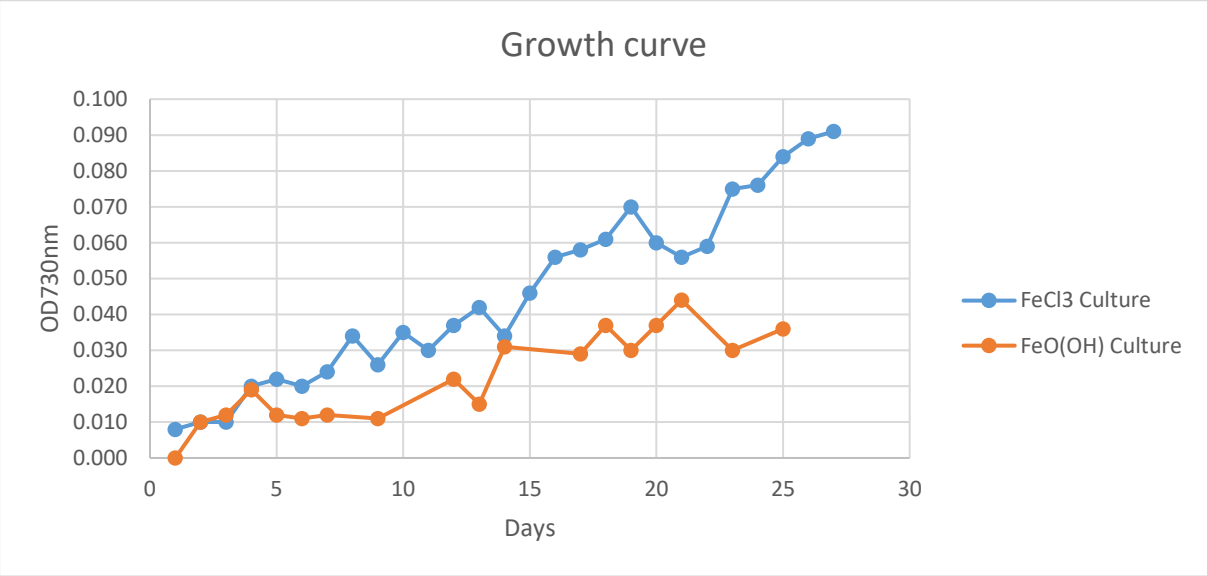

Figure 5-1 OD730nm vs Days for cells grown in culture $FeCl_3$ and FeO(OH).

Figure 5-2 shows the experimental Log growth curve and Figure 5-3 shows the theoretical growth curve of cell population growth. The theoretical curve includes frequent measurements that were done in hourly intervals and the experimental curve includes measurements that were done in 24-hour intervals. For both of the cultures, the lag phase is not observed on the experimental growth curves and overall, not all four phases are clearly distinguishable on the experimental graph which will be discussed in the next chapter.

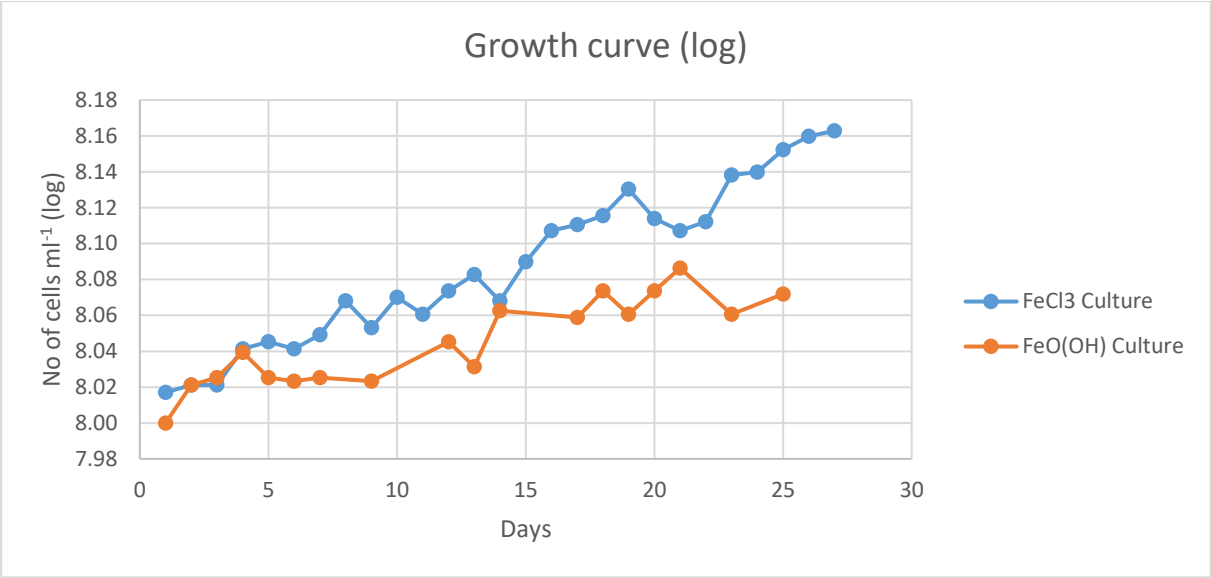

Figure 5-2 Log(number of cells mL^{-1}) vs Days for $FeCl_3$ and FeO(OH) culture.

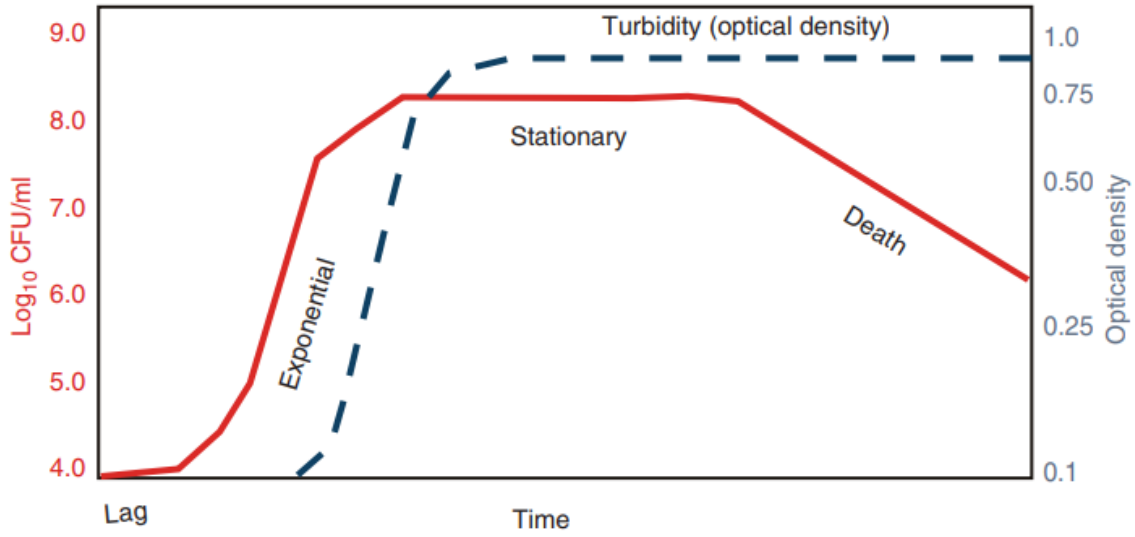

Figure 5-3 An ideal growth curve. The cell population consisting of; Lag, log(exponential), stationary and death phases. (Maier and Pepper, 2015)

5.3 Temperature and pH

5.3.1 $FeCl_3$

The temperature and pH were recorded starting from day 13 due to human error. The pH meter was calibrated every day just before the measurements were recorded. Both culture and control mediums were adjusted to have the same pH, 8.00 at the beginning of the experiment. As can be seen from Figure 5-4 and Figure 5-5, the temperature is sable throughout the experiment ranging in between 24.00-26.30 °C. pH drops from the initial 8.00 to 7.68 and ranges between 7.49-7.77 (culture), 7.37-7.79 (control), respectively.

Table 5-4 Temperature and pH for $FeCl_3$ culture. Recorded values throughout the experiment for both the medium containing the cells (Culture) and the control (Abiotic)

Day	Temperature ºC	Culture pH	Abiotic pH
0	-	8.00	8.00
13	-	7.68	7.65
14	-	7.58	7.53
15	-	7.61	7.58
16	-	7.77	7.79
17	-	7.75	7.68
18	-	7.77	7.74
19	-	7.73	7.71
20	-	7.70	7.60
21	25.42	7.63	7.52
22	25.30	7.64	7.62
23	25.70	7.49	7.56
24	26.30	7.63	7.62
25	24.90	7.59	7.68
26	25.40	7.62	7.52
27	24.90	7.67	7.68
28	24.00	7.66	7.60
29	24.40	7.64	7.37

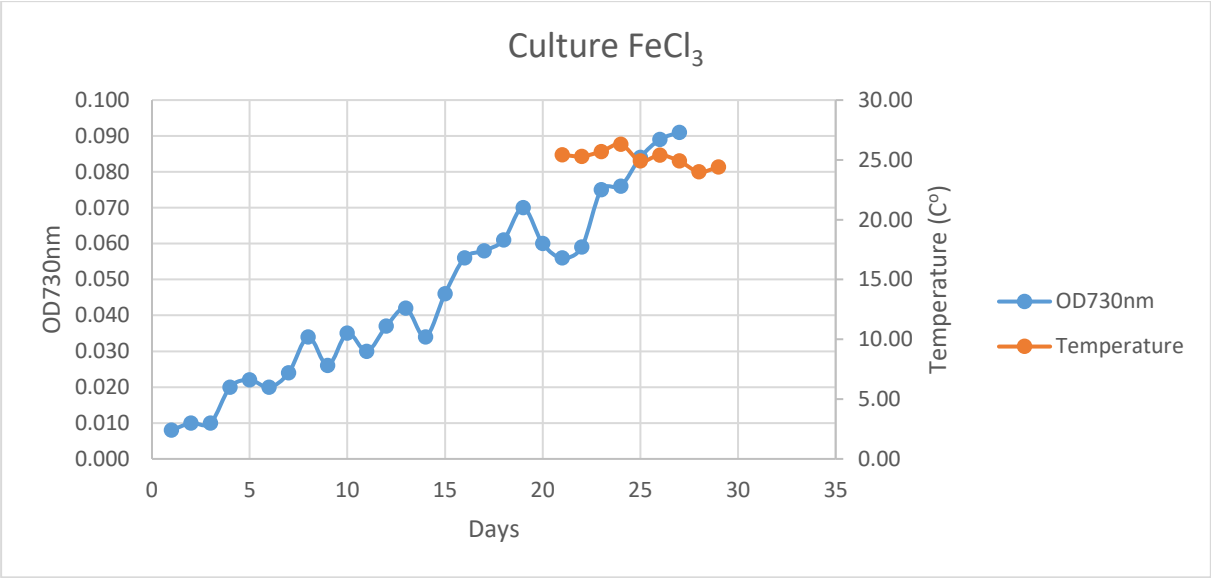

Figure 5-4 OD730nm and Temperature vs incubation days for $FeCl_3$.

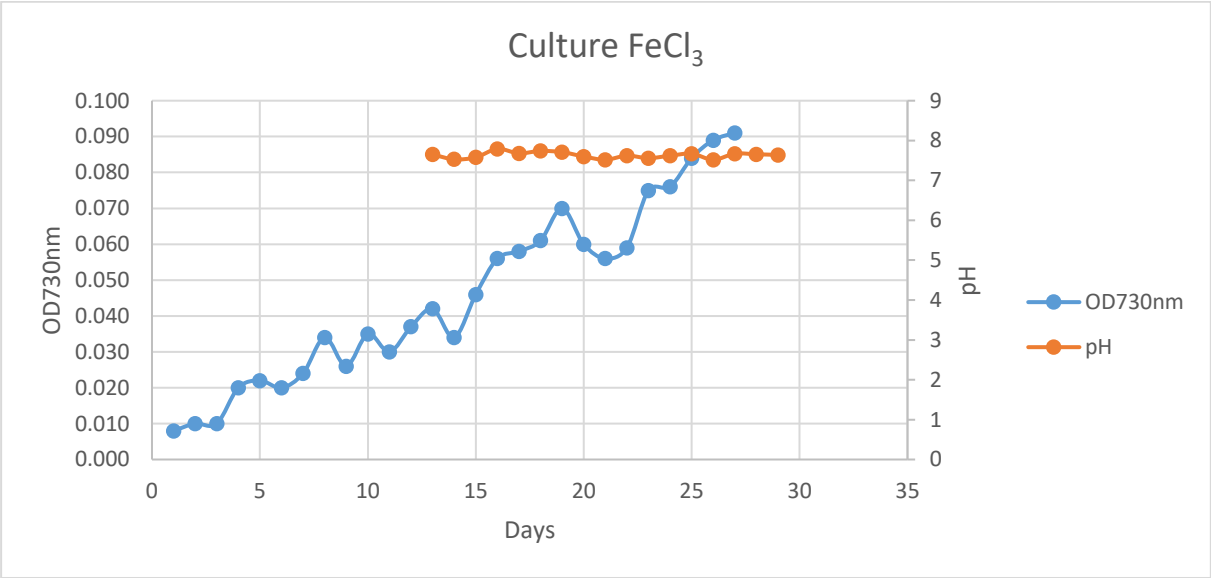

Figure 5-5 OD730nm and pH vs incubation days for $FeCl_3$.

5.3.2 FeO(OH)

The pH for both the culture medium and abiotic were adjusted to 8.06 at the beginning of the experiment before the cells were added into the medium. For culture medium the pH value drops down to 7.58 and fluctuates between 7.21-7.58. The variations in pH can be seen from the orange line in Figure 5-7 with a sudden drop from the initial adjusted pH and steady throughout the experiment. The same trend can be seen in the control medium as well where the values range between 7.43-7.88 with the highest pH (7.88) recorded on day 16, respectively

(Table 5-5). As can be seen on Figure 5-6. The temperature looks stable throughout the experiment with ±1-2 °C variations.

Table 5-5 Temperature and pH for FeO(OH) culture. Recorded values throughout the experiment for both the medium containing the cells (Culture) and the control (Abiotic).

Day	Temperature C°	Culture pH	Abiotic pH
0	-	8.06	8.06
1	25.42	7.58	7.60
2	25.30	7.58	7.58
3	25.70	7.58	7.56
4	26.30	7.48	7.51
5	24.90	7.26	7.45
6	25.40	7.44	7.59
7	24.90	7.48	7.68
8	24.00	7.44	7.68
9	24.40	7.49	7.65
10	24.10	7.31	7.62
11	24.90	7.29	7.43
12	23.60	7.44	7.43
13	25.40	7.44	7.61
14	24.10	7.44	7.66
15	24.40	7.41	7.69
16	24.80	7.44	7.88
17	26.80	7.21	7.56
18	24.60	7.41	7.56
19	24.40	7.36	7.52
20	24.60	7.38	7.55
21	24.90	7.37	7.52
22	24.30	7.37	7.55
23	24.60	7.37	7.52
24	24.50	7.35	7.52
25	24.70	7.36	7.61

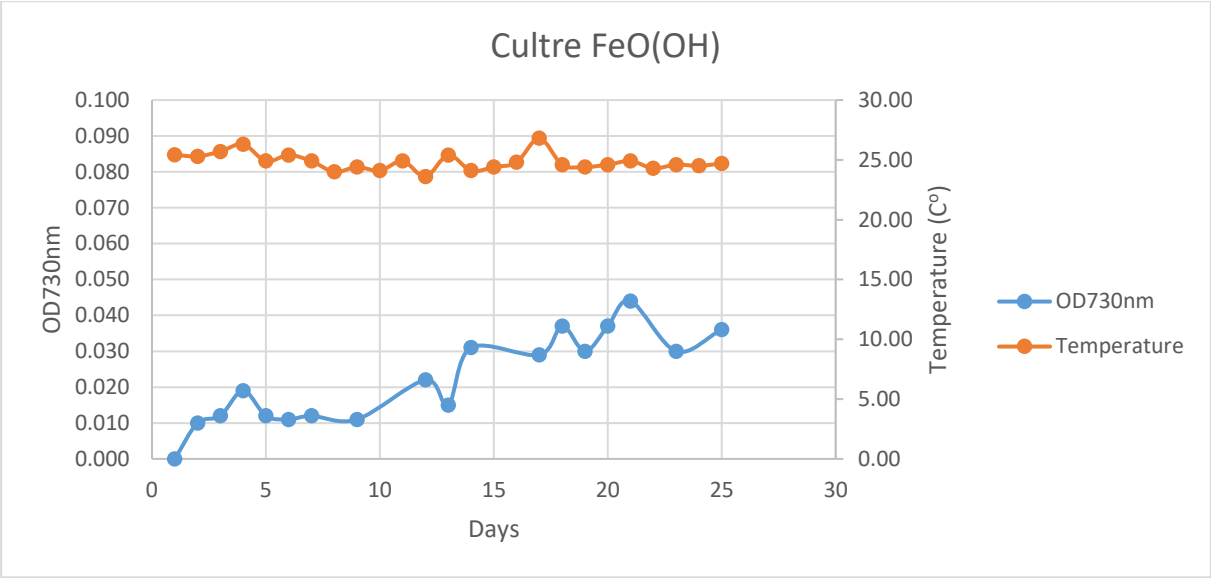

Figure 5-6 OD730nm and Temperature vs incubation days for FeO(OH).

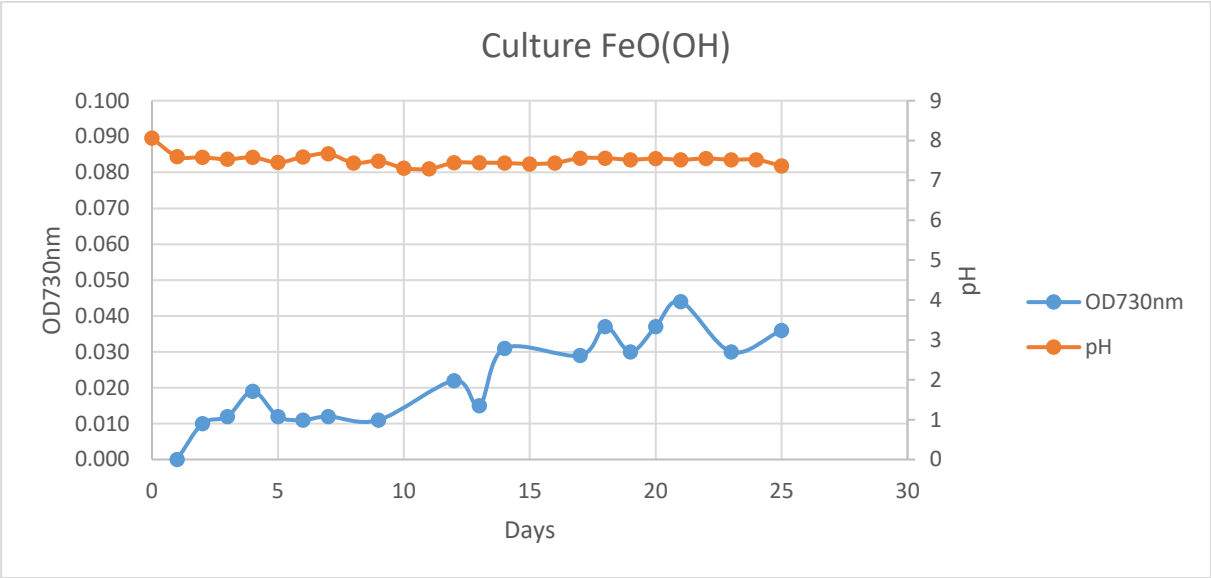

Figure 5-7 OD730nm and Temperature vs incubation days for FeO(OH).

5.4 Chlorophyll a

Chlorophyll a concentrations were calculated by using the Equation 2;

$$\mu g\ chl\ a/litre = ((FL - BL) \times f \times E \times 1000)/(V \times 1000)$$

Equation 2 Chlorophyll a concentration calculation. Where FL: instrumental reading of sample, BL: reading of blank (100% methanol), f: calibration factor, p.t = 0.45, extraction volume: 10 mL, filtered volume: 1 mL.

Due to human error, the methanol extracted chlorophyll a measurements were done using the wrong compartment in the instrument which was to measure direct in vivo fluorescence. From day 16 until day 24 the measurements were done in correct compartment for the extracted chlorophyll a and also for the previously used in vivo fluorescence. As a result, it was observed that there is a linear relationship between the two parameters and all the values were converted (Table 5-6).

Table 5-6 In vivo fluorescence and extracted chlorophyll a. Values measured between the days 16-24 for FeO(OH) culture.

		Days								
		16	**17**	**18**	**19**	**20**	**21**	**22**	**23**	**24**
IN VIVO FL	**1**	1323.12	1412.37	1221.34	561.23	940.81	1065.50	939.62	1899.25	1867.81
	2	1332.28	1225.08	1462.99	1052.88	912.11	1319.91	1055.33	1777.31	2637.24
	3	1119.99	926.53	1438.37	1309.51	1198.29	1203.39	987.40	2568.38	1228.31
	mean	1258.46	1187.99	1374.23	974.54	1017.07	1196.27	994.12	2081.65	1911.12
Chl a/NA	**1**	20.83	14.79	10.12	8.84	15.35	18.20	15.93	42.36	31.99
	2	21.19	23.00	17.14	16.62	15.05	20.04	18.14	35.56	44.95
	3	17.98	4.45	24.28	22.93	20.69	23.03	16.65	31.62	22.34
	mean	20.00	14.08	17.18	16.13	17.03	20.42	16.91	36.51	33.09

The calculations were done by creating a line of best fit that goes through 0 on the extracted chlorophyll a vs in vivo fluorescence graph and using the equation;

$$y = 0.016154851\text{x}$$

Equation 3 Linear relationship between in vivo FL and chl a/NA. Where, y = chl a/NA, m = gradient, x = in vivo FL.

The correlation coefficient is calculated to be r = 0.940651, which states a strong correlation between measured in vivo fluorescence and chl a/na. The r^2 = 0.884824, this means that 88.48% of total variation in in vivo fluorescence can be explained by the linear relationship. Adjusted R^2 (adjusted for the number of predictors ie. samples in the model) is 0.868371 which gives 86.84 % of total variation in the sample population. Regression analysis is carried out to show

the relationship between the measured in vivo fluorescence and extracted chlorophyll a where the p value is 0.000158 which means that there is a 0.0158% chance that the result occurred only as a result of chance.

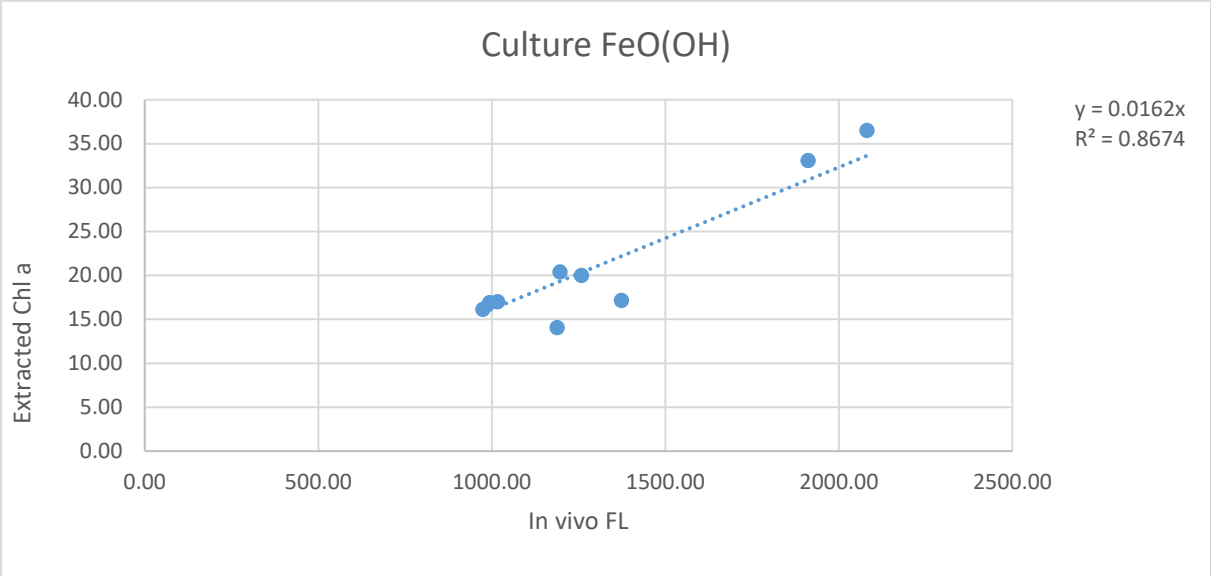

Figure 5-8 Extracted chlorophyll a versus in vivo fluorescence. A linear relationship between the two parameters is observed.

5.4.1 $FeCl_3$

The following chlorophyll a values on Table 5-7, were all blank corrected and the negative values are the values that were below limit of detection. Chlorophyll a measurements were done for the control medium in order to check for contamination and the recorded values were below the detection limit or insignificant. Chlorophyll a (g) $cell^{-1}$ was also calculated from the number of cells to show how the direct chlorophyll a concentration in each cell. Chl a (g) $cell^{-1}$ values are directly proportional to the recorded chlorophyll a concentrations (µg L^{-1}).

Table 5-7 Chlorophyll a concentrations for $FeCl_3$ culture. Values reported for both culture medium and control (abiotic). Three replicates were analysed and the mean value was used in results demonstration. Chl a (g) cell^{-1} is also calculated from the number of cells.

Day	Culture Chl a	Abiotic Chl a	Chl a (pg) Cell^{-1}
2	32.30	-2.07	307.65
3	62.57	-1.54	595.92
4	116.47	-0.01	1058.82
5	128.75	-0.01	1159.87
6	84.76	2.60	770.50
7	127.54	1.79	1138.77
8	117.56	-0.31	1004.77
9	144.71	-0.43	1280.62
10	17.38	2.10	147.87
11	14.96	1.63	130.07
12	11.17	-0.47	94.27
13	13.89	2.40	114.83
14	13.85	2.28	118.35
15	19.08	2.40	155.12
16	15.31	3.92	119.58
17	10.20	2.66	79.06
18	12.98	2.10	99.48
19	9.93	0.91	73.57
20	18.64	0.45	143.39
21	15.35	-1.69	119.92
22	108.14	-1.65	835.09
23	135.83	-10.05	987.87
24	142.61	-10.05	1033.42
25	93.87	-7.37	661.08

Below on Figure 5-9, chlorophyll a concentration is plotted against incubation days and there is a rapid increase from day 1 until day 5 where the chlorophyll concentration reaches up to 128.75 µg L^{-1}. Thereafter, there is a fluctuation between days 6 and 9. From day 9 there is a drastic decline in chlorophyll a concentration which drops down to 17.38 µg L^{-1} and stays in

that range until day 21. From day 21 and onwards, the chlorophyll a concentration steeps up to 108.14 µg L^{-1} and follow a steady increase until day 25. The mean and standard deviation of change of rate were calculated as; 15.37 (*p*g) $cell^{-1}$ day^{-1} and ±347.38, respectively.

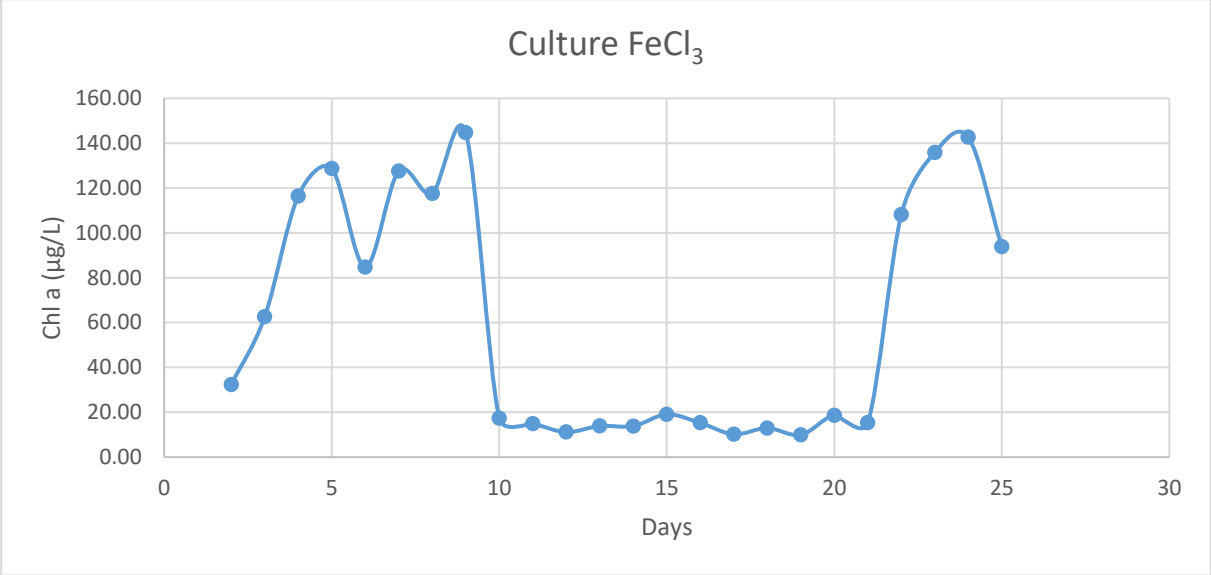

Figure 5-9 Chl a vs Days for $FeCl_3$ culture. Chlorophyll a (Chl a) concentration in µg L^{-1} plotted against incubation days for $FeCl_3$.

5.4.2 FeO(OH)

The following chlorophyll a values on Table 5-8, were all blank corrected and the negative values are the values that were below limit of detection. Only two values are recorded for control culture since it was only done to check contamination and the two values obtained were below the detection limit and insignificant to consider, respectively. Chl a (g) $cell^{-1}$ was calculated from the number of cells which is directly proportional to the chlorophyll a measured in µg L^{-1}.

Table 5-8 5-9 Chlorophyll a concentrations for FeO(OH) culture. Measurements for control were done only in day 1 and 2. Analysis was done in three replicates and the mean value was used in demonstrating the results. Chl a (g) cell^{-1} is also represented.

Day	Culture Chl a	Abiotic Chl a	Chl a (pg) Cell^{-1}
1	0.79	-2.08	7.90
2	49.32	0.88	469.73
3	86.32	-	814.37
4	105.20	-	960.75
5	72.11	-	680.28
6	100.89	-	956.28
7	100.66	-	949.59
8	123.25	-	951.71
9	116.00	-	1099.51
10	108.11	-	825.23
11	99.35	-	746.97
12	87.69	-	790.00
13	87.41	-	813.16
14	89.10	-	771.43
15	73.53	-	720.88
16	82.15	-	764.20
17	77.03	-	672.74
18	90.57	-	764.28
19	61.51	-	534.88
20	64.60	-	545.17
21	77.63	-	636.31
22	62.93	-	-
23	141.99	-	1234.73
24	129.60	-	-

Below the Figure 5-10 shows a rapid increase in chlorophyll a concentration from day 1 to 4 reaching up to 105.20 µg L^{-1}. There is a drop at day 5 where the chlorophyll concentration declines down to 72.11 µg L^{-1} but keeps increasing steadily from onwards until day 8. Thereafter the values show a steady decline by fluctuating between 116.00-61.51 µg L^{-1} followed by a sharp increase in day 23 and 24 with recorded values of 141.99 and 129.60,

respectively. The mean and standard deviation of rate of change were calculated to be; 44.17 (pg) cell^{-1} day^{-1} and ±193.19, respectively.

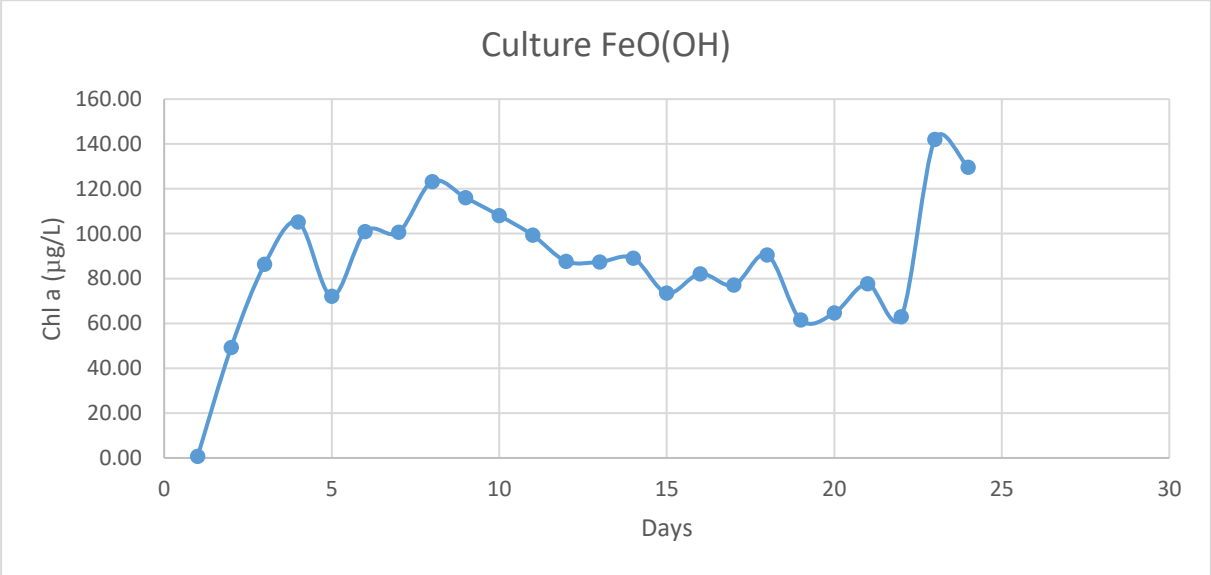

Figure 5-10 Chl a vs Days for FeO(OH) culture. Chlorophyll a concentration in µg L^{-1} plotted against incubation days for FeO(OH).

5.5 Intracellular and particulate iron

The final intracellular and particulate Fe concentrations were calculated as follows. Initial Fe56 concentrations from ICP-MS results were corrected for UltraCLAVE blank, intracellular/particulate filter blank and this value was multiplied by the final volume after dilution and divided by the initial filter volume Appendix A:

The intracellular and particulate Fe concentrations were converted into nM for a better comparison with the literature that is reported in nM, however, the intracellular Fe per cell was reported in pmol Fe cell^{-1} due to the values being very small. Here on Table 5-11, it was assumed that the cells that were treated with oxalate had solely intracellular Fe and hypothetically it can be suggested that the filtered particulate Fe included both the Fe that was in the cells and the Fe that was in the extracellular medium. So, by subtracting the intracellular concentration from particulate, extracellular iron concentrations were obtained. This was done to estimate approximately how much iron is associated with the cells extracellularly.

For $FeCl_3$, the intracellular and particulate filtration was done on the following incubation days; 7, 10, 13, 15, 17, 20, 26. For FeO(OH) experiment, the filtration was done on days; 6, 11, 13, 15, 22, 25. This was done in accordance to cell growth, to see Fe concentrations in different stages of growth. A control for both intracellular and particulate filters were analysed on day 10 giving concentrations of 8.79 nM and 27.98 nM, respectively (Table 5-10).

Table 5-10. Particulate and Intracellular Fe concentrations in control medium.

Sample info	Day	Fe56(MR) Conc. nM
Particulate Fe Control	10	27.98
Intracellular Fe Control	10	8.79

Table 5-11. Particulate, Intracellular and Extracellular Fe concentrations in $FeCl_3$ culture. Iron concentration per cell is calculated from blank corrected Fe56 values that are also corrected for filtration volume, shown in pmol Fe $cell^{-1}$.

$FeCl_3$ Sample info	Day	Fe56(MR) Conc. nM	*p*mol Fe $Cell^{-1}$
Particulate Culture	7	128.04	1.14
	10	99.82	0.85
	13	106.21	0.88
	15	114.92	0.93
	17	91.59	0.71
	20	100.77	0.78
	26	140.30	0.97
Intracellular Culture	10	46.09	0.39
	13	58.38	0.48
	15	58.74	0.48
	17	38.44	0.30
	20	37.25	0.29
	26	56.76	0.39
Extracellular	10	53.73	0.46
	13	47.83	0.40
	15	56.18	0.46
	17	53.15	0.41
	20	63.52	0.49
	26	83.53	0.58

Table 5-12. Particulate, Intracellular Fe concentrations in FeO(OH) culture. Iron concentration per cell is calculated from blank corrected Fe56 values that are also corrected for filtration volume, shown in pmol Fe cell^{-1}.

		Fe56(MR) Conc.	
FeO(OH) Sample info	**Day**	**nM**	***p*mol Fe Cell^{-1}**
Particulate Culture	6	29.30	0.28
	11	29.88	0.22
	13	24.58	0.23
	15	23.01	0.23
	22	36.09	-
	25	23.27	0.20
Intracellular Culture	6	LoD	-
	11	30.36	0.23
	13	LoD	-
	15	LoD	-
	22	37.75	-
	25	78.68	0.67

5.5.1 $FeCl_3$

On day 7, only particulate iron was measured which had a concentration of 128.04 nM. The following measurement day 10 has intracellular Fe concentration of 46.09 nM and the extracellular concentration is slightly above at 53.73 nM. As can be seen from Figure 5-11, on the days 13 and 15 the intracellular Fe concentration is higher than the extracellular Fe and the highest intracellular Fe was recorded on day 15 with 58.74 nM. Thereafter, the intracellular Fe concentration stays below extracellular concentration for days 17, 20 and 26. The highest particulate Fe concentration which is assumed to include intracellular and extracellular Fe was measured on day 26 which had a value of 140.30 nM (Table 5-11).

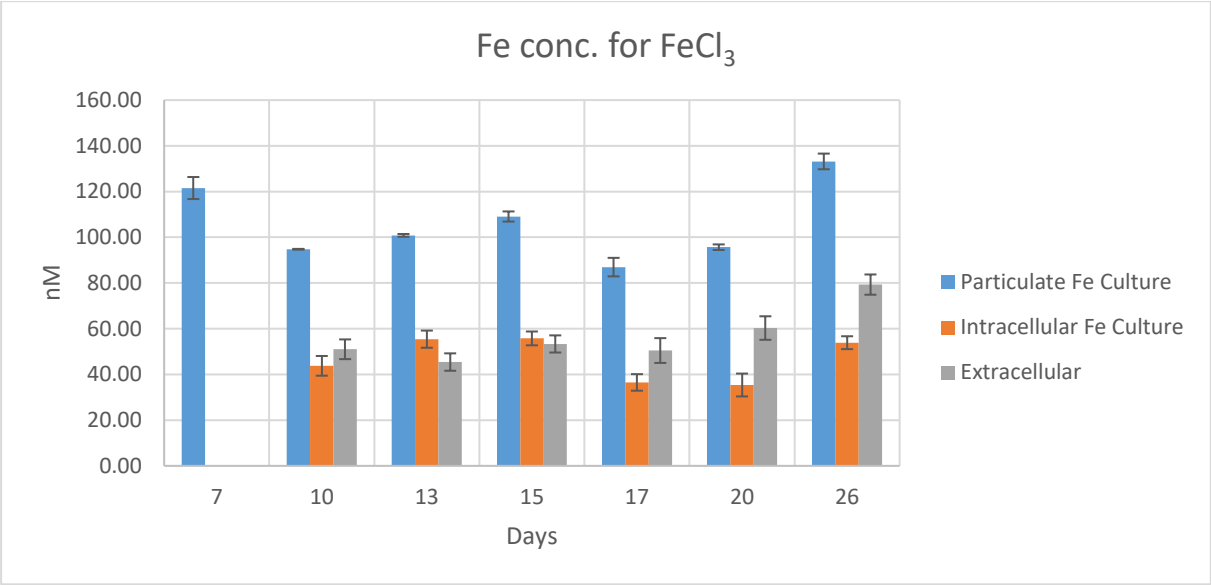

Figure 5-11 Fe concentrations for $FeCl_3$ culture. Particulate, intracellular and extracellular Fe concentrations plotted against incubation days for culture with initial $FeCl_3$ concentration of 50 nM.

The error bars were calculated using standard deviation of the three replicate samples which shows the variations in the data.

5.5.2 FeO(OH)

The following graph shows the changes in particulate, intracellular and extracellular concentrations. On days 6, 13 and 15 the intracellular Fe concentrations were so low that they were below the detection limit which are shown in LoD in Table 5-12. The hypothesised Extracellular Fe values are calculated and found all to be negative so they are not presented. Compared to the $FeCl_3$ culture, significantly less particulate Fe was recorded over the sampling days. Intracellular Fe concentration is more or less steady for to the $FeCl_3$ culture, whereas this trend disappears on FeO(OH) culture with some days intracellular Fe recorded is below detection limit and some days it is close to that of particulate or very high as can be seen on the last day.

On day 11 it can be seen that, the particulate Fe concentration (29.88 nM) and the intracellular Fe concnetration (30.36 nM) are not far away from each other and only differ in 0.48 nM which suggest most of the Fe recorded that day was intracellularly concentrated. The same pattern can also be seen on day 22 where the particulate Fe is measured as 36.09 nM and the intracellular Fe is recorded as 37.75 nM. The highlighted values on day 25 for intracellular Fe are not mentioned in further chapters because the concentration is significantly higher than the particulate Fe which is clearly due to contamination.

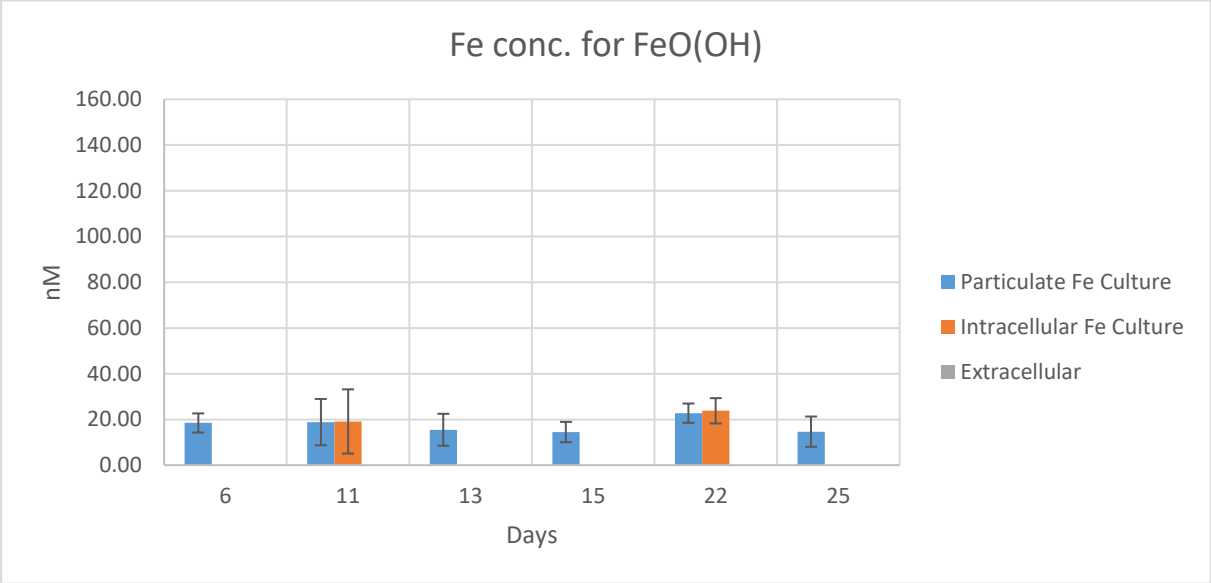

Figure 5-12 Fe concentration for FeO(OH) culture. Particulate, intracellular and Fe concentrations versus incubation days for culture initially having 50 nM of FeO(OH).

The error bars were calculated using standard deviation of the three replicate samples which shows the variations in the data. The error bars on Figure 5-11 and Figure 5-12 show very large variants in both particulate and intracellular Fe, stating low accuracy.

6 Discussion

6.1 Growth

Cells grown in culture with $FeCl_3$ show a steady increase in the number of cells mL^{-1} as can be seen from the Table 5-2, starting from day 1 with 104E+06 number of cells mL^{-1} increasing up to 146E+06 on day 27. Towards the end of the experiment the cells were expressing stress that was observed by the change in the colour of the culture medium from green to a yellowish colour which could explain the decrease in the number of cells to 126E+06 cells mL^{-1} on the final day (28). The culture medium containing FeO(OH), had an initial value of 100E+06 cells mL^{-1} and from thereafter the steady increase followed. However, from day 5 until day 9 there is a decrease in the number of cells mL^{-1} which can be explained by the following. The OD730nm of the cells were measured in the Biotechnology Department at NTNU by a PhD student and each sampling day, the cells would be stored in the fridge until they were collected and measured. The *Synchococcus* strain used in this experiment was a tropical organism which preferred high temperatures such as 38 °C and light 250 μmol photons m^{-2} s^{-1} (optimum temperature and light) as reported by (Ludwig and Bryant, 2012). Considering this, the cell growth might have been halted as a physiological stress response to the cold and dark when they were transferred from their original medium which was around room temperature (25 °C). Additionally, the random decreases in number of cells/mL throughout the experiment is assumed to be resulting from the aforementioned.

When the two cultures are compared, overall, the increase in number of cells/mL for the $FeCl_3$ is higher compared to the cells grown in FeO(OH), with 40% and 18% increase in number of cells mL^{-1} respectively. Additionally, an overall growth trend can be seen on figure 5. where a higher growth over time in cells grown in $FeCl_3$ is observed compared to the cells grown in FeO(OH). This might be due to the differences in their solubility and availability to cells, even though, initially the same concentration of Fe (50nM) was added into the two mediums in the form of $FeCl_3$ and FeO(OH). As mentioned in the previous chapters, $FeCl_3$ is very soluble in water and in contrast, goethite, FeO(OH) is significantly less soluble as with other Fe(III) oxide species (Schwertmann, 1991, PubChem, 2004). Hence $FeCl_3$ would be more bioavailable for cellular uptake which explains why more growth in cells grown in this type of Fe is detected. This conclusion was derived by ignoring the OD730 nm for the last day (day 28) on $FeCl_3$ which is explained above.

An ideal growth curve is shown on Figure 5-3 and from the log growth curve (Figure 5-2) it can be seen that there is already a dense inoculum from the beginning of the experiment and

thereafter, a very slow increase in growth is observed in both cultures. The growth curve on Figure 5-3, consists of different stages of growth; lag, exponential (log), stationary and death phases, respectively. The lag phase is described as the adaptation time of the cells to their new environment before the exponential phase. According to Maier and Pepper (2015), in low inoculum size with 1E+04 cells mL^{-1} the lag phase continues until the cell population reaches 1E+06 cells mL^{-1} which could take about 1.5 days. On the other hand, in higher inoculum size of 1E+07 cells mL^{-1}, the lag phase would be observed for 0.5 days (Maier and Pepper, 2015). This could suggest that since both of the experiments were started with high cell density (1E+08 cells mL^{-1}), the lag phase could have been missed due to cells being measured every 24 hours instead of more frequently such as 12 hours or 8 hours.

Exponential phase or the log phase is the stage where the rate of increase in number of cells in the culture is proportional to the number of cells present any time (Maier and Pepper, 2015). This would mean that a rapid exponential growth in the cell number would be observed. As mentioned with the lag phase, there is already a very high number of cells from incubation day 1 hence, the log phase also cannot be observed for both of the cultures. According to a study done by Samperio-Ramos et al. (2017), a culture added with 50 nM Fe in the form of $FeCl_3$ starts with 7E+04 number of cells mL^{-1} and increases to 7.3E+06 cells mL^{-1} on day 12 which described as the stationary phase (Samperio-Ramos et al., 2017). In this study, the cell number increases significantly over time, whereas in this experiment, there is already a dense culture from day 1 and the increase in number of cells is very slow or not very significant compared to the literature value (Samperio-Ramos et al., 2017). Considering the increase in the number of cells mL^{-1} calculated and literature values, it can be assumed that the cells were in the stationary phase throughout with no or little growth.

6.2 Temperature and pH

Both $FeCl_3$ and FeO(OH) cultures were kept in room temperature (25 ± 2-3 °C) throughout the experiment. A study carried out by Samperio-Ramos et al. (2017), on *Synechococcus* sp. PCC 7002 and Fe, keeps the culture mediums at constant temperature of 25 °C as with this experiment (Samperio-Ramos et al., 2017). However, as previously mentioned, the optimal temperature for *Synechococcus* sp. PCC 7002 is reported as 38 °C (Ludwig and Bryant, 2012). Another study carried out by Wilhelm et al. (1996), maintains a temperature of 37 °C throughout the incubation period (Wilhelm et al., 1996). According to a research done on determining the maximum growth temperature of 8 different *Synechococcus* strains, the

optimum growth temperature of the studied strains is between 30-35 °C (Prihantini et al., 2016). This could suggest that the temperature the mediums were kept at throughout the experiment, might have influenced the growth rates obtained in both, $FeCl_3$ and FeO(OH) cultures.

At the beginning of the experiments, the $FeCl_3$ and FeO(OH) culture pH's were adjusted to 8.00 and 8.06, respectively. This was done to achieve optimum growth, as Silva et al (2017) reports, the maximum growth rate (about 1.4 ± 0.2 day^{-1}) for *Synechococcus* sp. PCC 7002 is observed at pH 8.5 and states that for this specific type of *Cyanobacteria* neutral or slightly alkaline pH (7.5-9.0) would enhance growth (De Farias Silva et al., 2017). Both in $FeCl_3$ and FeO(OH) cultures, a drop in pH from the initial adjusted pH (8.00 and 8.06, respectively) is observed for both culture and control mediums. This could be due to the supply of CO_2 into the medium which resulted in decrease in pH. However, bicarbonate (HCO_3) in the Aquil medium as well as the counter ions, might have prevented the pH from decreasing further down and overall, keeping the pH in equilibrium throughout the incubation period. Hence, no additional buffering system such as bicarbonate buffer or tris was used in the experiment. It was observed that, using a buffer system (bicarbonate or tris) decreases the cell growth hence, no buffer was used to obtain optimum growth (Hunnestad and Vogel, 2017). The pH stayed in equilibrium because to the prepared SOW already had a buffering in it due to buffer based stock solutions as well as HCO_3 being used in the making of the Aquil. The ability of counter ions described as high reactive ions to form buffers is discussed by Silva et al (2017). As a result of the constant CO_2 bubbling, additional bicarbonate ion is formed (HCO_3^-) which in return is neutralised by the charges of counter cation where the cation shifts the equilibrium on Equation 4 to the right until an equilibrium is achieved. Additionally, the now neutralised HCO_3^- is taken up by the *Cyanobacteria* along with P and N ions (De Farias Silva et al., 2017). Hence, counter ions in the salts used in the making of SOW might have formed this buffer system resulting in a pH equilibrium.

$$CO_{2(aq)} + H_2O \overset{k1}{\longleftrightarrow} H_2CO_3^* \overset{k2}{\longleftrightarrow} HCO_3^- + H^+ \overset{k3}{\longleftrightarrow} CO_3^{2-} + 2H^+$$

with dissociation constants $k_1 = 10^{-3.6}, k_2 = 10^{-6.381}, k_3 = 10^{-10.377}$.

Equation 4 Carbonate equilibrium (De Farias Silva et al., 2017).

6.3 Chlorophyll a

Measured chl a concentrations for culture $FeCl_3$ shows a steady increase followed by a sudden drop in chl a µg L^{-1} which lasts for about 10 incubation days. Lis et al. (2015) reports that, in iron limited conditions a decrease in growth rate and decrease in intracellular photosynthetic

pigments including chlorophyll a is observed in *Synechococcus* sp. PCC 7002 (Lis et al., 2015). A similar trend is also reported by Wilhelm et al. (1996) where from the beginning of the experiment the cellular chlorophyll levels slightly increase and show a significant drop thereafter with decreasing Fe availability which is explained as an initial response of *Cyanobacteria* to low levels of iron. After a while, the decline in chlorophyll a, stops and an increase in cellular chlorophyll a is again observed which is thought to be start of a recovery period (Wilhelm et al., 1996). The same pattern is seen on the $FeCl_3$ culture where the low cellular chlorophyll a period is followed by a steep increase. The reason behind the decrease in cellular chlorophyll a with decreasing Fe availability is explained by the enzymes that are involved in chlorophyll biosynthesis being iron-dependent (Wilhelm et al., 1996). This assumption means that the Fe availability in the system directly affects the level of chl a $cell^{-1}$, however no correlation between Chl a (pg) $Cell^{-1}$ and pmol Fe $Cell^{-1}$ is observed in this experiment for culture $FeCl_3$. This could suggest that the data obtained could be resulting from instrumental or human error.

The change in cellular chlorophyll a for FeO(OH) culture follows the aforementioned trend reported by Wilhelm et al. (1996) and the decrease in chlorophyll a is not as sharp as it is observed in $FeCl_3$ culture, it rather follows a steady decline (Wilhelm et al., 1996). However, the relationship between Chl a (pg) $Cell^{-1}$ and pmol Fe $Cell^{-1}$ in FeO(OH) culture could not be observed since there is only one data point for intracellular Fe where the rest of the incubation days, intracellular iron was below the detecting limit. Hence, the direct influence of Fe availability on chlorophyll a is unclear. Hypothetically, if it is assumed that the decline in cellular chlorophyll a is due to lack of Fe availability for both of the cultures, then the response in $FeCl_3$ can be described as more pronounced, showing a larger decline and remaining low for a while. If there was a significant correlation between Chl a (pg) $Cell^{-1}$ and pmol Fe $Cell^{-1}$, it could be stated that both cultures had encountered iron limitation as could be observed from chlorophyll a stress response.

Additionally, when the growth rate and chlorophyll a concentrations are compared, it can be seen that increase in the number of cells/mL does not necessarily increase cellular chlorophyll a concentrations. However, in an axenic culture, a direct relationship between OD and chlorophyll a content is observed where, as OD increases, chlorophyll a content also increases. This is because chlorophyll a is evenly distributed in cells and OD measures the light passing through the solution that is scattered by the cells and its components including, chlorophyll a. Hence the extracted chlorophyll a content measured by fluorescence would have a direct relationship with the measured OD at 730 nm (Held, 2011) . In this case, this relationship could

not be observed due to the cells being on stationary phase. The stationary phase is not necessarily an inactive phase and weather some cells are dying and an equal number of cells are dividing or there is no population growth at all cannot be determined (Kenneth Todar, 2008-2012). Additionally it has been reported that, *Synechococcus* sp. PCC 7002 cells lose their pigments when the death phase is initiated in the stationary growth phase (Sakamoto et al., 1998). Hence, this could suggest that, extracted chlorophyll a concentration does not reflect cell growth during stationary phase.

The mean values calculated for Chl A (pg) $Cell^{-1}$ for $FeCl_3$ culture and FeO(OH) are 509.5 ± 445.85 and 579.55 ± 246.98 Chl A (pg) $Cell^{-1}$, respectively. The higher standard deviation in $FeCl_3$ culture suggests a larger variation in measured values and a slightly smaller mean Chl A (pg) $Cell^{-1}$ compared to the FeO(OH) culture. The more soluble $FeCl_3$ did not result in higher cellular chlorophyll a concentration and the values obtained were in fact similar.

6.4 Intracellular and particulate iron

6.4.1 $FeCl_3$

In $FeCl_3$ culture, due to possible contamination, high concentration of Fe values might have been detected. This assumption is made considering initially only, 50 nM of Fe was added to the culture, however, values above 50 nM for both particulate and intracellular Fe are detected suggesting entrance of Fe to the system, potentially brought by dust during filtration process. The intracellular Fe measured in $FeCl_3$ added control (abiotic) suggest there might be contamination in the medium where Fe concentration of 8.79 nM was measured. When looking at OD730 measurements for this culture, it can be seen that on day 10 when the intracellular Fe sampling was carried out, a reading of 0.002 was recorded which is insignificant and could be due to noise detected by the spectrophotometer. Since there is not significant cell density detected on this day, this suggest that the contamination might have occurred during the treatment of samples with oxalate wash and NaCl rinse.

For both particulate and intracellular Fe, the detected concentrations are significantly high and when looked at variations in chlorophyll a concentration, the sudden decline in chlorophyll a concentration is most likely due to an instrument or human error. The decline in chlorophyll a concentration occurs from day 10 and lasts until day 20 however, high concentrations of intracellular Fe was detected during these days which suggest that the decrease in chlorophyll a could not be due to iron starvation. The first sampling done for intracellular Fe concentration starts from day 10 which is 46.09 nM and from this day there is a small variation in intracellular

Fe concentrations. The calculated Extracellular Fe throughout the sampling days range from 47.83-63.52 nM and 83.53 nM detected on the last sampling day (26). The slow and steady uptake of Fe from day 10 could be due to the cells being in stationary phase. During stationary phase the size of a population remains constant and since, there is not significant growth, the cells might not require as much as Fe as they do during log phase.

6.4.2 FeO(OH)

The intracellular iron for this culture could not be detected on the sampling days 6,13 and 15 because the values were below limit of detection, suggesting no significant cellular iron uptake for these days (Table 5-12). Particulate Fe concentrations detected on the same sampling days are; 29.30, 24.58 and 23.01 nM, respectively. This could imply that there is Fe in the culture medium however, the cells are having a harder time to access this particulate Fe and they need to work harder to utilise and acquire it. The days 11 and 22 where intracellular Fe was detected, all the concentrations were found to slightly higher than the particulate Fe. The detected intracellular Fe concentration should not be higher than the particulate Fe considering particulate concentration includes intracellular and extracellular, and should thus be higher than the separate values. Through the oxalate wash or NaCl rinse process, Fe might have been added to the samples resulting in contamination which gave higher intracellular Fe values. However, the intracellular Fe concentrations are corrected for the oxalate wash filter blanks which removes the influence of the oxalate and NaCl rinse. This suggest that there might be other issues regarding this method which resulted in contamination of intracellular Fe samples.

There are no measurements on intracellular Fe done before day 6 so how much iron was in the cells before then is unknown. Additionally, on day 22, the OD730 nm was not measured due to human error so the Fe uptake per cell cannot be observed in this day. The detected values for intracellular Fe for day 11 is 30.36 nM, 0.23 pmol Fe $Cell^{-1}$ and for day 22 is 37.75 nM. This could mean that, during those days, the cells were able to access and accumulate large amounts of Fe. Hence, due to very high concentrations of intracellular Fe detected in cells, no correlation between the trend in chlorophyll a that could be resulting from lack of Fe and cellular Fe concentration can be observed.

The particulate Fe concentration ranges between 23-30 nM with a higher value detected on day 22 (36.09 nM). Sudden increases in intracellular Fe from LoD to 30.36 nM and to 37.75 could be explained by the following mechanisms. In this case, PilA1 mediated iron reduction could be the Fe acquisition mechanism used by *Synechococcus* sp. PCC 7002. The organism might

have used this mechanism to access the insoluble goethite, FeO(OH) and convert most of the particulate Fe into intracellular Fe which had resulted in detection of higher intracellular Fe concentrations (Lamb et al., 2014).This way the extracellular particle bound Fe(III) is reduced to Fe(II) before it can be taken up by the cells. It can also be suggested that the efficient use of pili mediated iron reduction might be the reason for intracellular Fe concentrations on day 11 and 22. Hence, when there was not sufficient DFe or soluble Fe, the cells were able to utilise and access the particulate bound Fe(III) resulting in sudden increases in intracellular Fe concentrations. According to Årstøl (2017) *Synechococcus* sp. PCC 7002 has genes that seem to code for structural pilin proteins however, the role of these species homologue for the PilA1-gene in *Synechocystis* 6803 is currently being investigated (Årstøl, 2017). Additionally, the details of iron reduction mechanism via pili is unknown such as the electron transporters as mentioned by Lamb et al. (2014) (Lamb et al., 2014).

A siderophore mediated iron acquisition mechanism is also suggested for *Synechococcus* sp. PCC 7002 by Kranzler et al. (2013) involving synechobactin. This photoreactive ligand bound to Fe(III) goes under a light induced charged transfer reaction resulting in reduction of Fe(III) to Fe(II) that is available for cellular uptake (Kranzler et al., 2013).This could be the case for the FeO(OH) culture when there was not sufficient intracellular iron, the cells would produce these siderophores, increase Fe uptake and when the intracellular Fe was used up (photosynthetic activities, growth, etc.), this process would repeat as a stress mechanism which would explain the sudden increase in the intracellular Fe concentrations.

6.4.3 $FeCl_3$ versus FeO(OH)

Compared to the $FeCl_3$ experiment, significantly less particulate Fe is detected for FeO(OH) culture which could be associated with the high solubility of amorphous $FeCl_3$ compared to the morphous goethite, FeO(OH). Additionally in FeO(HO) culture, less intracellular Fe was detected compared to $FeCl_3$ culture which could suggest that the cells were indeed able to take up the more soluble form of Fe better than the less soluble FeO(OH). However, there is still high intracellular Fe detected for cells grown in goethite, FeO(OH) which is explained by the reductive efficiency of *Synechococcus* sp. PCC 7002 via PilA1. Despite the low solubility of goethite mineral the organism was able to acquire Fe through electron transfer and reduction of particulate bound Fe(III) to Fe(II). The efficiency of the pili mediated iron reductive mechanism can be seen from the Fe(II) detected directly from the culture medium by FIA-CL

The formation of Fe(II) was detected for 70% and 67% of the sampling period for cells grown in $FeCl_3$ and goethite (FeO(OH)), respectively. The average concentration of Fe(II) in $FeCl_3$ is 0.46nM ± 0.37 compared to 0.39nM ± 0.35 for cells grown in FeO(OH) culture (Villegas, 2018). When looking at the Fe(II) concentration for both cultures, it can be seen that the overall Fe(II) detected in cell cultures are very low considering 50 nM Fe that was added to the cultures at the beginning of the experiments. This could be due to the cell mediums being at around room temperature which has resulted in very quick oxidation to Fe(III).

No significant information can be obtained from Fe(II) regarding the reductive efficiency of *Synechococcus* sp. PCC 7002 however, from particulate and intracellular Fe concentrations, it can be seen that particulate bound Fe(III) is accessed and utilised by the organism. It is also important to note that no significant total Fe was detected in this experiment and the reason behind this is not clear (Villegas, 2018).

7 Conclusion

This project examined weather iron speciation influences the iron acquisition mechanism in *Synechococcus* sp. PCC 7002. Two different iron species; $FeCl_3$ and goethite (FeO(OH)) in cultures containing *Synechococcus* sp. PCC 7002 were analysed over a 26 and 25 day incubation period, respectively. The optical density (OD730 nm) measurements showed that the cells in both cultures were in stationary phase thus no relationship between chlorophyll a and growth was observed. The results obtained from cells grown in $FeCl_3$ showed that particulate and intracellular Fe were both detected in high concentrations. The variations in chlorophyll a data did not reflect any significant responses about the photosynthetic activity of cells due to instrumental/human error. The culture which had FeO(OH) as the iron source did not have as much as Fe compared to the $FeCl_3$ culture, both particulate and intracellularly detected. Overall, the results suggested that the more soluble $FeCl_3$ is more easily taken up by the cells than the significantly less soluble goethite FeO(OH). However, despite the low solubility of goethite FeO(OH), high intracellular Fe was detected possibly acquired by PilA1 mechanism. Hence, the type of iron mineral (speciation) as well as reductive efficiency of PilA1 mechanism influence the iron acquisition in *Synechococcus* sp. PCC 7002. Furthermore, more research is needed to be carried out to confirm the hypothesis of this project.

8 Future Work

For the future work this project could be improved by making several adjustments. Factors such as light supply must be consistent throughout the experiment. The light source should be known and the responsible person for the laboratory lighting should be informed about the sensitivity of this experiment so that the light is not manipulated by anyone but the person in charge of the experiment. Sensitive biological parameters such as optical density measurements should be done soon after sampling to reduce the adverse effects on cells that could occur from storage time and conditions. Optical density measurements should be carried out in more frequent intervals especially at the beginning of the experiment to observe the important biological changes and growth phases. For future work, the experiment should be started with a small inoculum size in order to detect growth in all stages. The measurements of all parameters including pH and temperature must be consistent and recorded from the beginning of the experiment until the end. The experiments should be carried out in three parallels to produce more analytically accurate data and high repeatability and reproducibility. In this case, this was not possible to do so because the culture mediums were each in 20 L PE bottles which took a large space and the laboratory environment was not spacious. Finally, different minerals of Fe can be used such as; hematite ($Fe_2O_{3)}$ and magnetite (Fe_3O_4) to have a wider understanding of the influence of speciation on PilA1 mechanism and Fe acquisition in *Synechococcus* sp. PCC 7002.

9 Bibliography

ABD-ALLA, M. H. 1998. Growth and siderophore production in vitro of Bradyrhizobium (Lupin) strains under iron limitation. *European Journal of Soil Biology,* 34**,** 99-104.

ACHTERBERG, E. Acid cleaning procedure.

ARMBRUSTER, D. A. & PRY, T. 2008. Limit of Blank, Limit of Detection and Limit of Quantitation. *The Clinical Biochemist Reviews,* 29**,** S49-S52.

ÅRSTØL, E. 2017. *Iron Uptake in the Cyanobacteria*

Synechococcus sp. PCC7002. MS thesis, Norwegian University of Science and Technology.

BALASUBRAMANIAN, R., SHEN, G., BRYANT, D. A. & GOLBECK, J. H. 2006. Regulatory roles for IscA and SufA in iron homeostasis and redox stress responses in the cyanobacterium Synechococcus sp. strain PCC 7002. *J Bacteriol,* 188**,** 3182-91.

BENNER, R. 2011. Loose ligands and available iron in the ocean. *Proceedings of the National Academy of Sciences,* 108**,** 893-894.

BIGELOW, N. Algal Media Recipes. Available: https://ncma.bigelow.org/media/wysiwyg/Algal_recipes/NCMA_algal_medium_Aquil.pdf.

BIOTECHNOLOGY DEPARTMENT, N. 2018. OD730nm correlation with No of Cells per ml.

BOYD, P. & ELLWOOD, M. 2010. The biogeochemical cycle of iron in the ocean. *Nature Geoscience,* 3**,** 675-682.

BOYD, P. W., MACKIE, D. S. & HUNTER, K. A. 2010. Aerosol iron deposition to the surface ocean — Modes of iron supply and biological responses. *Marine Chemistry,* 120**,** 128-143.

BREITBARTH, E., ACHTERBERG, E. P., ARDELAN, M. V., BAKER, A. R., BUCCIARELLI, E., CHEVER, F., CROOT, P. L., DUGGEN, S., GLEDHILL, M., HASSELLÖV, M., HASSLER, C., HOFFMANN, L. J., HUNTER, K. A., HUTCHINS, D. A., INGRI, J., JICKELLS, T., LOHAN, M. C., NIELSDÓTTIR, M. C., SARTHOU, G., SCHOEMANN, V., TRAPP, J. M., TURNER, D. R. & YE, Y. 2010. Iron biogeochemistry across marine systems – progress from the past decade. *Biogeosciences,* 7**,** 1075-1097.

BROWNING, T. J., ACHTERBERG, E. P., YONG, J. C., RAPP, I., UTERMANN, C., ENGEL, A. & MOORE, C. M. 2017. Iron limitation of microbial phosphorus acquisition in the tropical North Atlantic. *Nature Communications,* 8**,** 15465.

CROOT, P. & HELLER, M. 2012. The Importance of Kinetics and Redox in the Biogeochemical Cycling of Iron in the Surface Ocean. *Frontiers in Microbiology,* 3.

DE FARIAS SILVA, C., GRIS, B., SFORZA, E., LA ROCCA, N. & BERTUCCO, A. 2016. *Effects of sodium bicarbonate on biomass and carbohydrate production in Synechococcus PCC 7002*.

DE FARIAS SILVA, C. E., SFORZA, E. & BERTUCCO, A. 2017. Effects of pH and Carbon Source on Synechococcus PCC 7002 Cultivation: Biomass and Carbohydrate Production with Different Strategies for pH Control. *Applied Biochemistry and Biotechnology,* 181**,** 682-698.

DESIGNS, T. 2017. Trilogy Laboratory Fluorometer User's Manual. *In:* 998-7210, P. N. (ed.).

DVOŘÁK, P., CASAMATTA, D. A., POULÍČKOVÁ, A., HAŠLER, P., ONDŘEJ, V. & SANGES, R. 2014. Synechococcus: 3 billion years of global dominance. *Molecular Ecology,* 23**,** 5538-5551.

EGIL SAKSHAUG, G. H. J., KIT M. KOVACS 2009. *Ecosystem Barents Sea,* Trondheim, Tapir Academic Press.

FRISO, G., GIACOMELLI, L., YTTERBERG, A. J., PELTIER, J.-B., RUDELLA, A., SUN, Q. & WIJK, K. J. V. 2004. In-Depth Analysis of the Thylakoid Membrane Proteome of Arabidopsis thaliana Chloroplasts: New Proteins, New Functions, and a Plastid Proteome Database. *The Plant Cell,* 16**,** 478-499.

GEIDER, R. J. & LA ROCHE, J. 1994. The role of iron in phytoplankton photosynthesis, and the potential for iron-limitation of primary productivity in the sea. *Photosynthesis Research,* 39**,** 275-301.

GEOTRACES. 2010. Changing the paradigm on the oceanic iron cycle. *GEOTRACES* [Online]. Available: http://www.geotraces.org/science/science-highlight/1372-iron-oceanic-cycle.

GEOTRACES 2014. Sampling and Sample-handling Protocols for GEOTRACES Cruises. GEOTRACES.

GERRINGA, L. J. A., ALDERKAMP, A.-C., LAAN, P., THURÓCZY, C.-E., DE BAAR, H. J. W., MILLS, M. M., VAN DIJKEN, G. L., HAREN, H. V. & ARRIGO, K. R. 2012. Iron from melting glaciers fuels the phytoplankton blooms in Amundsen Sea (Southern Ocean): Iron biogeochemistry. *Deep Sea Research Part II: Topical Studies in Oceanography,* 71-76**,** 16-31.

HASSLER, C. S. & SCHOEMANN, V. 2009. Discriminating between intra- and extracellular metals using chemical extractions: an update on the case of iron. *Limnology and Oceanography: Methods,* 7**,** 479-489.

HELD, P. 2011. Monitoring of Algal Growth Using Their Intrinsic Properties Available: https://www.biotek.com/resources/application-notes/monitoring-of-algal-growth-using-their-intrinsic-properties/.

HUNNESTAD, A. V. & VOGEL, A. I. M. 2017. *RE: Personal Communication.*

HUNTER, K. A. & BOYD, P. W. 2007. Iron-binding ligands and their role in the ocean biogeochemistry of iron. *Environmental Chemistry,* 4**,** 221-232.

KENNETH TODAR, P. 2008-2012. The Growth of Bacterial Populations. Available: http://textbookofbacteriology.net/growth_3.html.

KRANZLER, C., RUDOLF, M., KEREN, N. & SCHLEIFF, E. 2013. Chapter Three - Iron in Cyanobacteria. *In:* CHAUVAT, F. & CASSIER-CHAUVAT, C. (eds.) *Advances in Botanical Research.* Academic Press.

LAMB, J. J., HILL, R. E., EATON-RYE, J. J. & HOHMANN-MARRIOTT, M. F. 2014. Functional Role of PilA in Iron Acquisition in the Cyanobacterium Synechocystis sp. PCC 6803. *PLOS ONE,* 9**,** e105761.

LANNUZEL, D., VANCOPPENOLLE, M., VAN DER MERWE, P., DE JONG, J., MEINERS, K., GROTTI, M., NISHIOKA, J. & SCHOEMANN, V. 2016. Iron in sea ice: Review and new insights. *Elementa: Science of the Anthropocene* 4**,** 130.

LICHTENTHALER, H. K. & BUSCHMANN, C. 2005. *Chlorophylls and carotenoids: Measurements and characterization by UV-Vis spectroscopy*.

LINDSEY, R. & SCOTT, M. 2010. What are Phytoplankton? *NASA: The Earth Observatory.*

LIS, H., KRANZLER, C., KEREN, N. & SHAKED, Y. 2015. A Comparative Study of Iron Uptake Rates and Mechanisms amongst Marine and Fresh Water Cyanobacteria: Prevalence of Reductive Iron Uptake. *Life,* 5**,** 841-860.

LIS, H., SHAKED, Y., KRANZLER, C., KEREN, N. & MOREL, F. M. M. 2014. Iron bioavailability to phytoplankton: an empirical approach. *The Isme Journal,* 9**,** 1003.

LIU, Y., HOU, S. & ZHANG, Y. 2009. The acid cleaning method of labware for trace element analysis in snow and ice samples.

LUDWIG, M. & BRYANT, D. 2012. Synechococcus sp. Strain PCC 7002 Transcriptome: Acclimation to Temperature, Salinity, Oxidative Stress, and Mixotrophic Growth Conditions. *Frontiers in Microbiology,* 3.

MAIER, R. M. & PEPPER, I. L. 2015. Chapter 3 - Bacterial Growth. *Environmental Microbiology (Third edition).* San Diego: Academic Press.

MARTIN, J. H. *Determination of Particulate Organic Carbon (POC) and Nitrogen (PON) in Seawater* [Online]. Available: http://usjgofs.whoi.edu/eqpac-docs/proto-18.html [Accessed 01/05/2018].

MARTIN, J. H. 1990. Glacial-interglacial CO2 change: The Iron Hypothesis. *Paleoceanography,* 5**,** 1-13.

MILESTONE. 2018. UltraCLAVE

Simultaneous, Fully Automated

Microwave Digestion System. Available: milestonesci.com/wp-content/.../08/UltraCLAVE_Brochure.pdf.

MYERS, J. A., CURTIS, B. S. & CURTIS, W. R. 2013. Improving accuracy of cell and chromophore concentration measurements using optical density. *BMC Biophysics,* 6**,** 4.

NTNU, N. U. O. S. A. T. 2018. Cleanlab cleaning procedure.

PERCIVAL, S. L. & WILLIAMS, D. W. 2014. Chapter Five - Cyanobacteria. *Microbiology of Waterborne Diseases (Second Edition).* London: Academic Press.

PRICE, N. M., HARRISON, G. I., HERING, J. G., HUDSON, R. J., NIREL, P. M. V., PALENIK, B. & MOREL, F. M. M. 1989. Preparation and Chemistry of the Artificial Algal Culture Medium Aquil. *Biological Oceanography,* 6**,** 443-461.

PRIHANTINI, N. B., ADDANA, F., SJAMSURIDZAL, W. & YOKOTA, A. 2016. The effect of temperature on the growth of genus Synechococcus isolated from four Indonesian hot springs and Agathis small lake of Universitas Indonesia. *AIP Conference Proceedings,* 1729**,** 020063.

PUBCHEM 2004. PubChem Compound Database.

RAD, B. 2000. Chelex ® 100 and Chelex 20 Chelating Ion Exchange Resin Instruction Manual. *In:* LABORATORIES, B.-R. (ed.). Alfred Nobel Dr, Hercules CA 94547.

ROSE, A. L., SALMON, T. P., LUKONDEH, T., NEILAN, B. A. & WAITE, T. D. 2005. Use of Superoxide as an Electron Shuttle for Iron Acquisition by the Marine Cyanobacterium Lyngbya majuscula. *Environmental Science & Technology,* 39**,** 3708-3715.

RUDOLF, M., KRANZLER, C., LIS, H., MARGULIS, K., STEVANOVIC, M., KEREN, N. & SCHLEIFF, E. 2015. Multiple modes of iron uptake by the filamentous, siderophore-producing cyanobacterium, Anabaena sp. PCC 7120. *Molecular Microbiology,* 97**,** 577-588.

SAKAMOTO, T., DELGAIZO, V. B. & BRYANT, D. A. 1998. Growth on urea can trigger death and peroxidation of the cyanobacterium Synechococcus sp. strain PCC 7002. *Appl Environ Microbiol,* 64**,** 2361-6.

SAKSHAUG, E., JOHNSEN, G. & KOVACS, K. 2009. Seawater chemistry. *In:* SAKSHAUG, E. (ed.) *Ecosystem Barents Sea.* Trondheim: Tapir Academic Press.

SAMPERIO-RAMOS, G., SANTANA-CASIANO, J. M. & GONZÁLEZ-DÁVILA, M. 2017. Variability in the production of organic ligands, by Synechococcus PCC 7002, under different iron scenarios. *Journal of Oceanography*.

SCHLOSSER, C., ROCHA, C. L. D. L., STREU, P. & CROOT, P. L. 2012. Solubility of iron in the Southern Ocean. *Limnology and Oceanography,* 57**,** 684-697.

SCHOFFMAN, H., LIS, H., SHAKED, Y. & KEREN, N. 2016. Iron–Nutrient Interactions within Phytoplankton. *Frontiers in Plant Science,* 7.

SCHWERTMANN, U. 1991. Solubility and dissolution of iron oxides. *Plant and Soil,* 130**,** 1-25.

SINGH, S. K., KOTAKONDA, A., KAPARDAR, R. K., KANKIPATI, H. K., SREENIVASA RAO, P., SANKARANARAYANAN, P. M., VETAIKORUMAGAN, S. R., GUNDLAPALLY, S. R., NAGAPPA, R. & SHIVAJI, S. 2015. Response of bacterioplankton to iron fertilization of the Southern Ocean, Antarctica. *Frontiers in Microbiology,* 6**,** 863.

SPEER, B. R. Introduction to the Cyanobacteria. *Berkeley University of California.*

SYSTEMS, A. 2018. Vertical Laminar Flow Workstation. *AirClean Systems.*

TAGLIABUE, A., BOWIE, A. R., BOYD, P. W., BUCK, K. N., JOHNSON, K. S. & SAITO, M. A. 2017. The integral role of iron in ocean biogeochemistry. *Nature,* 543**,** 51.

TAYLOR, K. G. & KONHAUSER, K. O. 2011. Iron in Earth Surface Systems: A Major Player in Chemical and Biological Processes. *Elements,* 7**,** 83-88.

THOMAS, D. J., SULLIVAN, S. L., PRICE, A. L. & ZIMMERMAN, S. M. 2005. Common freshwater cyanobacteria grow in 100% CO2. *Astrobiology,* 5**,** 66-74.

TURNER DESIGNS. Frequently Asked Questions About Fluorometric Chlorophyll Analysis.

VILLEGAS, M. 2018. *RE: Iron and Iron(2+) Detection.*

VOGEL, A. I. M., LALE, R. & HOHMANN-MARRIOTT, M. F. 2017. Streamlining recombination-mediated genetic engineering by validating three neutral integration sites in Synechococcus sp. PCC 7002. *Journal of Biological Engineering,* 11**,** 19.

VON DER HEYDEN, B. P., ROYCHOUDHURY, A. N., MTSHALI, T. N., TYLISZCZAK, T. & MYNENI, S. C. B. 2012. Chemically and Geographically Distinct Solid-Phase Iron Pools in the Southern Ocean. *Science,* 338**,** 1199.

WEIER, J. 2001. John Martin. *NASA: Earth Observatory.*

WILHELM, S. W., P., M. D. & G., T. C. 1996. Growth, iron requirements, and siderophore production in iron-limited Synechococcus PCC 72. *Limnology and Oceanography,* 41**,** 89-97.

XUE, H., SIGG, L. & KARI, F. G. 1995. Speciation of EDTA in Natural Waters: Exchange Kinetics of Fe-EDTA in River Water. *Environmental Science & Technology,* 29**,** 59-68.

Appendix A: Fe56 ICP-MS results

Table A1 UltraCLAVE and filter blanks. ICP-MS data for blanks of particulate (water) Fe56 and intracellular (oxalate wash water) Fe56 and UltraClave blank values, dilution corrected.

		Final dilute after digestion				
		Density 0.6M HNO3 = 1.0167				**Fe56(MR)**
	Initial filter vol.	**Final vol. (mL)**				**Conc.**
Date	**mL**	**28.32**	**Sample info**		**µg L^{-1}**	**RSD, %**
		49.03	Blank UltraClave		0.15	13.00
		49.68			0.10	6.80
		47.39			0.12	3.50
		47.80			0.09	1.90
		50.00			0.12	3.80
		47.21			0.07	12.60
				Average	0.11	6.93
30/03/2018	25	47.92	Particulate water blank 25 mL		0.78	0.70
30/03/2018	25	71.41			0.72	5.60
30/03/2018	25	47.28			0.55	3.00
				Average	0.68	3.10
30/03/2018	25	48.05	oxalate wash water blank 25mL		1.72	2.20

30/03/2018	25	48.02			2.31	4.40
30/03/2018	25	48.38			1.27	1.60
				Average	1.77	2.73
			Blank UltraClave For filter 70+ (03/04/18)+		0.17	5.00
					0.10	5.00
					0.25	5.00
				Average	0.17	5.00

Table A2 Particulate and Intracellular Fe ICP-MS results for $FeCl_3$ and FeO(OH) culture. ICP-MS data of particulate and intracellular Fe56 for $FeCl_3$ (Aquil) and FeO(OH) (goethite) culture and control given in µg/L and calculated values from final volume in nM. Values below limit of detection reported as LoD.

		Initial filter vol.	**Final dilute after digestion Density 0.6M HNO3 = 1.0167**		**INTIAL MEASURMENT Fe56(MR) Conc.**		**FINAL CALCULATED Fe56(MR) Conc.**	
Date	**Day**	**mL**	**Final vol. (mL) 28.32**	**Sample info**	**µg L^{-1}**	**RSD, %**	**µg L^{-1}**	**nM**
06/03/2018	7	50	48.10	Aquil Culture particulate 50 mL	9.40	2.00	8.29	30.65
06/03/2018	7	25	47.41	Aquil Culture particulate 25 mL	4.74	1.10	7.49	27.70
06/03/2018	7	25	48.39	Aquil Culture particulate 25 mL	3.76	3.40	5.74	21.23
09/03/2018	10	25	48.24	Aquil Abiotic control particulate 25 mL	1.61	2.50	1.59	5.88
09/03/2018	10	25	48.24	Aquil Abiotic control particulate 25 mL	1.62	0.90	1.61	5.95

09/03/2018	10	25	48.46	Aquil Abiotic control particulate 25 mL	1.57	2.70	1.51	5.59
09/03/2018	10	25	48.57	Aquil Abiotic control particulate 25 mL	1.59	2.60	1.56	5.76
09/03/2018	10	25	47.81	Aquil Abiotic control intracellular oxalate wash	2.07	2.70	0.37	1.37
09/03/2018	10	25	48.63	Aquil Abiotic control intracellular oxalate wash	2.07	0.80	0.37	1.35
09/03/2018	10	25	48.18	Aquil Abiotic control intracellular oxalate wash	2.26	4.80	0.74	2.74
09/03/2018	10	20	49.27	Aquil Culture particulate 20 mL	2.94	2.80	5.28	19.55
09/03/2018	10	30	49.33	Aquil Culture particulate 30 mL	4.15	1.10	5.52	20.44
09/03/2018	10	25	47.73	Aquil Culture particulate 25 mL	3.91	2.60	5.96	22.05
09/03/2018	10	25	47.42	Aquil Culture intracellular oxalate wash	3.65	2.20	3.36	12.41
09/03/2018	10	25	47.51	Aquil Culture intracellular oxalate wash	3.53	1.10	3.15	11.64
09/03/2018	10	25	48.05	Aquil Culture intracellular oxalate wash	2.52	3.40	1.24	4.59
12/03/2018	13	25	47.60	Aquil Culture particulate 25 mL	3.92	1.00	5.96	22.04
12/03/2018	13	25	47.37	Aquil Culture particulate 25 mL	4.01	2.00	6.11	22.60
12/03/2018	13	25	48.04	Aquil Culture particulate 25 mL	3.80	1.50	5.78	21.38
12/03/2018	13	25	48.63	Aquil Culture intracellular oxalate wash	4.16	3.50	4.44	16.43
12/03/2018	13	25	53.49	Aquil Culture intracellular oxalate wash	3.14	3.20	2.71	10.01
12/03/2018	13	25	47.49	Aquil Culture intracellular oxalate wash	3.28	0.70	2.66	9.84
14/03/2018	15	25	47.65	Aquil Culture particulate 25 mL	4.32	2.40	6.74	24.92

14/03/2018	15	25	48.19	Aquil Culture particulate 25 mL	3.77	2.80	5.74	21.25
14/03/2018	15	25	48.28	Aquil Culture particulate 25 mL	4.32	2.80	6.83	25.25
14/03/2018	15	25	47.32	Aquil Culture intracellular oxalate wash	3.46	2.70	3.00	11.10
14/03/2018	15	25	48.25	Aquil Culture intracellular oxalate wash	3.25	1.60	2.66	9.83
14/03/2018	15	25	47.54	Aquil Culture intracellular oxalate wash	4.09	2.10	4.21	15.58
16/03/2018	17	25	49.36	Aquil Culture particulate 25 mL	3.82	3.00	5.97	22.10
16/03/2018	17	25	47.75	Aquil Culture particulate 25 mL	3.68	2.30	5.52	20.43
16/03/2018	17	25	48.42	Aquil Culture particulate 25 mL	2.80	1.40	3.89	14.40
16/03/2018	17	25	48.09	Aquil Culture intracellular oxalate wash	2.49	3.30	1.18	4.38
16/03/2018	17	25	47.62	Aquil Culture intracellular oxalate wash	3.00	1.50	2.14	7.90
16/03/2018	17	25	47.83	Aquil Culture intracellular oxalate wash	3.52	1.60	3.14	11.61
19/03/2018	20	25	48.31	Aquil Culture particulate 25 mL	3.78	0.50	5.77	21.36
19/03/2018	20	25	47.33	Aquil Culture particulate 25 mL	3.57	3.10	5.27	19.49
19/03/2018	20	25	49.30	Aquil Culture particulate 25 mL	3.78	1.50	5.89	21.78
19/03/2018	20	25	47.97	Aquil Culture intracellular oxalate wash	3.48	3.60	3.07	11.35
19/03/2018	20	25	47.87	Aquil Culture intracellular oxalate wash	3.26	3.90	2.65	9.79
19/03/2018	20	25	48.74	Aquil Culture intracellular oxalate wash	2.16	0.80	0.54	2.02
25/03/2018	26	25	49.44	Aquil Culture particulate 25 mL	4.30	1.70	6.94	25.69
25/03/2018	26	25	48.57	Aquil Culture particulate 25 mL	4.82	0.90	7.83	28.96
25/03/2018	26	25	48.88	Aquil Culture particulate 25 mL	5.29	1.80	8.80	32.54
25/03/2018	26	25	48.93	Aquil Culture intracellular oxalate wash	3.70	1.00	3.56	13.18

25/03/2018	26	25	47.68	Aquil Culture intracellular oxalate wash	3.80	1.10	3.67	13.57
25/03/2018	26	25	47.40	Aquil Culture intracellular oxalate wash	3.09	0.30	2.30	8.53
25/03/2018	6	25	47.30	Goethite Culture particulate 25 mL	1.48	4.10	1.31	14.70
25/03/2018	6	25	48.98	Goethite Culture particulate 25 mL	1.60	5.90	1.58	17.74
25/03/2018	6	25	47.54	Goethite Culture particulate 25 mL	1.86	3.70	2.04	22.96
25/03/2018	6	25	47.66	Goethite Culture intracellular oxalate wash	0.89	3.00	LoD	LoD
25/03/2018	6	25	50.95	Goethite Culture intracellular oxalate wash	0.94	3.80	LoD	LoD
25/03/2018	6	25	47.54	Goethite Culture intracellular oxalate wash	0.96	1.50	LoD	LoD
30/03/2018	11	25	48.21	Goethite Culture particulate 25 mL	1.24	1.70	0.86	9.69
30/03/2018	11	25	47.98	Goethite Culture particulate 25 mL	2.17	2.70	2.64	29.72
30/03/2018	11	25	47.21	Goethite Culture particulate 25 mL	1.59	2.50	1.52	17.08
30/03/2018	11	25	47.95	Goethite Culture intracellular oxalate wash	2.29	4.60	0.78	8.80
30/03/2018	11	25	49.47	Goethite Culture intracellular oxalate wash	3.46	1.90	3.12	35.12
30/03/2018	11	25	48.14	Goethite Culture intracellular oxalate wash	2.50	2.20	1.20	13.48
01/04/2018	13	25	48.49	Goethite Culture particulate 25 mL	1.61	1.50	1.59	17.95
01/04/2018	13	25	48.20	Goethite Culture particulate 25 mL	1.14	1.90	0.68	7.61
01/04/2018	13	25	49.03	Goethite Culture particulate 25 mL	1.74	2.00	1.86	20.91
01/04/2018	13	25	49.08	Goethite Culture intracellular oxalate wash	0.89	1.70	LoD	LoD
01/04/2018	13	25	47.31	Goethite Culture intracellular oxalate wash	1.06	2.00	LoD	LoD
01/04/2018	13	25	47.62	Goethite Culture intracellular oxalate wash	1.16	2.60	LoD	LoD
03/04/2018	15	25	47.64	Goethite Culture particulate 25 mL	1.62	0.80	1.45	16.35

03/04/2018	15	25	47.64	Goethite Culture particulate 25 mL	1.68	3.70	1.57	17.71
03/04/2018	15	25	47.31	Goethite Culture particulate 25 mL	1.30	1.20	0.84	9.42
03/04/2018	15	25	48.08	Goethite Culture particulate 25 mL	1.53	2.90	1.29	14.52
03/04/2018	15	25	47.76	Goethite Culture intracellular oxalate wash	0.95	3.80	LoD	LoD
03/04/2018	15	25	47.93	Goethite Culture intracellular oxalate wash	1.38	3.30	LoD	LoD
03/04/2018	15	25	47.99	Goethite Culture intracellular oxalate wash	1.62	2.90	LoD	LoD
10/04/2018	22	25	47.34	Goethite Culture particulate 25 mL	2.11	2.90	2.37	26.69
10/04/2018	22	25	47.39	Goethite Culture particulate 25 mL	1.94	1.20	2.06	23.23
10/04/2018	22	25	47.82	Goethite Culture particulate 25 mL	1.71	1.90	1.63	18.31
10/04/2018	22	25	48.44	Goethite Culture intracellular oxalate wash	2.87	1.40	1.79	20.17
10/04/2018	22	25	47.96	Goethite Culture intracellular oxalate wash	3.34	1.40	2.68	30.16
10/04/2018	22	25	48.02	Goethite Culture intracellular oxalate wash	2.92	1.10	1.87	21.05
13/04/2018	25	25	47.78	Goethite Culture particulate 25 mL	1.87	3.00	1.94	21.80
13/04/2018	25	25	47.77	Goethite Culture particulate 25 mL	1.48	2.50	1.20	13.48
13/04/2018	25	25	47.56	Goethite Culture particulate 25 mL	1.26	3.20	0.77	8.71
13/04/2018	25	25	48.14	Goethite Culture intracellular oxalate wash	1.14	3.50	LoD	LoD
13/04/2018	25	25	47.64	Goethite Culture intracellular oxalate wash	4.26	1.60	4.41	49.59
13/04/2018	25	25	47.46	Goethite Culture intracellular oxalate wash	1.70	2.60	LoD	LoD

Appendix B: Chlorophyll a results

Table B1 In vivo Chlorophyll a for $FeCl_3$ culture. Readings for $FeCl_3$ culture and control, including blank (100% methanol) readings.

			Culture $FeCl_3$				Abiotic $FeCl_3$			
Date	**Day**	**Blank (100% methanol)**	**1**	**2**	**3**	**mean**	**1**	**2**	**3**	**mean**
01/03/2018	2	107.23	568.02	483.76	602.96	551.58	73.42	72.27	90.41	78.70
02/03/2018	3	105.20	776.74	1071.08	1049.94	965.92	103.12	79.57	69.55	84.08
03/03/2018	4	77.10	1244.23	1826.82	1966.68	1679.24	84.36	85.02	61.64	77.01
04/03/2018	5	77.10	1686.83	1926.95	1930.52	1848.10	84.36	85.02	61.64	77.01
05/03/2018	6	89.90	2025.00	1050.77	691.54	1255.77	130.41	139.08	107.55	125.68
06/03/2018	7	92.09	1682.33	1982.60	1874.64	1846.52	97.19	112.34	140.77	116.77
07/03/2018	8	111.87	1811.09	1298.17	2077.67	1728.98	107.19	108.75	107.06	107.67
08/03/2018	9	113.86	1930.81	2376.37	2006.18	2104.45	115.90	104.37	103.72	108.00
09/03/2018	10	102.97	338.18	348.05	339.71	341.98	139.12	126.20	130.18	131.83
10/03/2018	11	93.57	325.85	256.54	315.60	299.33	120.35	112.50	114.99	115.95
11/03/2018	12	112.43	270.21	234.44	293.66	266.10	107.63	105.71	104.55	105.96
12/03/2018	13	108.45	304.60	326.16	267.97	299.58	135.51	162.35	126.49	141.45
13/03/2018	14	108.45	246.22	394.79	255.76	298.92	129.61	156.66	133.14	139.80
14/03/2018	15	108.45	315.66	388.94	408.12	370.91	123.43	131.82	169.21	141.49
15/03/2018	16	108.45	291.51	337.47	328.04	319.01	175.46	139.19	172.65	162.43
16/03/2018	17	103.02	233.70	286.15	210.09	243.31	143.21	136.71	138.98	139.63
17/03/2018	18	109.43	304.82	299.15	260.08	288.02	131.63	124.19	159.29	138.37

18/03/2018	19	108.21	199.21	248.82	286.47	244.83	128.58	117.96	115.60	120.71
19/03/2018	20	108.21	386.49	436.91	270.50	364.63	113.72	114.57	114.99	114.43
20/03/2018	21	138.31	255.88	396.03	396.46	349.46	122.81	114.55	108.03	115.13
21/03/2018	22	138.31	1388.66	1988.25	1500.81	1625.91	111.25	115.78	119.84	115.62
22/03/2018	23	138.31	1749.88	1924.68	2345.81	2006.79				
23/03/2018	24	138.31	1662.98	2316.09	2321.09	2100.05				
24/03/2018	25	101.36	2007.73	1901.12	269.11	1392.65				

Table B2 Converted Chlorophyll a (extracted) for $FeCl_3$. Readings for $FeCl_3$ culture and control, including blank (100% methanol) values.

			Culture $FeCl_3$				Abiotic $FeCl_3$			
Date	**Day**	**Blank (100% methanol)**	**1**	**2**	**3**	**mean**	**1**	**2**	**3**	**mean**
01/03/2018	2	1.73	9.18	7.82	9.74	8.91	1.19	1.17	1.46	1.27
02/03/2018	3	1.70	12.55	17.30	16.96	15.60	1.67	1.29	1.12	1.36
03/03/2018	4	1.25	20.10	29.51	31.77	27.13	1.36	1.37	1.00	1.24
04/03/2018	5	1.25	27.25	31.13	31.19	29.86	1.36	1.37	1.00	1.24
05/03/2018	6	1.45	32.71	16.98	11.17	20.29	2.11	2.25	1.74	2.03
06/03/2018	7	1.49	27.18	32.03	30.28	29.83	1.57	1.81	2.27	1.89
07/03/2018	8	1.81	29.26	20.97	33.56	27.93	1.73	1.76	1.73	1.74
08/03/2018	9	1.84	31.19	38.39	32.41	34.00	1.87	1.69	1.68	1.74
09/03/2018	10	1.66	5.46	5.62	5.49	5.52	2.25	2.04	2.10	2.13
10/03/2018	11	1.51	5.26	4.14	5.10	4.84	1.94	1.82	1.86	1.87

11/03/2018	12	1.82	4.37	3.79	4.74	4.30	1.74	1.71	1.69	1.71
12/03/2018	13	1.75	4.92	5.27	4.33	4.84	2.19	2.62	2.04	2.29
13/03/2018	14	1.75	3.98	6.38	4.13	4.83	2.09	2.53	2.15	2.26
14/03/2018	15	1.75	5.10	6.28	6.59	5.99	1.99	2.13	2.73	2.29
15/03/2018	16	1.75	4.71	5.45	5.30	5.15	2.83	2.25	2.79	2.62
16/03/2018	17	1.66	3.78	4.62	3.39	3.93	2.31	2.21	2.25	2.26
17/03/2018	18	1.77	4.92	4.83	4.20	4.65	2.13	2.01	2.57	2.24
18/03/2018	19	1.75	3.22	4.02	4.63	3.96	2.08	1.91	1.87	1.95
19/03/2018	20	1.75	6.24	7.06	4.37	5.89	1.84	1.85	1.86	1.85
20/03/2018	21	2.23	4.13	6.40	6.40	5.65	1.98	1.85	1.75	1.86
21/03/2018	22	2.23	22.43	32.12	24.25	26.27	1.80	1.87	1.94	1.87
22/03/2018	23	2.23	28.27	31.09	37.90	32.42				
23/03/2018	24	2.23	26.87	37.42	37.50	33.93				
24/03/2018	25	1.64	32.43	30.71	4.35	22.50				

Table B3 Calculated Chlorophyll a for $FeCl_3$ culture and control. Values in µg/L and chl a (pg) $cell^{-1}$.

		Culture $FeCl_3$				Abiotic $FeCl_3$				
Date	**Day**	**1**	**2**	**3**	**mean**	**1**	**2**	**3**	**mean**	**Chl a (pg) $Cell^{-1}$**
01/03/2018	2	33.50	27.37	36.04	32.30	-2.46	-2.54	-1.22	-2.07	307.65
02/03/2018	3	48.82	70.22	68.68	62.57	-0.15	-1.86	-2.59	-1.54	595.92
03/03/2018	4	84.85	127.20	137.37	116.47	0.53	0.58	-1.12	-0.01	1058.82
04/03/2018	5	117.02	134.48	134.74	128.75	0.53	0.58	-1.12	-0.01	1159.87
05/03/2018	6	140.68	69.85	43.74	84.76	2.94	3.58	1.28	2.60	770.50
06/03/2018	7	115.61	137.43	129.59	127.54	0.37	1.47	3.54	1.79	1138.77
07/03/2018	8	123.53	86.24	142.91	117.56	-0.34	-0.23	-0.35	-0.31	1004.77
08/03/2018	9	132.09	164.48	137.57	144.71	0.15	-0.69	-0.74	-0.43	1280.62
09/03/2018	10	17.10	17.82	17.21	17.38	2.63	1.69	1.98	2.10	147.87
10/03/2018	11	16.89	11.85	16.14	14.96	1.95	1.38	1.56	1.63	130.07
11/03/2018	12	11.47	8.87	13.17	11.17	-0.35	-0.49	-0.57	-0.47	94.27
12/03/2018	13	14.26	15.83	11.60	13.89	1.97	3.92	1.31	2.40	114.83
13/03/2018	14	10.02	20.82	10.71	13.85	1.54	3.50	1.79	2.28	118.35
14/03/2018	15	15.06	20.39	21.79	19.08	1.09	1.70	4.42	2.40	155.12
15/03/2018	16	13.31	16.65	15.96	15.31	4.87	2.23	4.67	3.92	119.58
16/03/2018	17	9.50	13.31	7.78	10.20	2.92	2.45	2.61	2.66	79.06
17/03/2018	18	14.20	13.79	10.95	12.98	1.61	1.07	3.62	2.10	99.48
18/03/2018	19	6.62	10.22	12.96	9.93	1.48	0.71	0.54	0.91	73.57

19/03/2018	20	20.23	23.90	11.80	18.64	0.40	0.46	0.49	0.45	143.39
20/03/2018	21	8.55	18.74	18.77	15.35	-1.13	-1.73	-2.20	-1.69	119.92
21/03/2018	22	90.90	134.48	99.05	108.14	-1.97	-1.64	-1.34	-1.65	835.09
22/03/2018	23	117.16	129.86	160.48	135.83					987.87
23/03/2018	24	110.84	158.32	158.68	142.61					1033.42
24/03/2018	25	138.59	130.84	12.19	93.87					661.08

Table B4 In vivo Chlorophyll a for FeO(OH) culture. Readings for $FeCl_3$ culture and control, including blank (100% methanol) readings

			Culture FeO(OH)				Abiotic FeO(OH)			
Date	**Day**	**Blank (100% methanol)**	**1**	**2**	**3**	**mean**	**1**	**2**	**3**	**mean**
20/03/2018	1	138.31	189.64	130.66	127.25	149.18	105.44	109.84	113.68	109.65
21/03/2018	2	138.31	814.23	903.43	732.63	816.76	150.64	150.46	150.33	150.48
22/03/2018	3	138.31	1324.06	1260.54	1392.67	1325.76				
23/03/2018	4	138.31	1466.18	1691.34	1598.83	1585.45				
24/03/2018	5	101.36	295.54	1367.81	1616.52	1093.29				
25/03/2018	6	101.36	1873.25	2358.72	235.47	1489.15				
26/03/2018	7	136.97	1321.70	1740.14	1502.89	1521.58				
27/03/2018	8	136.97	1758.53	2055.32	1683.11	1832.32				
28/03/2018	9	98.64	1752.05	2250.30	1080.50	1694.28				
29/03/2018	10	84.44	1567.92	2212.62	934.01	1571.52				
30/03/2018	11	79.13	1631.22	1691.84	1014.12	1445.73				

31/03/2018	12	118.76	1499.41	1482.37	993.25	1325.01
01/04/2018	13	75.36	926.56	1383.74	1523.14	1277.81
02/04/2018	14	91.18	1348.04	1361.48	1240.94	1316.82
03/04/2018	15	114.32	1422.75	948.09	1006.48	1125.77
04/04/2018	16	128.41	1323.12	1332.28	1119.99	1258.46
05/04/2018	17	128.41	1412.37	1225.08	926.53	1187.99
06/04/2018	18	128.41	1221.34	1462.99	1438.37	1374.23
07/04/2018	19	128.41	561.23	1052.88	1309.51	974.54
08/04/2018	20	128.41	940.81	912.11	1198.29	1017.07
09/04/2018	21	128.41	1065.50	1319.91	1203.39	1196.27
10/04/2018	22	128.41	939.62	1055.33	987.40	994.12
11/04/2018	23	128.41	1899.25	1777.31	2568.38	2081.65
12/04/2018	24	128.41	1867.81	2637.24	1228.31	1911.12

Table B5 Converted Chlorophyll a (extracted) for FeO(OH). Readings for $FeCl_3$ culture and control, including blank (100% methanol) values

			Culture FeO(OH)				Abiotic FeO(OH)			
Date	**Day**	**Blank (100% methanol)**	**1**	**2**	**3**	**mean**	**1**	**2**	**3**	**mean**
20/03/2018	1	2.23	3.06	2.11	2.06	2.41	1.70	1.77	1.84	1.77
21/03/2018	2	2.23	13.15	14.59	11.84	13.19	2.43	2.43	2.43	2.43
22/03/2018	3	2.23	21.39	20.36	22.50	21.42				
23/03/2018	4	2.23	23.69	27.32	25.83	25.61				

24/03/2018	5	1.64	4.77	22.10	26.11	17.66
25/03/2018	6	1.64	30.26	38.10	3.80	24.06
26/03/2018	7	2.21	21.35	28.11	24.28	24.58
27/03/2018	8	2.21	28.41	33.20	27.19	29.60
28/03/2018	9	1.59	28.30	36.35	17.46	27.37
29/03/2018	10	1.36	25.33	35.74	15.09	25.39
30/03/2018	11	1.28	26.35	27.33	16.38	23.36
31/03/2018	12	1.92	24.22	23.95	16.05	21.41
01/04/2018	13	1.22	14.97	22.35	24.61	20.64
02/04/2018	14	1.47	21.78	21.99	20.05	21.27
03/04/2018	15	1.85	22.98	15.32	16.26	18.19
04/04/2018	16	2.07	21.37	21.52	18.09	20.33
05/04/2018	17	2.07	22.82	19.79	14.97	19.19
06/04/2018	18	2.07	19.73	23.63	23.24	22.20
07/04/2018	19	2.07	9.07	17.01	21.15	15.74
08/04/2018	20	2.07	15.20	14.74	19.36	16.43
09/04/2018	21	2.07	17.21	21.32	19.44	19.33
10/04/2018	22	2.07	15.18	17.05	15.95	16.06
11/04/2018	23	2.07	30.68	28.71	41.49	33.63
12/04/2018	24	2.07	30.17	42.60	19.84	30.87

Table B6 Calculated Chlorophyll a for FeO(OH) culture and control. Values in µg/L and chl a (pg) cell^{-1}.

		Culture FeO(OH)				Abiotic FeO(OH)				
Date	**Day**	**1**	**2**	**3**	**mean**	**1**	**2**	**3**	**mean**	**Chl A (pg) Cell^{-1}**
20/03/2018	1	3.73	-0.56	-0.80	0.79	-2.39	-2.07	-1.79	-2.08	7.90
21/03/2018	2	49.14	55.62	43.21	49.32	0.90	0.88	0.87	0.88	469.73
22/03/2018	3	86.20	81.58	91.19	86.32					814.37
23/03/2018	4	96.53	112.90	106.18	105.20					960.75
24/03/2018	5	14.12	92.07	110.15	72.11					680.28
25/03/2018	6	128.81	164.10	9.75	100.89					956.28
26/03/2018	7	86.13	116.55	99.30	100.66					949.59
27/03/2018	8	117.88	139.46	112.40	123.25					951.71
28/03/2018	9	120.20	156.42	71.38	116.00					1099.51
29/03/2018	10	107.84	154.71	61.76	108.11					825.23
30/03/2018	11	112.83	117.24	67.97	99.35					746.97
31/03/2018	12	100.37	99.13	63.57	87.69					790.00
01/04/2018	13	61.88	95.12	105.25	87.41					813.16
02/04/2018	14	91.37	92.35	83.58	89.10					771.43
03/04/2018	15	95.12	60.61	64.86	73.53					720.88
04/04/2018	16	86.85	87.52	72.08	82.15					764.20
05/04/2018	17	93.34	79.72	58.02	77.03					672.74
06/04/2018	18	79.45	97.02	95.23	90.57					764.28

07/04/2018	19	31.46	67.21	85.86	61.51		534.88
08/04/2018	20	59.06	56.97	77.78	64.60		545.17
09/04/2018	21	68.12	86.62	78.15	77.63		636.31
10/04/2018	22	58.97	67.38	62.45	62.93		
11/04/2018	23	128.73	119.87	177.38	141.99		1234.73
12/04/2018	24	126.45	182.38	79.96	129.60		

Appendix C: pH and temperature measurements

Table C1 Recorded pH and temperature values for $FeCl_3$ culture and control.

			Culture pH				Abiotic pH			
Date	**Day**	**Temperature ºC**	**1**	**2**	**3**	**mean**	**1**	**2**	**3**	**mean**
27/02/2018	0		8.00	-	-	8.00	8.00	-	-	8.00
12/03/2018	13		7.72	7.65	7.67	7.68	7.66	7.7	7.62	7.65
13/03/2018	14		7.58	7.58	7.57	7.58	7.54	7.5	7.53	7.53
14/03/2018	15		7.62	7.61	7.6	7.61	7.59	7.6	7.58	7.58
15/03/2018	16		7.78	7.76	7.76	7.77	7.8	7.8	7.78	7.79
16/03/2018	17		7.76	7.76	7.73	7.75	7.69	7.7	7.68	7.68
17/03/2018	18		7.79	7.76	7.75	7.77	7.76	7.7	7.73	7.74
18/03/2018	19		7.73	7.74	7.73	7.73	7.72	7.7	7.7	7.71
19/03/2018	20		7.71	7.69	7.69	7.70	7.6	7.6	7.61	7.60
20/03/2018	21	25.42	7.64	7.65	7.61	7.63	7.52	7.5	7.52	7.52
21/03/2018	22	25.30	7.64	-	-	7.64	7.62	-	-	7.62
22/03/2018	23	25.70	7.49	-	-	7.49	7.56	-	-	7.56
23/03/2018	24	26.30	7.63	-	-	7.63	7.62	-	-	7.62
24/03/2018	25	24.90	7.65	7.57	7.55	7.59	7.68	7.7	7.65	7.68
25/03/2018	26	25.40	7.63	7.63	7.60	7.62	7.54	7.5	7.5	7.52
26/03/2018	27	24.90	7.70	7.66	7.66	7.67	7.66	7.7	7.69	7.68
27/03/2018	28	24.00	7.67	7.66	7.64	7.66	7.55	7.7	7.6	7.60

28/03/2018	29	24.40	7.65	7.65	7.62	7.64	7.29	7.4	7.41	7.37

Table C2 Recorded pH and temperature values for FeO(OH) culture and control.

			Culture pH				Abiotic pH			
Date	**Day**	**Temperature ºC**	**1**	**2**	**3**	**mean**	**1**	**2**	**3**	**mean**
19/03/2018	0	-	8.06	-	-	8.06	8.06	-	-	8.06
20/03/2018	1	25.42	7.6	7.58	7.56	7.58	7.6	7.6	7.6	7.60
21/03/2018	2	25.30	7.58	-	-	7.58	7.58	-	-	7.58
22/03/2018	3	25.70	7.58	-	-	7.58	7.53	-	-	7.56
23/03/2018	4	26.30	7.48	-	-	7.48	7.58	-	-	7.51
24/03/2018	5	24.90	7.23	7.27	7.28	7.26	7.45	7.43	7.47	7.45
25/03/2018	6	25.40	7.47	7.43	7.41	7.44	7.60	7.59	7.58	7.59
26/03/2018	7	24.90	7.5	7.47	7.47	7.48	7.70	7.67	7.66	7.68
27/03/2018	8	24.00	7.44	7.46	7.42	7.44	7.69	7.68	7.68	7.68
28/03/2018	9	24.40	7.52	7.45	7.49	7.49	7.63	7.65	7.66	7.65
29/03/2018	10	24.10	7.25	7.34	7.34	7.31	7.62	7.63	7.61	7.62
30/03/2018	11	24.90	7.33	7.27	7.27	7.29	7.45	7.49	7.35	7.43
31/03/2018	12	23.60	7.42	7.47	7.44	7.44	7.45	7.48	7.37	7.43
01/04/2018	13	25.40	7.46	7.44	7.42	7.44	7.59	7.62	7.61	7.61
02/04/2018	14	24.10	7.45	7.43	7.44	7.44	7.68	7.65	7.64	7.66

03/04/2018	15	24.40	7.44	7.41	7.39	7.41	7.72	7.68	7.66	7.69
04/04/2018	16	24.80	7.46	7.44	7.42	7.44	7.94	7.88	7.83	7.88
05/04/2018	17	26.80	7.21	-	-	7.21	7.56	-	-	7.56
06/04/2018	18	24.60	7.41	-	-	7.41	7.56	-	-	7.56
07/04/2018	19	24.40	7.36	-	-	7.36	7.52	-	-	7.52
08/04/2018	20	24.60	7.38	-	-	7.38	7.55	-	-	7.55
09/04/2018	21	24.90	7.37	-	-	7.37	7.52	-	-	7.52
10/04/2018	22	24.30	7.37	-	-	7.37	7.55	-	-	7.55
11/04/2018	23	24.60	7.37	-	-	7.37	7.52	-	-	7.52
12/04/2018	24	24.50	7.35	-	-	7.35	7.52	-	-	7.52
13/04/2018	25	24.70	7.39	7.35	7.35	7.36	7.62	7.61	7.6	7.61

Appendix D: Chlorophyll a Linear Regression

Important to note these show raw results, however some numbers have been rounded to fit in tables due to high number of figures.

Table D1 Linear regression correlation results.

Regression Statistics	
Multiple R	0.940651
R Square	0.884824
Adjusted R Square	0.868371
Standard Error	2.886372
Observations	9

Table D2 ANOVA results of regression analysis of chlorophyll a conversion.

	df	**SS**	**MS**	**F**	**Significance F**
Regression	1	448.0216	448.0216	53.77672	0.000158
Residual	7	58.31801	8.331145		
Total	8	506.3396			

Table D3 Linear regression statistical results.

	Coefficients	Standard Error	t Stat	P-value	Lower 95%	Upper 95%
Intercept	-3.62685	3.527685	-1.02811	0.338106	-11.9685	4.714796
IN VIVO FL	0.018674	0.002546	7.333261	0.000158	0.012652	0.024695